"In presenting the dissertation as a partial fulfillment of the requirements for an advanced degree from the Georgia Institute of Technology, I agree that the Library of the Institution shall make it available for inspection and circulation in accordance with its regulations governing materials of this type. I agree that permission to copy from, or to publish from, this dissertation may be granted by the professor under whose direction it was written, or, in his absence, by the dean of the Graduate Division when such copying or publication is solely for scholarly purposes and does not involve potential financial gain. It is understood that any copying from, or publication of, this dissertation which involves potential financial gain will not be allowed without written permission.

_____

MASS SPECTROMETRIC STUDIES OF THE SYNTHESIS, REACTIVITY, AND ENERGETICS OF THE OXYGEN FLUORIDES AT CRYOGENIC TEMPERATURES

A THESIS

Presented to

The Faculty of the Graduate Division

by

Thomas Joseph Malone

In Partial Fulfillment

of the Requirements for the Degree

Doctor of Philosophy in the

School of Chemical Engineering

Georgia Institute of Technology

February, 1966

MASS SPECTROMETRIC STUDIES OF THE SYNTHESIS,

REACTIVITY, AND ENERGETICS OF THE OXYGEN

FLUORIDES AT CRYOGENIC TEMPERATURES

Approved:

Date approved by Chairman: March 3 1966

ACKNOWLEDGMENTS

I am deeply indebted to Dr. H. A. McGee, Jr. for his encouragement, advice, and assistance throughout both my graduate and undergraduate studies. Many hours of discussion and willing assistance with many problems from my fellow graduate students, D. B. Bivens, W. J. Martin, and J. H. Wilson are also greatly appreciated as were the interest and suggestions of Dr. W. H. Eberhardt and Dr. W. M. Newton while serving as the reading committee. My appreciation is also expressed to Dr. W. T. Ziegler and Dr. S. L. Gordon for several helpful discussions.

Deep appreciation is due the National Science Foundation, Proctor and Gamble Company, and Ethyl Corporation for furnishing me fellowships during my graduate study. I also wish to thank the National Aeronautics and Space Administration for its support through NASA grants NsG-123-61, NsG-337, and NsG-657. Several samples used in this work were generously furnished by Dr. R. A. Mitsch of the 3M Company.

The understanding, encouragement, and assistance of my wife, Pat, my parents, Mr. and Mrs. H. J. Malone, Sr., and many other relatives are deeply appreciated. The expert glass blowing of Mr. Donald E. Lillie and the excellent typing of Mrs. Peggy Weldon are also gratefully acknowledged.

TABLE OF CONTENTS

TABLE OF CONTENTS (Continued)

TABLE OF CONTENTS (Continued)

LIST OF TABLES

LIST OF TABLES (Continued)

LIST OF ILLUSTRATIONS

LIST OF ILLUSTRATIONS (Continued)

LIST OF ILLUSTRATIONS (Continued)

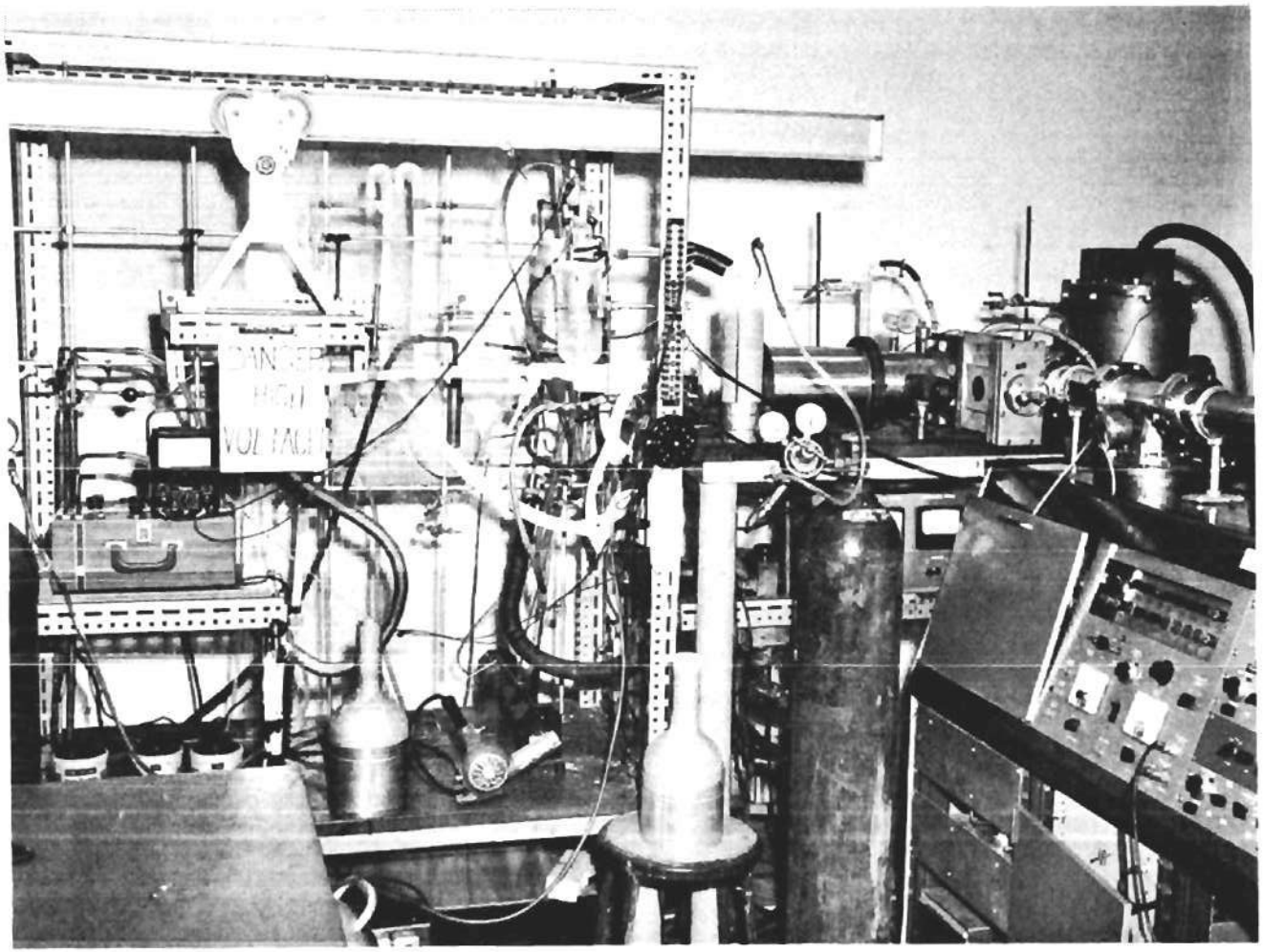

Figure 1. General View of Mass Spectrometer and Associated Cryogenic Equipment During External Synthesis of Low Temperature Oxygen Fluorides.

SUMMARY

The work reported in this thesis involved the development of a combination discharge tube reactor and mass spectrometer inlet system for investigation of very reactive chemical species at cryogenic temperatures; and the investigation of the synthesis, stability, energetics, and chemical reactivity of the reported low temperature oxygen fluorides, O_2F_2 and O_3F_2, as well as the unknown oxygen-fluorine free radicals, O_2F and OF.

The investigation of species that exist as stable entities only so long as they are maintained at cryogenic temperatures has required development of rather novel equipment and experimental techniques. The development of a multipurpose cryogenic reactor and mass spectrometer inlet system was completed (initial development was performed by Martin[3]) in this work. Using this apparatus, it is possible to synthesize mixtures of labile species at cryogenic temperatures by a variety of techniques (electrical discharge, pyrolysis, direct reaction, etc.), partially separate them (by simple distillation or differential condensation), and vaporize them directly into the ionizing electron beam of the mass spectrometer. Mass spectrometer sensitivity calculations were made which indicated that the cold labile species should be injected from an inlet port which actually touched the edge of the electron beam. These calculations predicted a decrease in sensitivity from its maximum by about a factor of 100 for the case where the sample inlet port was only 2.0 cm from the ionizing electron beam. This trend was strikingly verified in

the investigations of the O_2F radical for this work. The cryogenic reactor-inlet system that was developed as part of this research permits the optimum arrangement, that is, injection of the sample directly into the edge of the electron beam. The arrangement also permits detection of condensed species at temperatures where they exert a vapor pressure of only about 10^{-6} torr. The device has been used quite successfully in this work for the investigation of the low temperature oxygen fluorides.

The low temperature oxygen fluorides are believed to be the most powerful oxidizers known, being extremely reactive even at temperatures as low as 90°K. This has generated considerable interest in their possible use as propellant oxidizers and special purpose oxidizer additives, as well as in their use as reactive intermediates for the synthesis of other species that may be more stable and even more useful. The oxygen-fluorine free radicals were the object of much interest since none had ever been directly observed and it is believed that they might be extremely reactive and energetic.

Investigation of the mass spectrum of O_2F_2 over a broad temperature range indicated that its final decomposition products were only O_2 and F_2 as had been reported earlier. The $A(O_2F^+)$ and $A(OF^+)$ from O_2F_2 were measured to be 14.0 ± 0.1 ev and 17.5 ± 0.2 ev, respectively. Neither the positive nor the negative ion of dioxygen difluoride, $O_2F_2^+$ or $O_2F_2^-$, was detected in the mass spectrometer. From these measured $A(O_2F^+)$ and $A(OF^+)$, along with other available electron impact, microwave, thermochemical, and kinetic data, it was determined that O_2F^+ and OF^+ were being formed by the following mechanisms,

$$O_2F_2 + e \rightarrow O_2F^+ + F + 2e$$

and

$$O_2F_2 + e \rightarrow OF^+ + OF + 2e$$

respectively. These data also permitted the development of the bond energies of the O_2F_2 molecule and O_2F free radical. They were determined to be

$$D(F\text{-}O_2F) = 0.8 \text{ ev} \qquad D(O\text{-}OF) = 4.8 \text{ ev}$$

$$D(FO\text{-}OF) = 4.5 \text{ ev} \qquad D(O_2\text{-}F) = 0.8 \text{ ev}$$

These results are consistent with microwave, thermochemical, infrared, and kinetic data which all indicate that the O-O bonds are very strong in these species, whereas the O-F bonds are unusually weak.

Prior to the initiation of the present experimental work a qualitative theoretical analysis was conducted on the O_2F radical, using the arguments of the double quartet modification of the octet rule, to see if any strong conclusions concerning its existence or nonexistence would be possible. This analysis led to a proposal that the species could possibly be stabilized at low temperatures and would have an usually strong O-O bond and very weak O-F bond. The bond energies for the radical were obtained in the investigations of the O_2F_2 molecule, as discussed above, and obviously agree quite well with the qualitative proposal. The radical was actually detected in this work as a free species in the vapor phase, resulting from the pyrolysis of O_2F_2 in a tubular alumina furnace at about 250°K. This permitted a direct measurement of $I(O_2F)$ of 12.6 $\pm$ 0.2 ev and calculation of $I(O_2F_2) \leq 13.4$ ev, which are in close agreement with values estimated first in the development of the energetics of the

O_2F_2 molecule. This radical has also been detected in the past few months from epr studies of the liquid phase of O_3F_2 (contains O_2F in concentrations as high as 10 per cent by weight) and from ir studies of the products from the uv irradiation of F_2 in an O_2 matrix at 4°K. These mass spectrometric results for O_2F were quite exciting in that they not only represented the synthesis of a previously unknown species after predicting its possible stability, but they also resulted in the determination of its energetics which were in excellent agreement with its previously proposed electronic structure.

Several attempts were made to produce the O_2F radical by subjecting gaseous O_2-F_2 mixtures and O_2-OF_2 mixtures to an electrodeless radio frequency discharge at room temperature, but these experiments gave no evidence for the formation of the species. However, extensive studies of this type were not conducted.

Numerous attempts were made to produce the OF free radical which has been proposed to be a very reactive intermediate in many chemical reactions. For example, kinetic studies have indicated that OF_2 decomposes by way of the OF radical. Pyrolysis of OF_2 on hot filaments of molybdenum and nichrome that were conducted as part of this thesis did give some evidence for the evidence of the OF radical, but the evidence was not very conclusive. Similar experiments with hot filaments of niobium, tantalum, platinum, titanium, zirconium, and tungsten gave no evidence of formation of OF despite the fact that the very optimum mass spectrometric arrangement was employed, i.e., pyrolysis directly in the ionizing electron beam. In these experiments the OF_2 molecule should have experienced only a single collision with the hot filament before analysis, permitting the

study of the very first decomposition products. However, only free O atoms, O_2, and large amounts of F_2 were detected, indicating that OF_2 was decomposing directly to O and F_2 on the hot metal surfaces. Other pyrolysis experiments with OF_2 using tubular monel and alumina furnaces also gave no evidence for the formation of OF. In addition, no evidence for OF was obtained upon subjecting gaseous samples of OF_2, O-OF_2 mixtures or O_2-F_2 mixtures to an electrodeless radio frequency discharge.

The positive and negative ion spectra were obtained at every 2°-3°K intervals from 77°-165°K for the products of numerous O_3F_2 systhesis experiments using the cryogenic reactor-inlet system that was discussed above. However, no unequivocal evidence was obtained for the existence of O_3F_2 as a molecular entity in the vapor phase. The mass spectrum as a function of temperature indicated that relatively large amounts of OF_2 and ozone were formed during the syntheses. It also confirmed that O_3F_2 does decompose at 110°-120°K, forming O_2F_2 as reported, but these data also indicated that at least small quantities of OF_2 were formed during the decomposition. This last fact has not been reported previously.

In view of the failure to detect the O_3F_2 molecule as a molecular entity, a systematic qualitative theoretical analysis was conducted, using the double quartet approach that was used earlier for O_2F, on the O_3F_2 molecule as well as on most of the other molecules, radicals, and ions of oxygen and fluorine that seem possible (This analysis is presented in Appendix A). This analysis resulted in the conclusion that O_3F_2 might well have a chain structure and have the basic electronic features of a

loosely bonded O_2F and OF radical. This would indicate that O_3F_2 would decompose readily into O_2F and OF radicals which could react in turn along two different paths as follows;

$$2FO_2{\cdot}OF \rightleftharpoons 2FO_2{\cdot} + 2FO{\cdot} \begin{cases} \xrightarrow{\text{fast}} O_2F_2 + 2FO_2{\cdot} \xrightarrow{\text{slow}} 2O_2F_2 + O_2 \\ \longrightarrow OF_2 + O_2 \end{cases}$$

This mechanism would account for the formation of O_2F_2 and O_2, as well as OF_2 as indicated by these mass spectrometric studies. The above structure and mechanism for decomposition of O_3F_2 also agrees with all available epr, nmr, and ir data. It is obvious that this is not the final word on the O_3F_2 molecule. However, it is quite interesting that a qualitative theoretical analysis of this species predicts an electronic structure that seems to agree with most of the available experimental data. It will certainly be interesting to see if future studies of this unusual species support the structure and mechanism for decomposition that are proposed herein.

The theoretical analysis of a possible unsymmetrical isomer of dioxygen difluoride, $O{=}OF_2$, indicated that it could possibly exist as a stable entity but that it probably would not. In any case, it would be expected to be much less stable than the chain isomer, FOOF, which decomposes at about 200°K. No evidence was obtained in this work for the existence of this unsymmetrical isomer.

It would have been expected that at least small amounts of O_4F_2 would have been produced in the O_3F_2 synthesis experiments in this work. However, no evidence was obtained for its existence in the vapor phase.

There also was no evidence for the existence of the higher oxygen fluorides, O_5F_2 and O_6F_2, which have just been reported as possible stable entities below about 90°K.

A large part of the results discussed in this thesis have been recently published. The development of the energetics of the O_2F_2 molecule and O_2F radical have been published in the Journal of Physical Chemistry in the December, 1965, and January, 1966, issues, respectively. A detailed description of the cryogenic reactor-inlet system, developed for this work, is to be published in the April or May issue of Review of Scientific Instruments.

CHAPTER I

INTRODUCTION TO THE PROBLEM

Brief History and Purpose of the Studies

The great increase of interest in recent years in the broad and exciting area of low temperature chemistry motivated the work that is presented in this thesis. The initial objectives of the explorations of that little known realm of chemistry below about 150°K, which may well be called cryochemistry, have been the development of equipment and techniques for the synthesis and investigation of species that exist only at these extremes of environment.

The purposes of the present work have been two-fold. They are: (a) the development of a combination reactor and inlet system in which a mixture of very reactive chemical species can be synthesized, partially separated, and investigated at cryogenic temperatures with a time-of-flight mass spectrometer, and (b) the synthesis and mass spectrometric investigation of the physical and chemical properties over a broad temperature range of the known or pseudo-known oxygen fluorides OF_2, O_2F_2, O_3F_2, and O_4F_2 as well as the heretofore unobserved oxygen-fluorine free radicals, OF and O_2F. These species were chosen for study since they constitute a family of compounds that exist as stable entities, with the exception of OF_2, only so long as they are maintained at some very low temperature; they seem to exhibit very interesting, unusual, and hopefully useful properties; and very little is actually known about them. This particular family, as well as other instances of species exhibiting

this unusual cryogenic stability, have been discussed in a recent review by McGee and Martin.[1]

The only low temperature species of the oxygen fluoride family that has been studied previously in the vapor phase is O_2F_2. The microwave spectra of O_2F_2 have been obtained by Jackson[2] at dry ice temperature, but no unequivocal direct observations of the other low temperature oxygen fluorides have been reported. For example O_3F_2 is reported to be a blood red liquid at 90°K, but whether or not this red liquid is actually molecular O_3F_2 is quite unknown. Direct observations of these species are needed first to clarify their existence, and second, because of their significance in the study of cryochemistry. Mass spectrometry offers a possible means for the unambiguous observation of these molecules as well as a means to study their synthesis, their stability, their chemistry, and their energetics. Because of their unusual thermal instability at cryogenic temperatures, absolute temperature control is imperative at all times, and hence new equipment and procedures had to be developed.

The coupling of a mass spectrometer to a cryogenic chemical system is a new technique that is being developed at this Institute, and some of the early development of a thermal gradient, cryogenic inlet system has been briefly discussed by Martin.[3] This thesis discusses the design, development, and operation of a combination discharge tube reactor and cryogenic inlet system that encompasses the basic features of the inlet system discussed by Martin. Calculations were made to determine the optimum design and ultimate sensitivity of an inlet system of the general design described in this work. These calculations are discussed in detail in Appendix B and are summarized in Chapter II.

The actual investigations of the reported oxygen fluorides were conducted with the major emphasis on the low temperature oxygen fluorides, O_2F_2 and O_3F_2. However, numerous experiments were performed in an effort to synthesize and investigate the OF and O_2F free radicals as free species in the vapor phase. There has been considerable interest in isolating these species in order to prove the existence of oxygen-fluorine free radicals and to study their physical and chemical properties since it is believed that they might be extremely reactive and energetic even at low temperatures. No attempt was made in this work to prepare these radicals as free species in the liquid or solid state.

Most of the above objectives were completed with a great deal of success while a few of the experiments led to inconclusive results. This work was supported in part by the National Aeronautics and Space Administration through its grants NsG-123-61, NsG-337, and NsG-657 which were concerned, in part, with the preparation and investigation of highly endothermic compounds at cryogenic temperatures for possible use as propellants or as special purpose propellant additives such as hypergolic sensitizers or gelling agents.

Oxygen Fluoride Molecules

The low temperature oxygen fluorides are considered as possibly the most powerful oxidizers known and as a result have received considerable attention as rocket propellant oxidizers and oxidizer additives as well as reagents for chemical synthesis at cryogenic temperatures. A recent review by Streng[4] discusses the preparative techniques and summarizes the known physical and chemical properties of the four reported oxygen fluorides OF_2, O_2F_2, O_3F_2, and O_4F_2. Since that review is fairly

complete for the investigations reported before 1963, only the most pertinent properties of these species will be discussed here, and emphasis will be placed on the more recent information that has appeared since 1963.

Oxygen Difluoride (OF_2)

The first success in combining fluorine with oxygen was reported in 1927, by Lebeau and Damiens.[5] It is interesting to note that they first observed the formation of oxygen difluoride, OF_2, while attempting to purify fluorine gas by bubbling it through a caustic soda solution. This reaction is generally employed now for the commercial preparation of this compound. This species is a stable, colorless gas at room temperature and is a yellow liquid below 128°K(nbp). Chemically, oxygen difluoride is a powerful oxidizer, but its reactivity is considered to be lower than that of fluorine.

The stability of OF_2 at ordinary temperatures has permitted extensive investigations of both its physical and chemical properties. Hence, very little emphasis was placed on its study in this work. However, it was used as the parent species in numerous attempts to detect the OF radical by pyrolysis and radio frequency discharge techniques. Previous information about OF_2 that was particularly pertinent to these investigations were the mass spectrometric studies performed by Dibeler, Reese, and Franklin[6] which will be discussed in some detail in Chapter III and is summarized in Appendix C.

Dioxygen Difluoride (O_2F_2)

The formation of dioxygen difluoride, O_2F_2, was first achieved by Ruff and Menzel[7,8] in 1933, who subjected a gaseous mixture of O_2 and F_2 to an electric discharge at a low pressure (10-20 torr) and at liquid air temperature. At the present time, dioxygen difluoride is prepared directly from the elements in essentially the same manner by utilizing an electrical discharge as has been discussed in detail by Kirshenbaum and Grosse.[9] Different reaction systems and techniques for the synthesis of the oxygen fluorides have been discussed in some detail by several investigators.[10,11] Some of these systems, as well as a rather unique method developed during this work, will be discussed in some detail in Chapter II of this thesis.

Dioxygen difluoride is an orange-yellow solid, melting at 109.7°K to an orange-red liquid. It decomposes quite rapidly into O_2 and F_2 at temperatures close to its normal boiling point of 216°K, but it can be stored for a long period of time in darkness in pyrex glass cylinders cooled to 93°K.[4] It is an endothermic compound with a heat of formation from the elements of 4.7 Kcal/mole.[12]

Dioxygen difluoride was the object of extensive investigation in this work. This species had not previously been studied mass spectrometrically, its vapor phase had not been investigated below dry ice temperatures nor during its thermal decomposition, and the energetics of the molecule were unknown. It was a particularly interesting species in that early kinetic data seemed to indicate a branched structure, $O{=\!=}OF_2$. However, more recent microwave spectra reported by Jackson[2] showed that it is a nonplanar, symmetric chain molecule very similar to the hydrogen

peroxide molecule except that it has extraordinarily long O-F bonds of 1.58 Å and a surprisingly short O-O bond of 1.22 Å which is essentially equal to the bond length of the O_2 molecule of 1.21 Å.

Evidence for similar effects in other analogous compounds has been reported in the literature. Hirota[13] observed by electron diffraction that the S-S bond length in both S_2Cl_2 and S_2Br_2 is shorter than is usually found for a singly-bonded S-S link and that the S-Cl bond in S_2Cl_2 is longer than that found in SCl_2. In a similar study of N_2F_2, Bauer[14] found the N-F bond to be longer than expected for a normal single bond. Very recent work[15] with the disulfur difluoride compounds has shown that the S-S bond in the chain isomer, FSSF, is essentially double bond in character and is relatively short compared to the S-S bond in HSSH.

If the microwave data of Jackson are correct, it would be expected that the O-F bonds of FOOF would be very weak whereas the O-O bond would probably be nearly as strong as the double bond of molecular oxygen. From the energy measurements on O_2F_2 that were made and reported in this work it was shown that this is indeed the case. These are very exciting and significant results in that they represent the first successful mass spectrometric investigations of a species that is known to exist as a stable entity only at cryogenic temperatures.

The fact that the O-O bond length in O_2F_2 is very similar to that found for the oxygen molecule indicates that there must be some multiple bonding between the two atoms and that a singly-bonded covalent chain, which explains the structure of H_2O_2, is not sufficient to describe O_2F_2.

Using the valence bond description Jackson[2] stated that considerable contributions from ionic structures of the type $F^- \quad O{=}{=}O^+F$ would

lead to a shortening of the O-O bond and a lengthing of the O-F bond. The large contribution from doubly-bonded resonance structures for O_2F_2 would also account for the fact that it has a very high barrier for internal rotation.

In Jackson's paper an alternative explanation for the unusual structure of O_2F_2 was proposed by Libscomb using a molecular orbital description. He proposed that an antibonding π-molecular orbital of the O_2 molecule, say πy^*2p forms a bond with the 2py-orbital of the fluorine to give an electron pair in a three-center orbital. A similar situation would exist for the πz^*2p-orbital and the second fluorine atom. Libscomb pointed out that the three-center bond would also account qualitatively for the fact that the barrier to internal rotation in O_2F_2 is considerably higher than that reported for H_2O_2.

Linnett[16] has also proposed an explanation for the unusual structure of O_2F_2 using the double quartet modification of the octet rule. No attempt will be made in this work to present the ideas and arguments proposed by Linnett, but a very detailed presentation of the formal arguments and justification for the double quartet modification of the octet rule has been published recently.[17] This approach will be used rather extensively in Appendix A for describing the electronic structures of the reported oxygen fluorides, as well as unreported molecules, radicals, and ions of oxygen and fluorine. It is of interest to note that this rather new approach of describing the electronic structures of molecules has been hailed by J. O. Hirschfelder[18] as one of the most recent major advances in quantum mechanics.

Using this approach, Linnett showed that there are probably several

electronic configurations that contribute to the overall structure of O_2F_2 (see Appendix A), but the configurations that are probably the largest contributors are given by

(A) and (B)

where the solid dots represent electrons of one spin and the deltas represent electrons of the opposite spin. The lines represent pairs of electrons of opposite spin that are not considered close pair electrons (i.e., they do not occupy the same spatial orbital). The above electronic structures proposed by Linnett for O_2F_2 indicate that the O-F bonds would correspond to single electron bonds and would account for their unusually long lengths. Also, the indicated four electron O-O bond would account for the very short O-O bond length. Linnett further pointed out that configuration (B) would have a minimum interelectronic repulsion energy when the two OOF planes have an interplane angle of 90° which is essentially the actual value (87.5°) determined from the microwave studies of Jackson. A twisting of these planes from 90° would bring the two electrons of one spin in the O-O bond close to each other and would result in a higher energy. This idea would also account for the high barrier for internal rotation that was observed by Jackson.

The facts that two isomers of disulfur difluoride, FSSF and $S{=}SF_2$, have been observed and that kinetic data on O_2F_2 led some investigators to believe that it had a branched rather than chain structure, generated an interest in considering the possible existence of two isomers of this species as part of this thesis. Jackson's microwave work represented a

study of the vapor phase of the species at dry ice temperature (-78°C) while most of the chemical studies were conducted at much lower temperatures, with the O_2F_2 as a liquid or solid. This seemed to suggest the possibility that a branched isomer, $O{=\!=}OF_2$, might exist at lower temperatures which might not have been detected at the relatively high temperature of Jackson's work.

A theoretical analysis of a branched isomer of this compound, using the double quartet modification of the octet rule approach, was conducted before the initiation of the experimental work for this thesis, in order to see if it would indicate any strong conclusions concerning the existence or nonexistence of this species. Using the criteria proposed by Linnett[17], it was decided that the following two electronic configurations

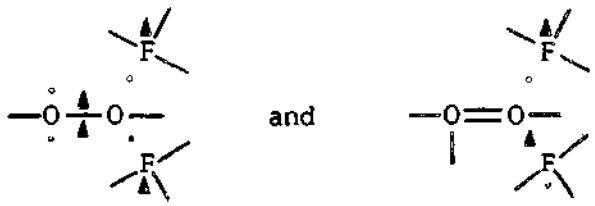

(C) (D)

could possibly give a stable structure, but that it would be of relatively high energy in that it has a somewhat unfavorable formal charge distribution. However, it can be shown (see Appendix A) that this charge distribution is essentially the same as that of ozone which is known to be reasonably stable. Hence, it was proposed[19] that this unreported unsymmetrical isomer of O_2F_2 might possibly exist at relatively low temperatures, but that it would definitely be much less stable than the chain isomer,

FOOF. No evidence for the existence of this unsymmetrical isomer was obtained in this work as will be shown in Chapter III. However, Arkell has made the interesting observation by infrared techniques that OF_2 was formed during the photolysis of F_2 in an O_2 matrix at 4°K. He suggested that possibly OF_2 formed by way of a transient intermediate such as

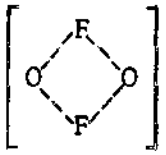

(E)

which could rearrange in only two ways, due to the restriction of the matrix, giving either O_2F_2 or $OF_2 + O$. It seems quite possible that the formation of the OF_2 could involve the formation of the unsymmetrical isomer, $O{=\!=}OF_2$, as an intermediate. Using the double quartet arguments for the hydrogen peroxide molecule result in the immediate conclusion that a branched isomer of that compound definitely would not exist, and such an isomer has never been observed experimentally. In addition, these arguments do predict that both isomers of disulfur difluoride, FSSF and $S{=\!=}SF_2$, would exist, and they have both been observed experimentally.[15] However, it should be pointed out that it is not obvious that the arguments of the double quartet model are valid for the case of sulfur compounds in which the valence shell is not restricted to eight electrons.

Ozone Difluoride (O_3F_2)

Ozone difluoride, O_3F_2, was first prepared by Aoyama and Sakuraba[20] in 1938 when they subjected a 3:2 gaseous mixture of oxygen and fluorine

near 15 torr to an electrical discharge in a reactor maintained at liquid air temperature. The same investigators showed also that O_3F_2 is formed by the action of ultraviolet light on a liquid mixture of oxygen and flurine.[21] For many years the claims of these Japanese scientists were not accepted for standard reference books or were regarded with skepticism. This lack of acceptance of their results was due to the fact that they did not give a quantitative analysis of their product. However, their results were generally accepted after Kirshenbaum and Grosse[9] prepared this species in 1958 by using the same techniques and investigated many of its physical and chemical properties.

Ozone difluoride is a dark red, viscous liquid at 90°K which makes it possible to easily distinguish it from O_2F_2 which is an orange solid at this temperature. It is an endothermic compound and has been reported to decompose quantitatively, with heat evolution of 2.0 Kcal/mole, at about 115°K, according to the equation[11,12]

$$2\ O_3F_2 \rightarrow O_2 + 2\ O_2F_2 \qquad (1)$$

Kirshenbaum[11] and Solomon[22] have reported that O_3F_2 can be distilled in the range of 96°-114°K at a pressure of 0.1 to 1.5 torr with only slight decomposition and can be refluxed at 116°K. These are very important facts in that it is necessary for a species to be distillable so that it can be transferred through the cryogenic mass spectrometer inlet system that was used in this work.

Ozone difluoride is considered as probably the most potent oxidizer known, but it is actually safer to handle than ozone. A somewhat unusual property that it exhibits is that when added to liquid oxygen to

its saturation concentration of about 0.1 mole per cent the resulting solution is hypergolic toward liquid hydrogen and low molecular weight hydrocarbons.[10] Numerous tests with these O_2-O_3F_2 solutions have shown that it is hypergolic with most of the fuels used as rocket propellants. Similar tests indicate that at least a 35 per cent solution of fluorine in liquid oxygen is required to get hypergolic ignition with hydrogen.[23] The 0.1 per cent O_3F_2 solution would definitely be more desirable since it has essentially the same physical properties as pure oxygen and is much safer to handle than the fluorine solution. This unusual hypergolic effect of the O_2-O_3F_2 solutions would permit the construction of rocket engines without ignition systems and would be of particular advantage in propulsion systems which must be shut off and restarted during flight. These properties of O_3F_2 show that cryochemical substances need not be relegated to the class of interesting but useless oddities but that they may be of wide practical importance.*

The necessity of maintaining O_3F_2 at temperatures below 115°K for its investigation has considerably hindered its study. The fact that it has never been directly observed has prevented the unequivocal determination that molecular O_3F_2 actually exists. Its composition has been determined only by thermally decomposing it and measuring the ratio of oxygen and fluorine that is formed.

Nuclear magnetic resonance studies of O_2F_2, O_3F_2, and O_2F_2-O_3F_2 mixtures have been performed by Solomon.[24] These results are quite interesting in that only a single F^{19} signal was obtained for the pure species

*The Air Reduction Company was awarded an Air Force contract for the production of O_3F_2 to be used as a liquid oxygen additive.

as well as for the mixtures. The signal from O_3F_2 was at a different frequency than that from O_2F_2, but it did not decrease in intensity as the sample of O_3F_2 was heated, even though this heating did result in the decomposition of O_3F_2 into O_2F_2 and O_2. Instead, the signal simply shifted its position toward that of pure O_2F_2. At no time during the decomposition were two different signals characteristic of pure O_2F_2 and O_3F_2 observed simultaneously. A possible explanation for this observation is discussed in Chapter III.

In infrared studies[25] of the products formed during the photolysis of $O^{18}F_2$ in an O_2^{16} matrix at 4°K, the interesting observation was made that the $O^{18}F_2$ concentration decreased and $O^{16}F_2$ was formed. The following exchange mechanism

$$O^{18}F_2 + O_2^{16} \rightleftharpoons FO^{18}O^{16}O^{16}F \rightarrow O^{16}F_2 + O^{16}O^{18} \qquad (2)$$

involving O_3F_2 was suggested as a possible explanation of the disappearance of the O^{18} atom in $O^{18}F_2$. This proposed mechanism is quite interesting in that it will be shown in Chapter III to agree with the mechanism that is proposed in this thesis for the decomposition of O_3F_2.

Solomon[26] has recently studied the reactions of O_2F_2 and O_3F_2 with SO_2 On the basis of an analysis of the products of these reactions he has stated that O_3F_2 appears to be a better source of O_2F than is O_2F_2. This conclusion is supported by epr studies, which will be discussed later, which indicate a much greater concentration of the O_2F radical in O_3F_2 than in O_2F_2.

Ozone difluoride was a particularly interesting species to investigate for this thesis in view of the considerable controversy as to

whether it actually exists as molecular O_3F_2. Some investigators believe that it may well be an equilibrium mixture of lower molecular weight species such as possibly O_2F and OF or 2 O_2F and O_2F_2. The mass spectrometric investigation of this species with a cryogenic inlet system, which is described in Chapter II, was the first attempt to detect it directly in the vapor phase. It is believed that these studies represent a significant contribution to the elucidation of this complex problem concerning the existence, structure, and reactivity over a fairly broad temperature range of this unusual species.

Tetraoxygen Difluoride (O_4F_2)

Another member of the oxygen fluoride family, tetraoxygen difluoride, O_4F_2, was first synthesized by Grosse, Kirshenbaum and Streng in 1961.[27,28] Very little is actually known about this species. At 77°K, it is a reddish brown solid, but it differs in color from O_3F_2 and sometimes forms clusters of long needle-like crystals. It melts at 82° ± 2°K and is stable at least for a few hours at 90°K where it has a vapor pressure of less than 1.0 torr. It has been reported[27] that between 90°K and 110°K it decomposes slowly to form O_3F_2 and O_2, with the former yielding O_2F_2 and O_2 at temperatures above 115°K. Since O_2F_2 in turn decomposes to O_2 and F_2 at about 200°K, all the O_4F_2 is supposedly decomposed finally into O_2 and F_2 gas at room temperature.

The only determination of the composition of O_4F_2 was made by warming the species to room temperature and measuring the ratio of the O_2 and F_2 formed. Several tests have been made to dispel earlier beliefs that the species was O_2F_2 or O_3F_2 with trapped O_2 or a mixture of O_3 + 3 O_3F_2.[28] Further evidence[29,30] that O_3F_2 and O_4F_2 are definitely

different species is the fact that the molar extinction coefficients of O_3, OF_2, O_2F_2, O_3F_2, and O_4F_2 are greatly different. Still further evidence is given by the electron paramagnetic resonance studies of these species which will be discussed in the next section of this chapter.

Arkell[25] has used infrared spectroscopy to study the products formed upon warming a solid matrix containing O_2F radicals. He reported the formation of O_4F_2, due to dimerization of O_2F radicals and assigned bands at 588 and 1519 cm^{-1} to the O-F and O-O stretching fundamentals, respectively, in O_4F_2. He pointed out that these bands are unusually close to the respective absorptions in O_2F, which will be discussed later, and indicates that the structural character of O_2F is maintained in the O_4F_2 molecule. That is, the dimerization of O_2F is not accompanied by gross physical change in the O_2F moiety. This is very analogous to the O_2-O_4 system discussed by Pauling[31] in which he states that O_4 "consists of two O_2 molecules, with nearly the same configuration and structure as when free, held together by bonds much weaker than ordinary covalent bonds." Assuming that the O_4F_2 species is analogous to this, it would correspond to two O_2F radicals joined by a very weak O-O bond and could dissociate very easily with heating which would account for its thermal instability. This is directly analogous to the isoelectronic N_2F_4-NF_2 system in which N_2F_4 dissociates into NF_2 with heating.

From a comparison of calculated O-O and O-F stretching force constants for O_4F_2, Arkell concluded that the O-O bonds in this species are essentially double bond in character while the O-F bonds are very weak. This indicates considerable contribution from ionic forms of this species in a manner similar to that suggested by Jackson[2] for O_2F_2. The

corresponding ionic forms would be

$$F-O-O-O^{+}=O \qquad F^{-} \quad F^{-} \qquad O=O^{+}-O-O-F \quad (3)$$

for O_4F_2. This thesis suggests an alternative explanation for the O-O double bond character and weak O-F bonds in this species from an application of the double quartet description. This development is discussed in detail in Appendix A.

During the period that the work for this thesis was being conducted, Nielsen[32] investigated the reaction products resulting from the irradiation of OF_2 at 77°K. He employed a mass spectrometer similar to that used in these experiments and supposedly observed and identified O_2F_2 as well as O_3F_2 and O_4F_2 as reaction products. However, the ions attributed to O_3F_2 and O_4F_2 were never observed below 130°K in his experiments, and in some cases these species were not observed until the temperature was greater than 200°K. Since O_3F_2 has a vapor pressure greater than 1.0 torr at 112°K it should have certainly been observed at this much lower temperature. Regardless of this fact, it is well known that both of these compounds decompose very rapidly at temperatures (105° - 120°K) much lower than those reported by Nielson (130° - 211°K). In view of the above, as well as the fact that no cooled sample delivery system was used, but rather the gaseous species were transported from a reservoir at cryogenic temperatures into the spectrometer through a small tube at room temperature, it seems impossible for his reported identification of O_3F_2 and O_4F_2 to be reliable. It will be shown rather conclusively in Chapter III that the ions Nielson attributed to O_3F_2 and O_4F_2 were probably impurities in the feed gas or small amounts of impurity species

formed during the irradiation of the OF_2 samples.

Higher Oxygen Fluorides

The existence of higher oxygen fluorides, O_5F_2 and O_6F_2, was postulated in 1961 by Streng, et al.,[27] These investigators have just reported[33] having prepared these species by subjecting stoichiometric mixtures of oxygen and fluorine to an electrical discharge at 60°K and at pressures of 0.5-8.0 torr. Their main characterization of the species was the determination of their empirical formulas. That is, they decomposed the species to O_2 and F_2 and determined the O_2:F_2 ratio. Infrared analysis of the species indicated that no O_3 or OF_2 was formed during the syntheses, and they pointed out that the only possible oxygen compound that could falsify their analysis was ozone. The fact that no ozone or OF_2 was detected in O_5F_2 or O_6F_2 is quite surprising in that several studies, including the mass spectrometric studies of this thesis, have shown that both of these species, OF_2 and O_3, are formed in the syntheses of O_2F_2 and O_3F_2. Streng, et al. also reported that attempts to make still higher oxygen fluorides than O_6F_2 resulted in the formation of only known oxygen fluorides and ozone. It seems strange, indeed, that ozone would be formed in the syntheses of the lower oxygen fluorides and attempts to synthesize still higher oxygen fluorides, whereas in the syntheses of O_5F_2 and O_6F_2 none would be formed. In addition, they stated that the O_6F_2 species decomposed at 90°K forming lower oxygen fluorides and ozone. In view of these strange results and the lack of more unequivocal evidence than just their empirical formulas, it seems that the claim for the existence of O_5F_2 and O_6F_2 as molecular entities should not be considered conclusive.

From the discussions to this point it is obvious that there were very important questions that needed to be answered regarding the structure, energetics, physical properties, and chemical reactivity of the reported oxygen fluorides. The existence or non-existence of O_3F_2 and O_4F_2 as stable entities is of primary importance and definitely points out the need for equipment and techniques to directly observe and investigate these species.

Electron Paramagnetic Resonance of the Reported Oxygen Fluorides

The electron paramagnetic resonance studies of the low temperature oxygen fluorides are of particular interest in that they represent a relatively extensive investigation of these species in the liquid and solid states. However, these studies still did not permit their direct observation as true chemical compounds. Maguire[34] reported that epr studies indicated that O_3F_2 was paramagnetic while O_2F_2 was not. Much more extensive epr studies have been performed very recently on the four known oxygen fluorides by Kirshenbaum, et al.[35](cf. Kasai and Kirshenbaum[36]). The following discussion summarizes the results obtained in those studies.

Oxygen Difluoride (OF_2)

Samples of OF_2* were studied at 77°K and were found to be diamagnetic, as expected. However, a weak signal was observed which could correspond to 6×10^{-7} mole per cent of the OF_2 being paramagnetic, but it was believed that the signal was due to an impurity.

*The OF_2 gas was a specialty product obtained from the Baton Rouge Development Laboratory, General Chemical Division, Allied Chemical Corporation.

Dioxygen Difluoride (O_2F_2)

Pure O_2F_2 as well as 3 volume per cent solutions of O_2F_2 in the diamagnetic solvent $CClF_3$ (Freon 13) were studied. In either case, a strong, well-resolved signal was obtained. Maintaining the pure sample at 195°K for various lengths of time (10 minutes to 4 hours) resulted initially in the increase of the signal and eventually in the decrease of the signal. At any stage, if the sample was quenched back to 77°K and maintained at that temperature, no further change in the signal intensity was observed. Therefore, it was concluded that the signal was not due to O_2F_2 itself nor to its final decomposition products, O_2 and F_2, but was probably due to intermediate radicals formed in the sequence of decomposition. Depending on the thermal treatment of the O_2F_2, the amount of the paramagnetic species observed amounted to 0.05 to 0.5 mole per cent of the original sample.

The epr data were interpreted as implying that the paramagnetic species had an unpaired electron experiencing a hyperfine interaction with only one fluorine nucleus. In view of the reportedly very short O-O bond and very long O-F bonds in O_2F_2, it was concluded that the paramagnetic species was due to the O_2F free radical rather than the OF radical. The bond strengths of the O_2F_2 molecule and the O_2F free radical that were determined as part of this thesis would certainly substantiate this conclusion.

A weak signal was observed which was attributed to another unidentified free radical whose intensity varied from sample to sample independent of the remainder of the epr pattern. Another weak signal was observed at half magnetic field strength and was interpreted as implying

the existence of a species in the triplet state. The intensity of this signal remained unchanged when the principal signal, here attributed to O_2F, increased after a heat treatment, and it was demonstrated that the origin of the triplet signal was independent of O_2F.

Ozone Difluoride (O_3F_2)

Pure O_3F_2 was found to be too strongly paramagnetic to obtain a resolved epr spectrum. When dilute solutions (0.2-0.4 vol. per cent) of O_3F_2 in diamagnetic $CClF_3$ (Freon 13) were used, the epr spectra were identical, except for increased line width, with those observed with O_2F_2. The concentration of the free radical in pure O_3F_2 was estimated to be 5-10 mole per cent, i.e., 50 to 100 times as great as the radical concentration in pure O_2F_2.

Since the same signal was obtained for both O_2F_2 and O_3F_2, the possibility that the O_2F_2 samples were contaminated with small amounts of O_3F_2 had to be considered. Some of the O_2F_2 samples studied at 77°K were held at 195°K for several hours and their epr spectra were subsequently re-examined. If the O_2F_2 signal was due to O_3F_2 as a contaminant, it would have decreased in intensity since O_3F_2 decomposes to O_2F_2 and O_2 at 115°K, but instead the signal increased. Hence, the possibility that the presence of O_3F_2 as an impurity could have been responsible for the epr spectrum of O_2F_2 was discarded.

A broad resonance at half-field for pure O_3F_2 was again interpreted to indicate a species in the triplet state. That signal was twice as strong as that observed with pure O_2F_2 and was found to also be independent of the principal signal.

The free radical present in O_3F_2 was considered to be due to the

O_2F free radical which was present as a result of either a decomposition reaction or a thermal equilibrium[36] of the form,

$$2(O_3F_2) \rightleftharpoons O_2F_2 + 2(O_2F) \qquad (4)$$

The intensity of the electron spin resonance signal of a solution containing one volume per cent of O_3F_2 and one volume per cent of O_2F_2 in Freon 13 as a solvent was compared with that of a similar solution but containing one volume per cent of O_3F_2 alone. If the equilibrium reaction above was responsible for the O_2F, the intensity of the former solution should be weaker than that of the latter by a factor of 2-3. Instead, it was stronger. Thus, it was concluded that the decomposition reaction characterized above was probably responsible for the abundant O_2F radical in O_3F_2.

Neumayr and Vanderkooi[37] have obtained evidence that supports this work of Kirshenbaum, et al.[35] They conducted epr studies on the ultraviolet decomposition products of FSO_2OOF and related compounds in a $CFCl_3$ matrix at 77° - 163°K. The irradiation of FSO_2OOF as a pure solid and in the $CFCl_3$ matrix gave rise to the same radicals, that is, O_2F and FSO_2. They stated that the O_2F radical was relatively long-lived at 83°K and gave a spectrum at 93°K that was identical with the one obtained by Kirshenbaum, et al. by decomposition of O_2F_2 and O_3F_2. They also showed that the source of their signal, presumably the O_2F radical, could only be obtained from the decomposition of FSO_2OOF, O_2F_2, or O_3F_2 but not from FSO_2OOSO_2F, FSO_2OF, or OF_2.

Tetraoxygen Difluoride (O_4F_2)

The epr spectrum of solutions of 0.2 mole per cent of O_4F_2 in the diamagnetic solvent carbon tetrachloride, CF_4, at 77°K were obtained.[33] The spectrum from O_4F_2 was different from that obtained for O_2F_2 and O_3F_2, and hence it was concluded that O_2F was not present in solutions of O_4F_2. The intensity of the strong signal from these dilute solutions indicated that the mole per cent of the paramagnetic species in O_4F_2 was 10 per cent or higher.

Oxygen-Fluorine Free Radicals

The existence of oxygen-fluorine free radicals has been a question of interest since the early 1930's. There has been a surge of interest in these oxygen-fluorine radicals in the past few years as possible rocket propellant oxidizers since it is apparent that they will be extremely reactive and energetic species. The following discussion summarizes the experimental evidence for the existence of the OF and O_2F radicals, the very limited energetic data on them, and their proposed electronic structures.

OF Radical

Direct evidence for the existence of the oxyhalide diatomic radicals OCl, OBr, and OI has been obtained from flame emission spectra,[38,39] and from flash photolysis coupled with ultraviolet absorption spectra.[40,41] However, similar attempts to detect the OF radical spectroscopically from the flash photolysis of an O_2-F_2 mixture have failed even though simultaneous recording of the ultraviolet absorption spectra was employed. Ruff and Menzel[7,8] claimed that they had synthesized the OF radical by pyrolysis

of O_2F_2 which in turn decomposed with further heating to O_2 and F_2. Frish and Schumacher[42,43,44] later refuted these claims after performing numerous experiments which indicated that only O_2 and F_2 were formed from the pyrolysis and that there was no basis for assuming the existence of the OF radical.

Shumacher and co-workers have investigated the photolysis and pyrolysis of OF_2 and have concluded that the mechanism for decomposition of OF_2 under these conditions involves a short-lived OF radical intermediate. For example, from the photolysis experiments[45,46] it was concluded that the following mechanism agreed with the kinetic data.

$$F_2O + h\nu_{(365m\mu)} \rightarrow F + OF \qquad (5)$$

$$F + F + M \rightarrow F_2 + M \qquad (6)$$

$$OF + OF \rightarrow O_2 + F_2 \qquad (7)$$

The pyrolysis of OF_2 in quartz, glass, and magnesium vessels was studied by Koblitz and Schumacher[47,48] at 250°, 260° and 270°C, and an activation energy of 40.6 $\pm$ 3 Kcal/mole was deduced for the decomposition process. The kinetic data and quantum yield calculated for these experiments indicated the formation of OF as an intermediate, but there was no direct detection of the radical.

A very recent mass spectrometric study of the thermal decomposition of OF_2 was performed by Dauerman, Salser, and Tajima.[49] The pyrolysis was studied under flow conditions in a nickel furnace in the presence of excess helium and at temperatures in the 600°-800°C range. No evidence

for the presence of OF was obtained. Instead, the only products reported were O atoms, O_2, F atoms, and F_2. A critical energy, presumably D(F-OF), for the decomposition was calculated to be 40.5 $\pm$ 4 Kcal/mole. A major shortcoming of these experiments was that the exit of the furnace was approximately 1.9 cm from the ionizing electron beam. The possible consequences of such an arrangement will be discussed in Chapter III where the results of the mass spectrometric studies of the pyrolysis of OF_2 and O_2F_2, which were studied as part of this thesis research, will be discussed.

Kinetic data for numerous reactions have indicated the existence of the OF radical as an intermediate. For instance, the primary decomposition process for the thermal decomposition of fluorine nitrate, NO_3F, has been proposed[50] to be

$$NO_3F \rightarrow NO_2 + OF \tag{8}$$

followed by

$$NO_2 + NO_3F \rightarrow NO_2F + NO_3 \tag{9}$$

and

$$NO_3 + OF \rightarrow NO_2F + O_2 \tag{10}$$

the final decomposition products being NO_2F and O_2. The rate determining step for the overall reaction of OF_2 and NO_2 has been concluded[51] to be

$$NO_2 + OF_2 \rightarrow NO_2F + OF \tag{11}$$

It has also been proposed that the photochemical reaction between fluorine atoms and ozone,[52] as well as the thermal reaction of OF_2 and tetrafluorohydrazine, N_2F_4,[53] occur with the formation of the OF radical as an intermediate. One of the most convincing pieces of evidence for the existence of OF was obtained from the photochemical reaction of OF_2 with sulfur trioxide,

$$OF_2 + SO_3 \xrightarrow[365\ m\mu]{h\nu} F - \overset{\overset{O}{\|}}{\underset{\underset{O}{\|}}{S}} - OOF \qquad (12)$$

It has been argued[54,55] that this reaction must proceed by way of the OF free radical.

The first direct evidence for the existence of OF was obtained by Arkell, Reinhard, and Larson[56] using matrix isolation and infrared spectroscopy. In their experiments OF_2 was photolyzed in a nitrogen or argon matrix at 4°K. Infrared absorptions of 1028.5 cm^{-1} in argon and 1025.5 and 1030.5 cm^{-1} in N_2 were proposed to correspond to the fundamental frequencies of the OF radical. The appearance of the OF radical as a doublet in N_2 and a single absorption in argon was discussed in terms of the most probable causes of multiplets--aggregation, rotation, and multiple sites. It was estimated that a trapped radical concentration of about 0.6 per cent of the total material in the matrix was obtained. Upon warming of the matrix to 40°-45°K (depending on whether N_2 or A was the matrix), the bands attributed to OF disappeared. It was reported that in some of the experiments the OF_2 absorption increased upon disappearance of these bands, while in others formation of only small amounts of O_2F_2 were observed upon warming.

One of the most interesting points discussed by Arkell, et al.,[56] concerned the position of the OF radical absorption with respect to the other known OF stretching fundamentals. The absorption of 1028 cm^{-1} that was attributed to the OF radical in an argon matrix is the highest O-F stretching frequency of all O-F containing compounds, including OF_2. They stated that this would correspond to a bond energy higher than the average bond energy in OF_2 and that it may be as high as several previously estimated values of 45-56 Kcal/mole from pyrolysis studies[47,49] and from theoretical correlations.[57,58] However, it should be pointed out that this does not agree with a value of 25 Kcal/mole for the bond energy obtained by Dibeler, et al.,[6] from electron inpact studies of OF_2, which will be shown to be in excellent agreement with electron impact data on O_2F_2 obtained as part of this thesis research. In addition, it will be shown that the high value for D(O-F) is not consistent with microwave, thermochemical, or kinetic data on O_2F_2.

The ionization potential of 13.0 $\pm$ 0.2 ev for the OF radical was obtained indirectly from electron impact studies[6] on OF_2. This value is somewhat higher than the value of 12.2 ev estimated by Price, Passmore, and Roessler[58] by interpolation from isoelectronic similarity curves of radicals and ions. Obviously, a direct measurement of the ionization potential of the OF radical is highly desirable in that it would permit the calculation of the OF bond energy which has been the subject of much discussion and controversy.

Very recent epr work by Neumayr and Vanderkooi[37] has shown that uv irradiation of both pure liquid OF_2 at 77°K and OF_2 in a $CFCl_3$ matrix give the same resolved isotropic doublet due to a paramagnetic species.

This species was relatively unstable at 89°K, undergoing a 70 per cent decomposition in 19 minutes in the $CFCl_3$ matrix. They stated that observations of the stability, concentration, and temperature effects observed with pure liquid OF_2 and with OF_2 in a matrix indicated that the epr spectrum could arise from either the OF radical or from a fairly unstable paramagnetic molecule. They also reported that gas phase epr studies of OF_2 gave evidence for the existence of the OF radical, but that the evidence was not very conclusive.

The failure to detect the OF radical as a free species in the vapor phase, despite numerous attempts to do so, is obviously due to its instability and/or extreme chemical reactivity. The low dissociation energy for OF of 25 Kcal/mole reported by Dibeler, et al.[6] and supported by new data given in this thesis would indicate that the species might well be relatively unstable. However, as discussed above, this low bond energy does not agree with estimates made from either theoretical arguments,[57,58] pyrolysis studies,[47,49] or infrared studies.[56]

Green and Linnett[59] have discussed the relative chemical stabilities of OF and NO from a theoretical viewpoint. Since NO is observed at room temperature, even though it is thermodynamically unstable, and OF has not been detected, they suggested that a reaction path is open to OF over which NO cannot pass. They proposed a four-center mechanism (see Appendix A) by which 2OF could readily form $O_2 + F_2$ and showed that a similar mechanism for the reaction of NO to $N_2 + O_2$ was not likely. Linnett[17] has also shown that 2OF would be unstable relative to $O_2 + F_2$ using the arguments of the double quartet model.

The fact that HO_2, which is isoelectronic with OF, has been

identified, has also been discussed by Green and Linnett.[59] They stated that HO_2 is fairly readily "reflected" by glass surfaces while fluorine compounds such as F_2 and HF attack glass. A similar behavior of OF would make it much more difficult to detect than HO_2 using glassware, for it would be destroyed at the wall of the reaction vessel. The effect of various reactor materials (quartz, numerous metals, and alumina) on the decomposition of OF_2 were investigated in this thesis.

It is obvious from the above discussions that the existence and properties of the OF radical have been the subject of much investigation and controversy since the initial claim of its preparation by Ruff and Menzel[7] in 1933. The failure of previous investigators to detect this species in the vapor phase, despite the abundant indirect evidence for its existence, generated a keen interest in it as a species for further study for this thesis. Numerous attempts to synthesize and detect this radical in the vapor phase by the pyrolysis of OF_2 and by subjecting OF_2 to a radio frequency discharge are discussed in Chapter III. In these studies the exit of the reactor was inserted directly into the ionizing electron beam of the mass spectrometer. It seems that this is the very best arrangement possible for detection of a species by mass spectrometry, but this optimum arrangement has not been obtained in previous similar investigations of the oxygen fluorides. The desirability of this "optimum" arrangement was predicted analytically and demonstrated experimentally in this work and will be discussed in some detail.

O_2F Radical

In contrast to the OF radical, the existence of the O_2F radical had not been proposed prior to the initiation of this present work.

However, this radical has been the object of considerable study in a number of different laboratories during the past year. With the increased interest in the possible existence of oxygen fluorine radicals and the failure to detect the OF radical, several investigators have attempted to detect the O_2F radical.

Prior to the initiation of the present experimental work, the possible existence of the O_2F free radical as a stable entity was examined from a theoretical point of view using the double quartet approach of Linnett. After a careful examination of all possible electronic configurations for the O_2F radical (see Appendix A) it was concluded that the following two configurations would probably be the major contributors to its overall structure.

(F) and (G)

On the basis of the qualitative theoretical analysis of this O_2F radical, it was proposed[19] that it could very well be a stable species and might be prepared at unusual conditions such as at very low temperatures. This was accomplished in this work and will be discussed in detail in Chapter III, and has also been accomplished by several other investigators in the past few months.

Comparison of the electronic structures, F and G, of the O_2F radical with those of O_2F_2, A and B, presented earlier, indicates that the structural parameters of the radical would be essentially the same as that of the O_2F moiety in O_2F_2. It is obvious that the electronic

configurations of the radical are essentially identical to the configurations of O_2F_2 with one of the fluorine atoms removed. From these electronic structures of O_2F, it would be concluded that the O-O bond would be essentially double bond in character while the O-F bond would be very weak as was the case in the O_2F_2 molecule. It is interesting to note at this point that the bond energies for this species were measured in this work and were in excellent agreement with these qualitative predictions.

The first observation of the O_2F radical was reported by Kirshenbaum, et al.[35] (cf. Kasai and Kirshenbaum)[36] from electron paramagnetic resonance studies of O_2F_2 and O_3F_2 which were discussed in detail earlier in this chapter. From those studies they have also suggested that the main electronic features of O_2F_2 proposed by Jackson[2] from his microwave studies are still maintained in O_2F, and they have proposed a molecular orbital description of the species. They assumed that one of the antibonding π-orbitals of the O_2 molecule, say πy^*2p, forms a bond with the 2py-orbital of the fluorine, and the electron in the other orbital, πz^*2p, stays unperturbed and gives rise to the paramagnetism.

Further evidence for the existence of O_2F was obtained very recently by Arkell[25] using matrix isolation and infrared spectroscopy. He reported that the O_2F radical has been produced during the photolysis of O_2-OF_2 mixtures or O_2-F_2 mixtures in O_2, N_2, or A matrices at 4°K. The radical in argon had infrared absorptions at 584 and 1494 cm^{-1} which disappeared during thermal cycling of the matrix to the diffusion temperature of 40°-45°K. From the calculated O-O and O-F stretching force constants, he concluded that the O-O bond is essentially double bond in character and the O-F bond is very weak. On the basis of these results

he proposed that the ionic form, $F^- O{=}{=}O^+$, is a major contributor to the structure of O_2F. When the system O_2:F_2:A was used, the products of diffusion were reported to be O_2F_2 and O_4F_2 which were formed by combination of O_2F with atomic fluorine and by dimerization of O_2F, respectively. The possibility that the O_2F_2 was formed by dimerization of OF was ruled out since no OF radical was observed in any of these studies.

Levy and Copeland[60] have proposed the existence of the O_2F radical as an intermediate in the oxygen-inhibited, thermal, gaseous reaction of hydrogen and fluorine. They discussed the kinetics of this reaction in terms of a chain reaction involving the O_2F radical and propagation steps;

$$H + F_2 \rightarrow HF + F \qquad (13)$$

$$F + O_2 + M \rightarrow FOO + M \qquad (14)$$

and

$$FOO + H_2 \rightarrow HF + O_2 + H \qquad (15)$$

In addition, they estimated the heat of formation of O_2F to be 3.5 Kcal/mole using kinetic data[44,61] on the thermal decomposition of O_2F_2. This value of the heat of formation leads to an O-F bond energy in O_2F of 15 Kcal/mole or 0.7 ev. It will be shown that this is in excellent agreement with the value obtained in this thesis research.

The work of Levy and Copeland[60] presents the only reported evidence for the existence of O_2F in the vapor phase, but it is only indirect evidence. The synthesis, direct detection, and mass spectrometric investigation of this free radical in the vapor phase was accomplished during

this thesis research and will be discussed in detail in Chapter III. These studies permitted the development of the energetics of the O_2F radical (i.e., ionization potential and bond energies) which were of particular interest in view of the species' unusual structure as indicated by the infrared studies.

The experimental technique used in this work to synthesize the O_2F radical is considered rather unique and interesting in that it involves the "pyrolysis" of an unstable species, O_2F_2, at a temperature of only 250°K. It is also interesting to note that the location of the exhaust port of the furnace directly in the electron beam was shown experimentally to be of paramount importance as was predicted analytically. The results of the investigation of this radical were particularly satisfying in that they represented the synthesis, detection, and investigation of a species that had been predicted to possibly be stable by rather simple theoretical arguments.

O_3F and O_4F Radicals

The O_3F and O_4F radicals have received very little attention up until the present time. The only reported identification of these species is by Arkell,[25] who stated that they were detected during the photolysis of F_2 in an O_2 matrix at 4°K. He reported that two absorptions at about 1503 and 1512 cm^{-1} appeared as partially resolved side bands on the 1496 cm^{-1} (O-O bond in O_2F) absorption, and he assigned them to the O_3F and O_4F radicals, respectively. He proposed that the formation of the O_4F radical occurred by either of the two reactions

$$F + O_2 \rightarrow O_2F \overset{O_2}{\rightarrow} O_4F \qquad (16)$$

or

$$F + O_4 \rightarrow O_4F \qquad (17)$$

The second case had to be considered as a possibility because he observed O_4 in the matrix. He further proposed that the O_3F radical was formed during the photolysis by

$$O_4F \xrightarrow{h\nu} O_3F + O \qquad (18)$$

The discussions of this chapter have made it clear that the low temperature oxygen fluorides and oxygen-fluorine free radicals are presently the object of a very large amount of interest and study. Many investigators are studying these species and as a result much information concerning their systhesis, structure, energetics, and chemical behavior is being published. These species represent a family of compounds exhibiting very unusual and interesting properties, from both a theoretical point of view as well as from the view of their future usefulness. Though they are definitely not well understood at the present time, it does seem that the mass spectrometric studies performed as a part of this thesis research, along with the electron paramagnetic resonance, infrared, and microwave studies conducted by other investigators, have definitely helped explain many of their unusual properties and behavior.

CHAPTER II

APPARATUS AND EXPERIMENTAL TECHNIQUES

Introduction

The major piece of equipment used in this work was a Bendix Time-of-Flight Mass Spectrometer, Model 12-107, coupled to a cryogenic chemical system. A rather detailed description of the mass spectrometer and special adaptations for energy measurements are given in an earlier thesis from this laboratory by Martin.[3] In addition, a fairly complete discussion of the theory and experimental methods for determining the energetics of molecules and free radicals by mass spectrometric techniques are presented in Martin's thesis. Hence, a discussion of these aspects of the experimental equipment and techniques will be omitted here.

A very brief description of the early development of a thermal gradient, cryogenic reactor and inlet system for the mass spectrometer was given by Martin.[3] The continued development and a quite complete discussion of the design considerations, mechanical description, and operation of a combination reactor and inlet system, encompassing the basic features of the system discussed by Martin, is presented in this chapter of this thesis. Special adaptations of this cryogenic system for various techniques for the synthesis of the oxygen fluorides will be presented. More detailed discussions of the design considerations and calculations will be given in Appendix B.

Cryogenic Reactor and Inlet System

Before chemistry at very low temperatures will progress very far, the common operations of bench scale experimentation must be translated to the point of convenient utilization at cryogenic temperatures, and perhaps the most fundamental operation of all is that of chemical analysis. The analytical facility described here was designed for the study of the synthesis, stability, reactivity, and energetics of that interesting class of compounds which usually must be synthesized and maintained below some rather low temperature if the compound is to exist as a stable entity or chemical reagent. Examples of such compounds that are either known or pseudo-known are O_2F_2, O_3F_2, H_2O_3, H_2O_4, BH_3, HNO, NO_3, N_2H_2, NH_4O_3, etc. Manipulations with these species must be conducted at temperatures below the onset of that loss process having the lowest activation energy, and this may be 100°K or lower.

The only earlier mass spectrometer adaptation that seems reasonably related to the present arrangement was described by Blanchard and LeGoff.[62] In their apparatus, the walls of the ionization chamber were cooled with liquid nitrogen, whereas in the present arrangement, a refrigerated delivery system injects the sample directly into the ionizing electron beam. In the earlier apparatus, a molecular beam from a nearby furnace could be directed onto the inner walls of the cooled ionization chamber. In experiments with a beam containing I_2 molecules and I atoms, and with the chamber temperature low enough to condense both species, no evidence was found for the presence of free I atoms upon slow warmup. Either the atoms failed to survive the quench or they recombined at temperatures below that at which they exerted a detectable vapor pressure.

General Design Considerations

Both the synthesis reactions and the subsequent studies of the reactivity and energetics of the species of interest must be conducted in cryogenically cooled systems. Experience has shown that simple transfer operations such as pipetting, liquid flow, or vaporization and recondensation become somewhat difficult operations when the working substance is thermally unstable at cryogenic temperatures. Also the pruification techniques that might be applicable to such systems are complicated by the temperature requirement, and hence each will require development prior to its use. Therefore, it was desirable to combine into one device, insofar as it was possible, the features of a versatile chemical reactor, some capability for separative operations, and chemical analysis by mass spectrometric means.

Almost without exception, reactions which proceed at cryogenic temperatures involve at least one reactant which is a free radical and which is usually generated by electric discharge, pyrolysis, photolysis, or by chemical reaction (such as a low pressure flame). So the experimental arrangement should also be versatile enough to reasonably accommodate these several free radical generation operations.

Simple or equilibrium distillation that is frequently used at more ordinary temperatures may be adapted for use with these unstable systems provided the vapor conduit between the boiler and the condenser is maintained at a temperature no greater than that of the boiler. Also, if a thermal gradient can be maintained along this flow channel, the constituents of the vapor will, to a degree, condense separately in bands depending upon their respective vapor pressures. The occurrence of this

latter phenomenon in cold traps is familiar to investigators having experience with vacuum rack manipulations of condensable gases. These notions, which were employed in the present device, were first used in a related situation by Sir James Dewar[63] in 1910 in the first successful quenching of a highly reactive species from an electric glow discharge. He found that solid CS would violently explode upon warming above liquid air temperature only if it was first separated from the undissociated CS_2 that had survived the discharge.

The mass spectrometer was selected as the primary analytical device for these investigations because, unlike electron spin resonance or infrared, which have both been widely and successfully used in related experiments, the mass spectrometer detects all species. It also affords a direct observation of the species of interest and the output data require a minimum of equivocal interpretation. An identification may be obtained in the present system provided only that a species exert a vapor pressure of about 3×10^{-6} torr and that the vapor will, upon electron impact, give a sufficient intensity and variety of either positive or negative ions. Both positive and negative ions are detectable in the Bendix time-of-flight (TOF) mass spectrometer provided only that the ion has a lifetime of the order of 50 microseconds. The identification is also aided by the use of an ionizing electron beam of controlled energy, and by the control of the temperature of the inlet system which takes advantage of the relative volatility and hence the separability of the several components that may be present from a particular experiment. The open structure of the source of the Bendix spectrometer, which makes it possible to assemble complex hardware adjacent to and even within the

source itself, was the deciding factor in the selection of that machine. A recent review summarizes many other adaptations of the TOF instrument in situations where this open source structure has been advantageous.[64] The disadvantages of the TOF instrument stem from the low duty cycle of 0.005 which results from a control pulse of 0.25 microseconds at a frequency of 20 Kc.

Maximum detectability corresponds to the observation of usable spectra at the lowest sample pressures, hence at the lowest temperatures of the condensed samples that are of interest here, and therefore in the region of greatest thermal and chemical stability of these rather labile compounds. It is possible to calculate[65] the intensity of molecules effusing into a vacuum from a circular inlet port of area πr^2 which has some particular ratio of length to radius, L/r. The molecular intensity, N_θ, at any solid angle, $d\omega$, located at some angle, θ, with respect to the center line of the port, may be developed in the form of the usual cosine distribution function multiplied by a deviation factor, J, which is a complicated function of L/r and θ,

$$N_\theta = [(N_t/\pi)(\cos\theta)(d\omega/dA)]J \qquad (1)$$

From the variation of J with L/r and θ, it is evident that both the intensity at any angle and the total flow will be a maximum for a sharp edge orifice for which case J has its maximum value of unity. N_t is the rate at which molecules enter the sample inlet channel and is given by the product of the molecular number density in the sample reservoir, the average molecular speed, and the inlet area, i.e., by $PA/(2\pi mkT)^{1/2}$. We are concerned, of course, with the ionization of molecules which have

suffered no collisions since leaving the inlet port. The sensitivity, S, is directly proportional to the number of these molecules that are ionized per unit time which is given by the product of the electron flux, N_e, the molecular or the target number density, $D(x,y,z)$, and the ionization cross section, σ_i. The target density, $D(x,y,z)$, is given by Equation (1) above, but expressed in rectangular coordinates, divided by the mean molecular speed, $\bar{v}$. Although the electron flux is uniform, the target density is a function of position within the effective collision covolume and hence one must integrate over this covolume to determine the total sensitivity, S, that is,

$$S = K \int_{\text{Covol.}} \sigma_i N_e D(x,y,z) dV \qquad (2)$$

where K is a proportionality constant. It is then possible to examine analytically the relative merits of various configurations of the inlet port relative to the rectangularly collimated electron beam of the TOF mass spectrometer. Since the probability that a given molecule will be ionized during its single pass through the electron beam is very small, it can be assumed that the number density of targets is undiminished as a result of ionization and is therefore correctly given by $D(x,y,z)$. Equation (2) can then be integrated to give,

$$\begin{aligned} S = \{4N_t N_e \sigma_i K/\pi\bar{v}\}\{ & a \ln[\Upsilon_2(b+\beta_1)/\Upsilon_1(b+\beta_2)] \\ & + b \ln[(\alpha_2+\beta_2-a)(\alpha_1+\beta_1+a)/(\alpha_2+\beta_2+a)(\alpha_1+\beta_1-a)] \\ & + c_2 \tan^{-1}(a/c_2) - 2c_2 \tan^{-1}[ac_2/(\alpha_2+b)(\alpha_2+\beta_2)] \\ & + 2c_1 \tan^{-1}[ac_1/(\alpha_1+b)(\alpha_1+\beta_1)] - c_1 \tan^{-1}(a/c_1)\} \end{aligned} \qquad (3)$$

where, $\alpha = (b^2 + c^2)^{1/2}$; $\beta = (a^2 + \alpha^2)^{1/2}$; $\gamma = (a^2 + c^2)^{1/2}$; and where the factor, J, has been taken to be constant and equal to its maximum value of unity, that is, Equation (3) is applicable to a sharp edge orifice. The geometry of the inlet port and beam configuration is specified by 2a and 2b which are the cross sectional dimensions of the beam as viewed from the port, and by c_1 and c_2 which are the perpendicular distances from the port to the near and far faces of the beam, respectively.

The relative merits of the various inlet channels having finite lengths may also be explored, but the integration of Equation (2) is now much more complicated. Omitting the concern for integrating over a collision covolume, the fraction of molecules entering an inlet channel of finite length which finally emerge within an angle θ with respect to the axis of the channel has been computed recently and tabulated for a wide variety of values of the parameters L/r and θ.[66]

Two alternative configurations of the inlet port relative to the electron beam of cross section 0.076 x 0.50 cm and effective length of 0.64 cm are possible with the Bendix instrument. The axis of the inlet port may be perpendicular to the ion flight path, or the drift tube, and facing the 0.076 x 0.64 cm side of the electron beam. Or the inlet port may be coaxial with the ion flight path and facing the 0.50 x 0.64 cm side of the electron beam. An indication of the calculated behavior of the two configurations for several values of the distance between the inlet port and the near face of the electron beam, c_1, is summarized in Table I and given in detail in Appendix B. Evidently both the perpendicular and the coaxial configurations provide about the same sensitivity at equal displacements from the near face of the electron beam. The paramount

Table 1. Variation of Sensitivity with Relative Configuration of Electron Beam and Inlet Port

Configuration	Geometrical Parameters (cm)				$\bar{v} F^*$ (from Eq. (3))
	a	b	c_1	c_2	
Perpendicular Arrangement	0.038	0.32	0.0	0.5	0.156
	0.038	0.32	0.2	0.7	0.0387
	0.038	0.32	0.8	1.3	0.0070
	0.038	0.32	1.4	1.9	0.0028
	0.038	0.32	2.0	2.5	0.0015
Coaxial Arrangement	0.250	0.32	0.0	0.076	0.134
	0.250	0.32	0.2	0.276	0.0594
	0.250	0.32	0.8	0.876	0.0087
	0.250	0.32	1.4	1.476	0.0036
	0.250	0.32	2.0	2.076	0.0018

*F is the fraction of molecules entering the inlet channel per unit time that appear in the collision covolume and is equivalent to $S/\sigma_i N_t N_e K$. Maximum detectability with respect to the relative configuration of the electron beam and the inlet port corresponds to a maximum value of F.

importance of minimizing the distance between the inlet port and the electron beam is clear, for if the inlet port is only 2 mm away from the beam, the sensitivity is down by about a factor of four for the perpendicular case. This behavior as well as the other trends that may be inferred from Table I have been experimentally verified. Equation (3) is equally applicable to any sort of a collision free inlet arrangement in which the above model is reasonable. A similar analytical study of the much greater sensitivity obtainable with a slit shaped inlet port may also be developed.

Largely as a consequence of the realizable mechanical conveniences, the perpendicular arrangement was selected for these investigations.

This system is, in some sense, rather similar to a heated filament inlet system for use with the Bendix instrument that was developed by Biemann[67] and in which thermally sensitive organic substances contained in a tiny capsule may be positioned inside the source adjacent to the ionizing electron beam of the instrument. Heating the capsule produces vaporization directly into the electron beam, and hence there are few collisions and therefore little reaction or degradation before ionization.

Mechanical Description

A schematic of the apparatus appears in Fig. 2 where the reactor-inlet system itself is shown in heavy black while its associated components are shown either in outline or in cross-hatching. The reactor inlet system is suspended from a single header (23) and consists essentially of two independently thermostated chambers (22), (17) that are centered within a polished stainless steel sleeve (21) which can move laterally through a double O-ring gland (5) into a vacuum lock arrangement (6). A 13.3 cm high vacuum gate valve (9) (Consolidated Vacuum

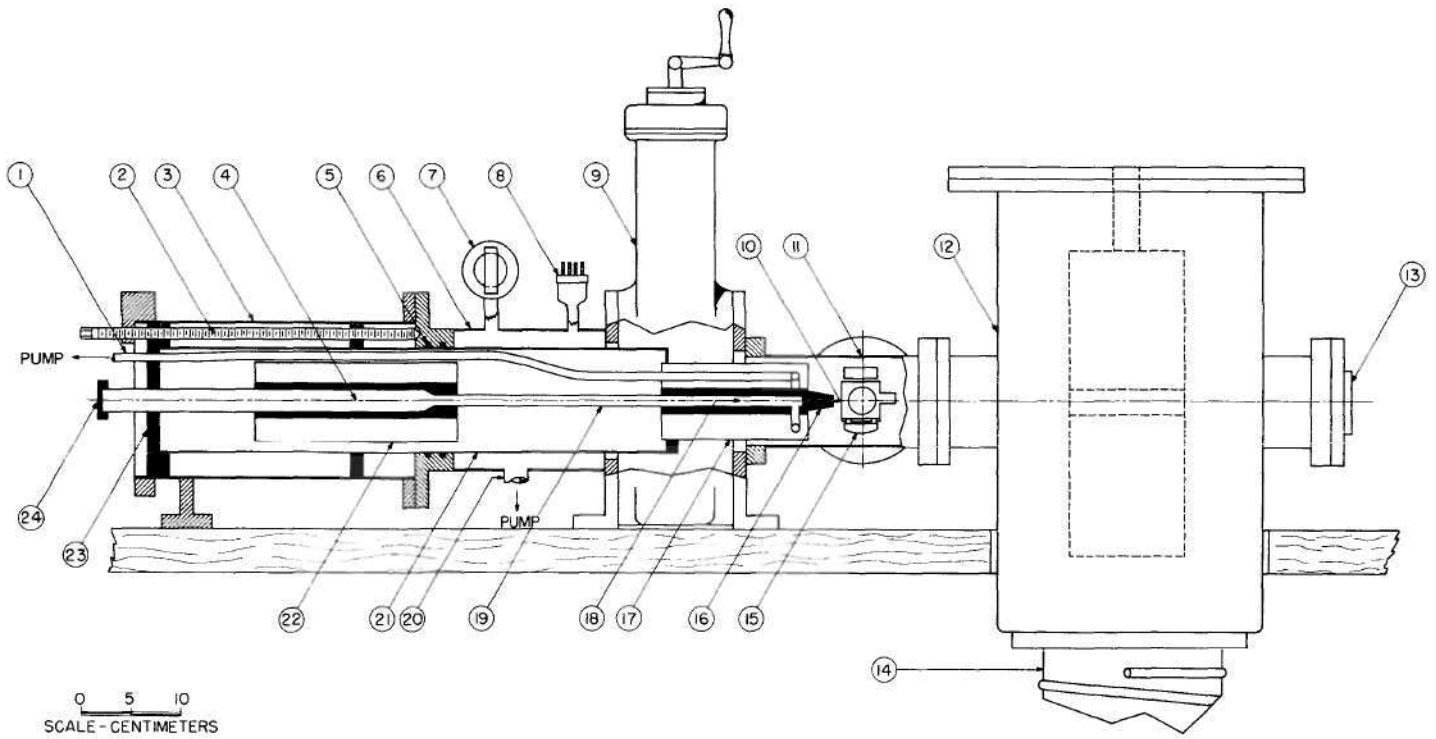

Figure 2. Schematic of Multi-Purpose Cryogenic Reactor and Mass Spectrometer Inlet System.

Corporation Model VCS-41A) separates the vacuum lock from the separately pumped source and drift tube of the spectrometer. This design is for convenience and permits the reactor-inlet arrangement to be withdrawn for adjustments or modifications without the necessity of breaking vacuum in the mass spectrometer system itself. The sample spaces within the two refrigerant chambers (4), (18) are connected by a 20 cm long x 0.25 cm wall tube (19), and together they form a coaxial tubular reactor and condensation space. Both chambers and the connecting tube are made of copper for rapid thermal equilibration and are nickel plated on the outside to reduce the emissivity and hence the refrigerant use rate. The entire reactor and condensation tube in which the low temperature species are prepared and manipulated was lined, for chemical inertness, with monel tubing which was sweated in place. At the expense of somewhat poorer heat transfer between the sample and the refrigerant, a snug fitting pyrex liner can be inserted into the reactor-condensation tube which effectively allows the sample to be manipulated within an all glass system. Thermostating of each chamber is accomplished by offsetting the natural inward heat leak with a controlled influx of refrigerant which is adjusted to be slightly in excess of that required to just balance the natural heat leak. Fine control is then maintained automatically by two recorder-controllers (Leeds and Northrup Company, Adjustable Zero-Adjustable Range-Speedomax H) which control the power dissipated in 100 ohm constantan heaters wound on the inside of each chamber. Electrical trimming of the heat balance can be much more precisely controlled than is possible with flow control of the liquid refrigerant. Proportional control of these heaters was not required since simple two-position operation

resulted in oscillations about the control point which increased to a maximum of only ±0.5°K when the apparatus was cooled to near 77°K.

The refrigerant delivery system to the two thermostated chambers (17), (22) is illustrated in Fig. 3. The flow of liquid N_2 from the coolant container into the two chambers is achieved by applying a gaseous N_2 overpressure of 5-15 psig in the vapor space over the liquid. Close control and monitoring of the influx of refrigerant is accomplished by adjustment of the two micrometer valves until the desired flow rate is attained as indicated by the two flowrators coupled to the refrigerant chamber exhaust lines. From the measured vented gas flow rate, one can immediately deduce the liquid refrigerant use rate.

The end of the condensation tube nearest the source is fitted with any one of several flat extension pieces (16) which are positioned to protrude into the ionization chamber of the spectrometer when an analysis is being performed; a channel in this extension piece conducts the sample from the condensation tube into the ion source (15). The inlet port itself (10) (0.089 cm dia.) may be positioned at any point relative to the electron beam including its being actually submerged in the beam, and hence ionization of the sample occurs prior to wall collisions. A sample molecule must be considered to be background after only one such wall collision. The inlet arrangement properly positioned in the source for analysis is shown schematically in Fig. 4. Design calculations which were confirmed subsequently by experimental measurements, show that the 0.4 x 1.6 cm cross section of the copper extension piece provides sufficient conductivity along its 2.5 cm length to insure that the sample is not heated significantly above the temperature of the inner refrigerant chamber

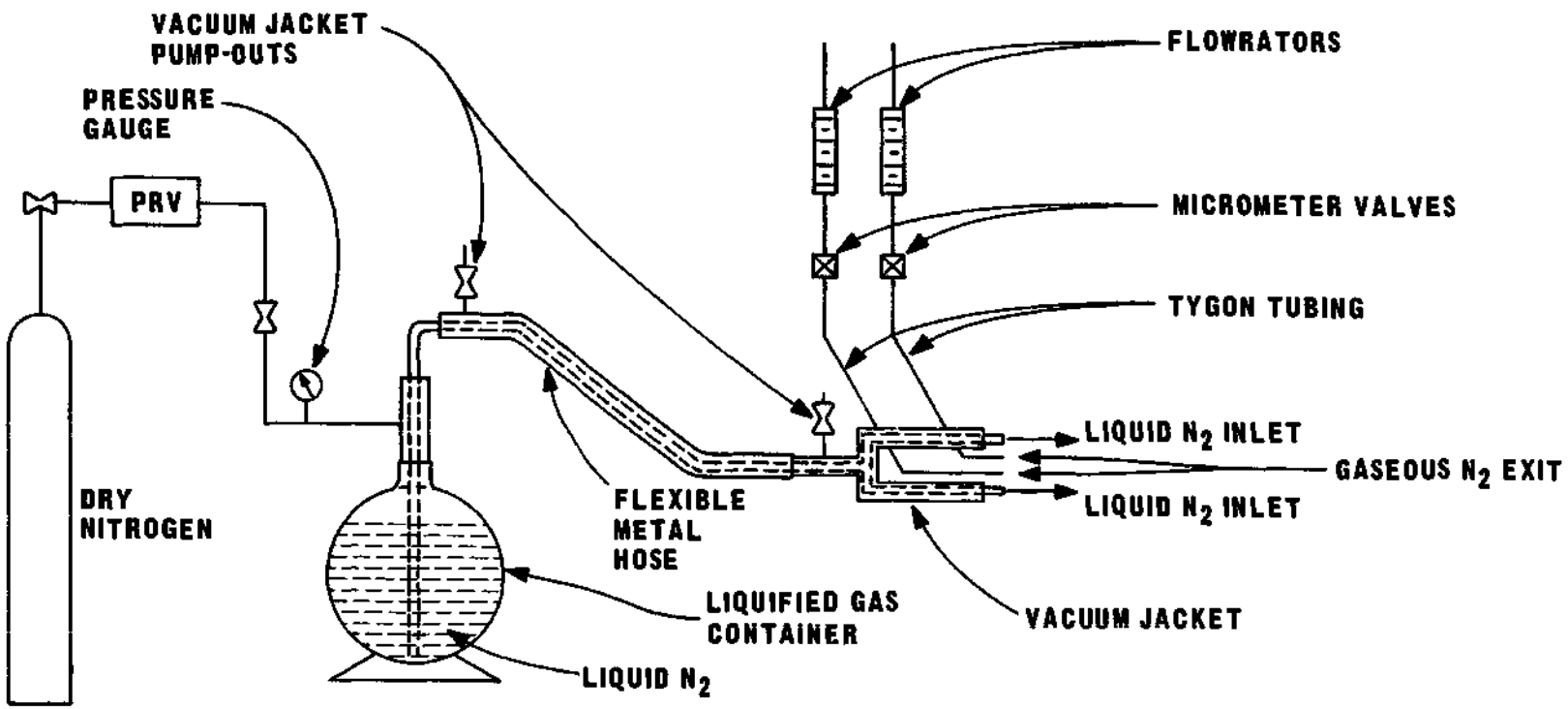

Figure 3. Schematic Diagram of Coolant Delivery System for the Cryogenic Reactor-Inlet System.

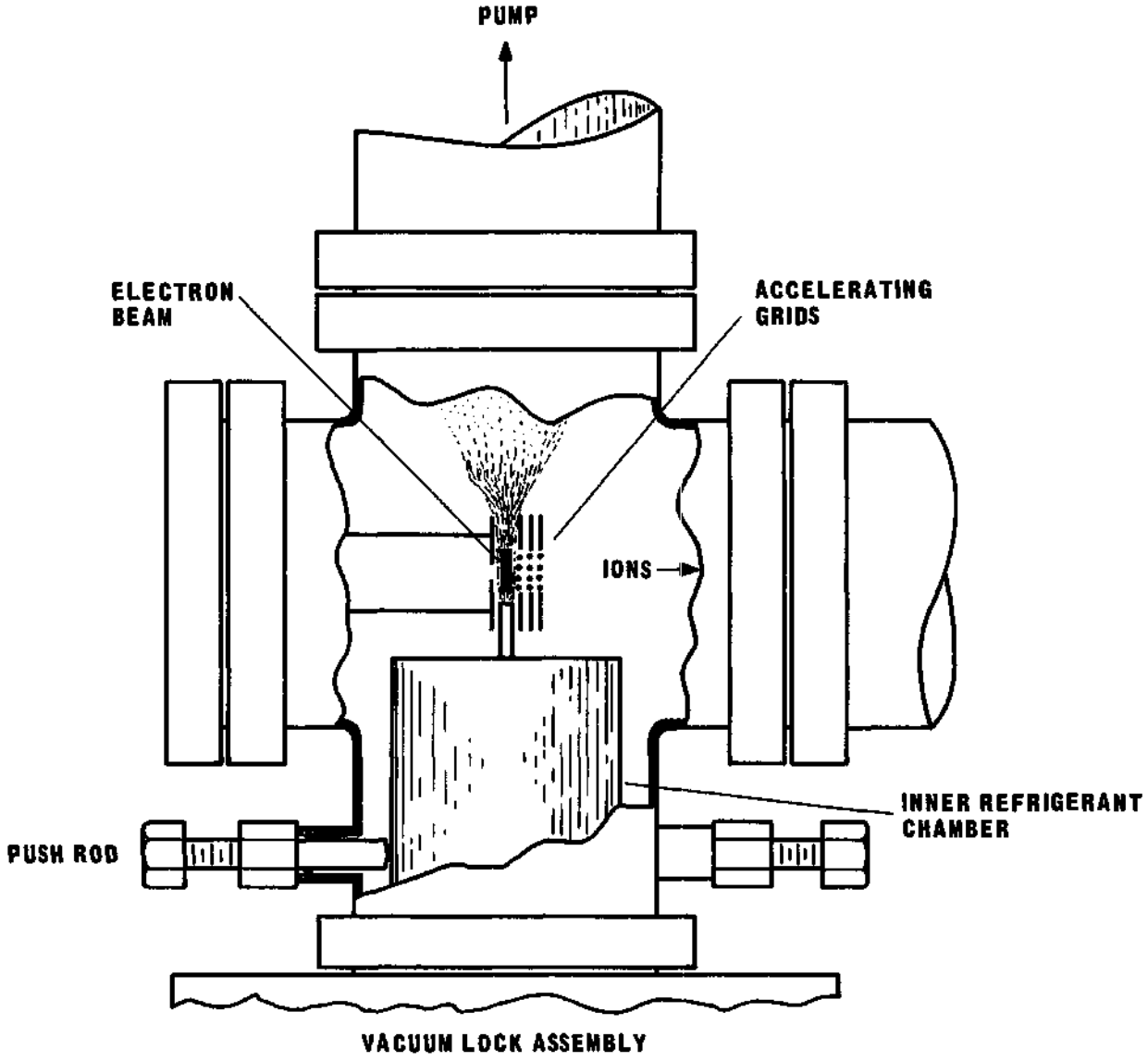

Figure 4. Top View of the "Cross" Vacuum Chamber Which Contains the Source Structure and Which is Depicted with the Cryogenic Inlet System in Analytical Position.

(17) when it passes through the inlet channel. The lateral positioning of the reactor inlet device is accomplished with a screw (2), and an observation port (13) is provided to visually follow the advance of the extension piece into the source structure. Sidewise positioning adjustments in the plane perpendicular to that of Fig. 1 are made during this advance by a pair of oppositely placed, vacuum sealed push rods which are mounted on the "cross" vacuum chamber (11). This rather delicate alignment situation is apparent in Fig. 4. When in analytical position, that is, as shown in Fig. 4, the sample gas from the condensation tube is injected directly into the ionizing electron beam, and a portion of it is ionized before collisions with surfaces at room temperature can occur. Fast pumping in the source region is provided by a nominal 750 l/sec system (14) (National Research Corporation Model HS 4-750).

This two chamber system with a temperature controlled interconnecting vapor conduit (19) may also be used for the physical separation of product mixtures from the reactor (4) by means of either simple distillation or by fractional condensation in a thermal gradient. However, for experiments in which this rough separation is undesirable or unnecessary, a single chamber device has been built which is completely glass lined for chemical inertness, and which is in essence merely the inner refrigerant chamber (17) alone. Either an extension piece similar to that described above or a gold foil leak may be used, but the foil leak cannot be advanced into the source and hence it can be no closer than 1.9 cm to the electron beam. The analysis summarized in Table I indicates that the foil leak results in a loss in sensitivity of nearly a factor of 100 over that obtained with the extension piece.

The 2.5 cm diameter reactor space (4) of the outer refrigerant chamber (22) was designed to accept a variety of synthesis operations. Glow discharges, furnace pyrolyses, and heated filament pyrolyses have been conducted in this reactor. In each instance a labile species from the high energy operation has been either quenched directly from the vapor, or it has entered into subsequent heterogeneous reactions on the cold walls of the reactor. Depending upon the experimental requirement, the reactor-condensation tube may be either pumped from the reactor header (24) or from the opposite end (1) which will thus cause a mass flow through the entire system.

Operation

Since a variety of different sorts of experiments were conducted in this apparatus, its operation is best described by considering specific cases. From these descriptions, it will be obvious that there are several possible permutations of the device.

In Situ Synthesis of the Oxygen Fluorides. In the initial stages of this research the low temperature oxygen fluorides were synthesized in a glass reactor in essentially the same manner as that described by Kirshenbaum and Grosse.[9] Using this technique it was demonstrated that 5-10 cm^3 of O_3F_2 could be made over a 5-7 hour period. However, this technique required that the samples be transferred from the reactor into the cryogenic inlet system for analysis. This transfer operation proved to be very difficult to accomplish without excess heating and contamination of the species. Hence, a rather unique method for preparing these compounds in situ in the inlet system was developed.

An electric discharge reactor was obtained by mounting a single

axially symmetric electrode and a reactant gas inlet (Fig. 5) on the reactor header (24). A pyrex tube encased the 0.32 cm diameter electrode from the header to a point some 7.5 cm inside the reactor space (4), which assured the glow was established only within the refrigerated volume. The reactant gas inlet line is extended beyond the header to exhaust directly into this discharge region. This system was used with a potential of 800-1500 volts (60 cycles) to establish a discharge in a mixture of oxygen and fluorine at 25-40 torr pressure in the annular space between the electrode and the grounded reactor walls cooled below 90°K. The unstable low temperature oxygen fluorides were thereby synthesized. Accumulation of an excess of either reactant in (4) during the synthesis operation was prevented by pumping out the lower end (1) of the reactor-condensation tube at a controlled rate. Since it was not necessary to monitor the reactor off-gases during the synthesis, the reactor-inlet assembly was allowed to rest with full atmospheric force of some 230 pounds pressing the end of the extension piece, which has a cross-section of about 0.151 cm^2 at the point of contact, against a teflon block. This acted as a valve to seal the reactor space from the low pressure in the vacuum lock (6) which was required for thermal insulation. Insulation pressures of 10^{-5} torr were readily maintained while operating with pressures of 30 torr in the reactor. About 4 liters of liquid nitrogen were required to cool and flood each chamber (17), (22). With the chambers flooded, metering of the vented nitrogen gas indicated boil off of 1.0 and 0.7 l/hr of liquid nitrogen, respectively, in the outer (22) and inner chambers (17) to offset the natural heat leak. When the annular electric discharge was on in the reactor space (4), the liquid nitrogen boil

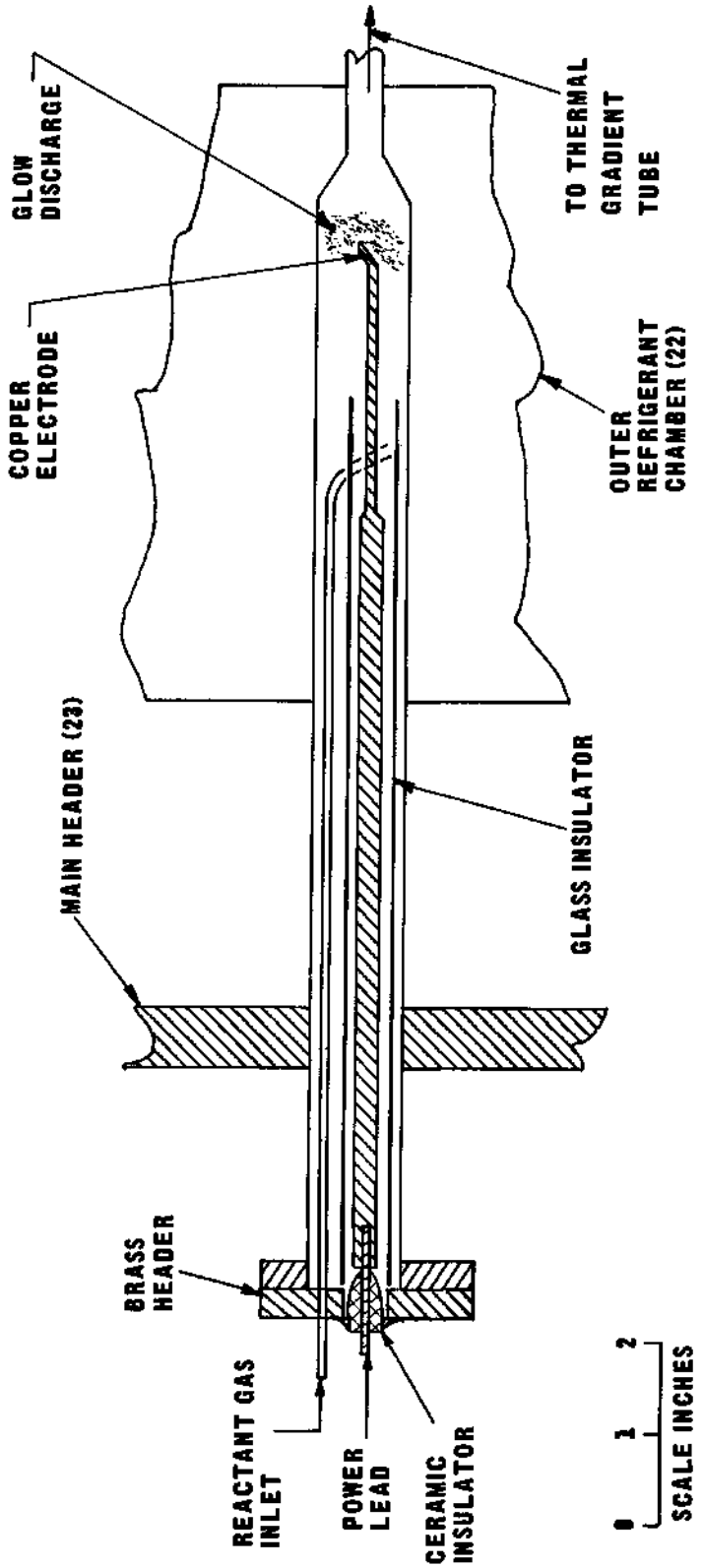

Figure 5. Schematic Diagram of the Gas Inlet and Single-Electrode Arrangement Used for the Synthesis of the Oxygen Fluorides In Situ in the Cryogenic Reactor-Inlet System.

off rate in the outer chamber was increased to 3.7 l/hr. A typical O_3F_2 synthesis run required 60 minutes during which 15 liters (NTP) of premixed oxygen and fluorine feed gas were pumped through the discharge. Upon completion, the discharge was turned off, and the reactor space was pumped to remove the excess feed gas. Care was required at this point since excessive pumping could remove product species which have high vapor pressures. From an operational point of view, one may assume that each species present will exert its full vapor pressure since the occurrence of solid solutions, partial miscibility, etc. can only reduce the vapor pressure. Using the lateral positioning screw (2), the system was then backed off of the teflon block valve against which the inlet port had been pressed, the large slide valve (9) was opened, and the system was advanced into the source. This forward advance was followed visually through the observation port (13) and was continued until the inlet port (10) at the end of the extension piece (16) was just touching the thin side of the rectangularly collimated 0.076 x 0.50 cm electron beam or until the spectrum intensity was maximized. Final positioning of the inlet port was accomplished by adjusting the horizontal pushrods until maximum sensitivity was obtained.

Upon attainment of the optimum position of the extension piece (16), the oxygen fluorides were distilled directly into the spectrometer by slowly raising the temperatures of the refrigerant chambers (17), (22). Since the ionizing electron beam was in grazing, tangential incidence with the sample inlet port (10), mass spectrometric analysis of the vapors was achieved without warmup above the temperature of (17). By adjusting the two refrigerant flow rates and the power dissipated in the heaters, the

temperature of the chambers are stabilized and automatically maintained at any value above the normal boiling point of the refrigerant. Both the voltage applied to the heaters and their per cent on-time are variables in the trimming of the heat load on the two refrigerant chambers. In general, a lower voltage and a correspondingly greater per cent on-time result in smaller temperature oscillations about the control point. Typical operating parameters with both chambers near 77°K show temperature fluctuations about the control point of ±0.5°K, heater voltage of 50, and per cent on-time of 40. The temperature fluctuations decrease with increasing temperature.

In some of the experiments it was desirable to have the cryogenic reactor space (4) and condensation tube (19) completely glass lined. This was accomplished with the single electrode arrangement by cutting a narrow slit in the side of the glass reactor-liner in such a position that a discharge could be established between the tip of the electrode and the reactor wall through the narrow opening. In these experiments the exit channel through the extension piece (16) was also glass lined. This proved to be a very satisfactory arrangement and permitted the investigation of the relative effects of metal and glass surfaces on the labile species studied in this work.

External Synthesis of the Oxygen Fluorides. In the course of the experimental investigation of the low temperature oxygen fluorides, it was decided that it was highly desirable to prepare the species externally in a device permitting visual observation of the product and in a manner duplicating that used by other investigators who have synthesized and studied O_2F_2 and O_3F_2. Earlier experiences with preparation of the

samples in a separate reactor, which required a very difficult transfer operation into the inlet system, proved to be disappointing as was mentioned earlier. Hence, a pyrex reactor similar to that used by Kirshenbaum and Grosse[9] was designed so that it could be attached directly to the mass spectrometer inlet system. This external reactor was mounted near the reactor header (24) of the low temperature inlet system so that a 43 cm long drain line could be used to conduct these externally generated compounds through the reactor header and into the center of the reactor space (4). Fig. 6 shows the reactor contained in a specially designed dewar that permits immersion of the drain line over its entire length in the same refrigerant (usually liquid oxygen, 90°K) as was used to cool the discharge tube reactor. In a typical O_3F_2 synthesis a voltage of 2000-2800 volts was used and a reactor pressure and temperature of 18-25 torr and 90°K, respectively, were maintained. This resulted in the formation of O_3F_2 as a red liquid on the walls of the glass reactor in just the manner described by other investigators. In experiments in which insufficient O_3F_2 was prepared to drain directly into the reactor space (4), the transfer was accomplished by permitting the liquid O_2 refrigerant to boil off slowly while simultaneously pumping continuously on the lower end (1) of the reactor condensation tube. This resulted in distillation of the sample into the cryogenic reactor-inlet system. The inlet system was in analytical position, as shown in Fig. 4, during this transfer operation to permit detection of any decomposition of the synthesis products. The investigation of the species as a function of temperature was conducted in the same manner as in the annular discharge experiments.

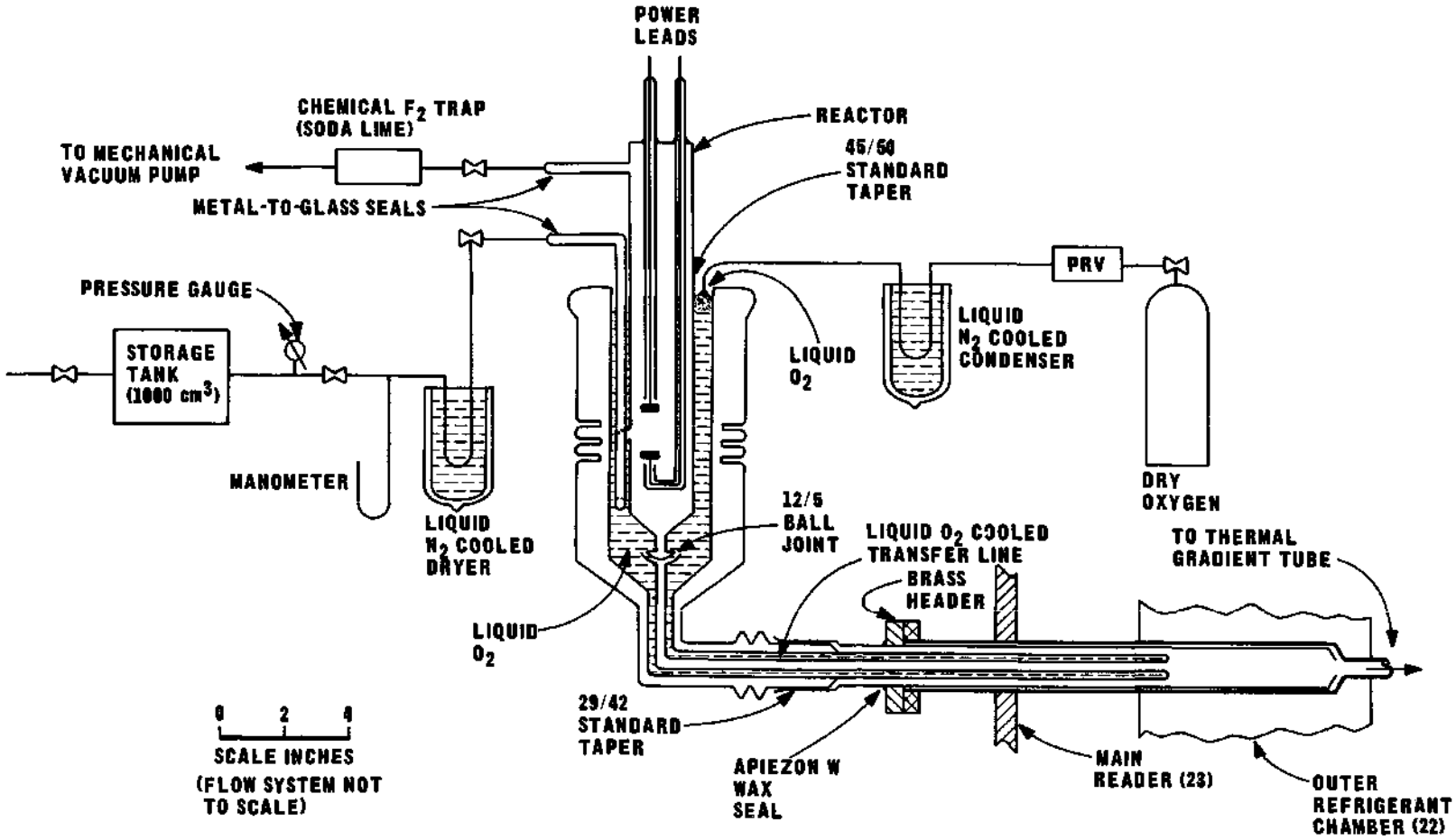

Figure 6. Schematic Diagram of the Cryogenic Reactor-Inlet System Attachment and its Associated Flow System for the External Synthesis of the Oxygen Fluorides.

The arrangement shown in Fig. 6 was used in experiments where the entire reactor-condensation tube and exit channel were glass lined. In other experiments in which these surfaces were not glass lined (monel walls), the glass reactor and dewar were connected to the reactor header (24) by a glass-to-metal seal rather than by the Apiezon W wax seal. Fig. 6 depicts the feed gas inlet arrangement for these experiments, which was the same for both the in situ and external generation of the oxygen fluorides.

The electrical networks used to produce the gaseous discharge for the oxygen fluoride syntheses are shown schematically in Fig. 7. A Jefferson luminous tube outdoor sign type transformer was used which was capable of producing a secondary voltage of 15,000 volts at currents up to 120 ma. A variable rheostat, R_1, (0-1645 ohms, 0.7 amps) was used to make the circuit ohmic. Since the secondary coil of the transformer was center-grounded, only one-half the secondary voltage was used in the annular discharge experiments as indicated by Fig. 7A. In those experiments a second variable rheostat, R_2, (0-213 ohms, 2.3 amps) was added. This permitted a very accurate determination of the discharge current (25-50 ma) by measuring a very small voltage drop (5-10 volts) across a well-known resistance (R_2 = 200 ohm). The discharge current for the external syntheses (25-75 ma) was determined by measuring the voltage drop (25-75 volts) across R_1 (1000 ohms).

Miscellaneous Inlet Systems

Furnace Attachment for the Cryogenic Inlet System

The copper extension piece (16) of the cryogenic reactor-inlet

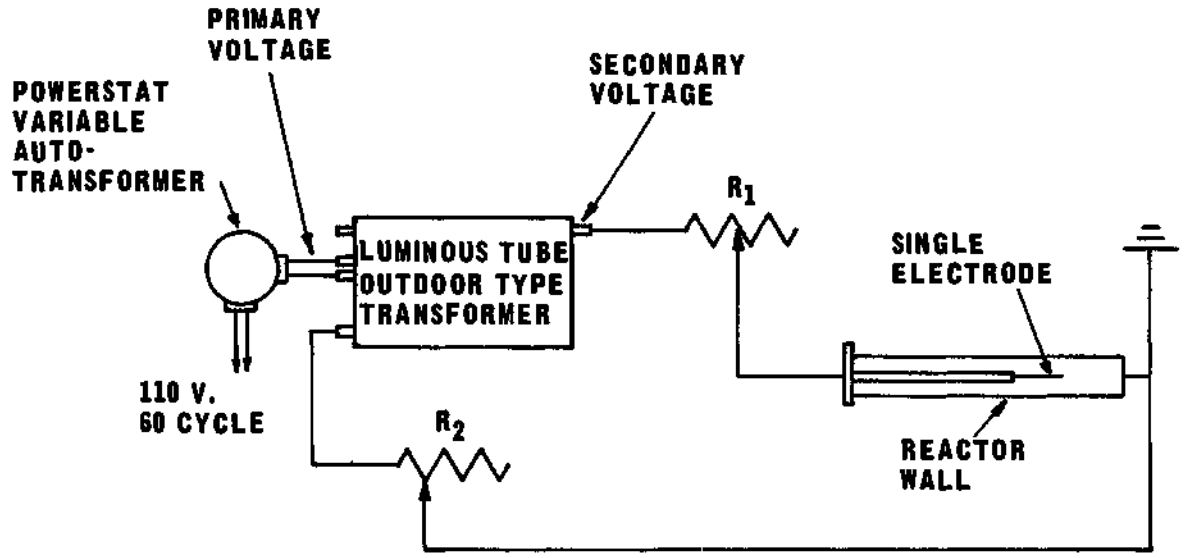

Figure 7a. Schematic Diagram of the Electrical Network for the <u>in situ</u> Synthesis of the Oxygen Fluorides.

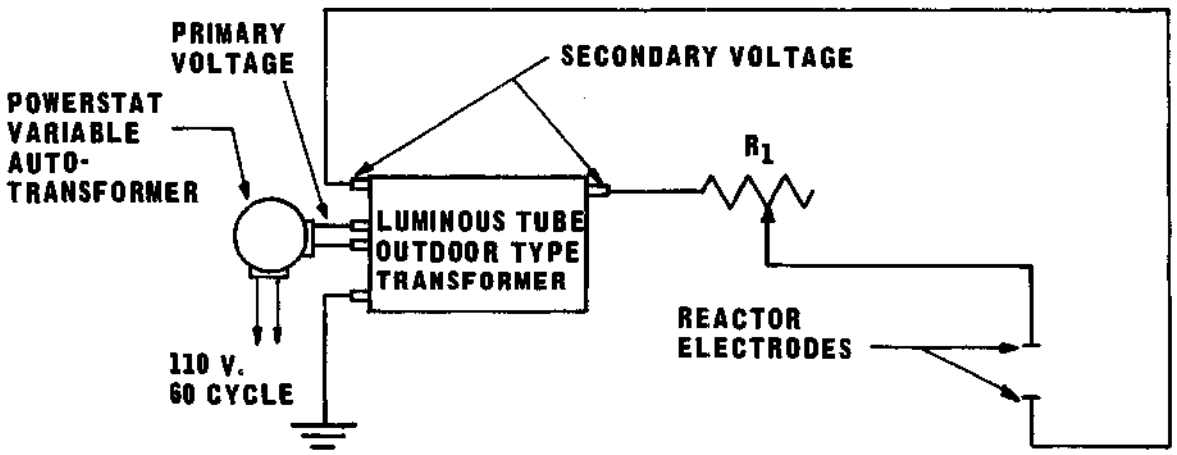

Figure 7b. Schematic Diagram of the Electrical Network for the External Synthesis of the Oxygen Fluorides.

system was replaced with a furnace which made it possible to study the initial and perhaps unstable or transitory pyrolysis products of the sample stored in the condensation tube. The furnace attachment (Fig. 8) consisted of a 3.8 cm long alumina tube (0.103 cm I.D.) heated over a 2.5 cm region by a tungsten resistance wire (0.0107 cm dia.). The alumina tube and heater wire were coated with Sauereisen Insa-Lute Adhesive Cement (No. 1 Paste) to assure uniform heating and were encased in a quartz sleeve to prevent surface ionization on the heater element itself. The temperature of the furnace was measured by a copper-constantan thermocouple at the center of the heated region. Flow through the furnace was controlled by maintaining the cryogenic inlet arrangement at a temperature such that the condensed species exerted a vapor pressure of approximately 1.0 torr.

The synthesis of the oxygen fluorides for these experiments was somewhat complicated by the fact that the furnace attachment was very fragile, and the exit port (10) could not be sealed off from the isolation vacuum by use of the teflon block valve as was described earlier. Consequently, it was necessary to close the valve (20) to the isolation vacuum pumping system and to conduct the synthesis with the vacuum lock (6) at the same pressure as the reactor space (4), i.e., at 25-40 torr. This resulted in such a large increase in the liquid nitrogen coolant boiloff rate that the reaction could not be run continuously. However, the synthesis was accomplished by filling the coolant chambers, (17) and (22), before starting the synthesis and continuing to force the liquid nitrogen into the chambers as rapidly as possible while the discharge was on. When all the excess refrigerant had boiled off, the discharge

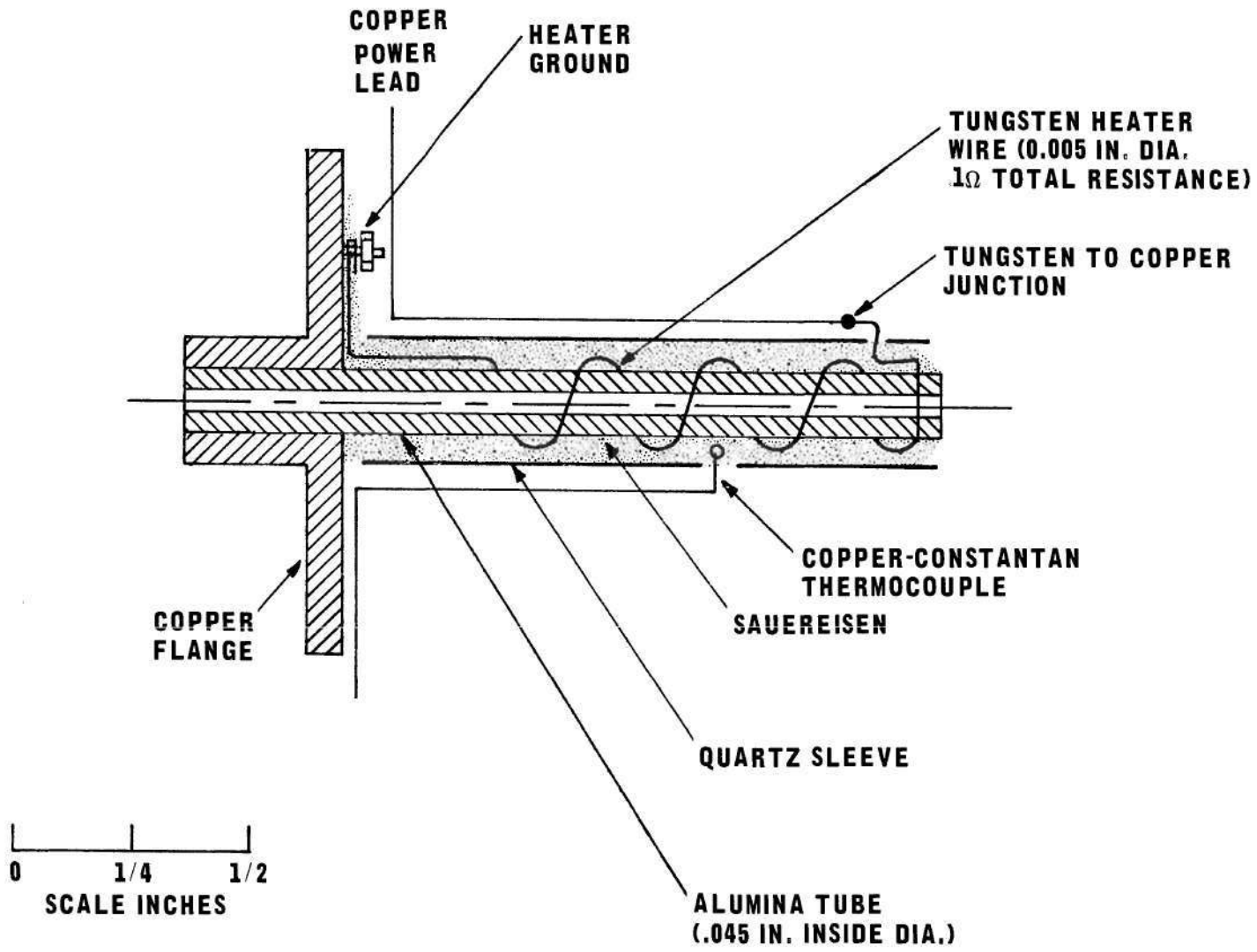

Figure 8. Schematic Diagram of Furnace Attachment for the Cryogenic Reactor-Inlet System.

was turned off and the same procedure was repeated. Using this technique, it was possible to run the discharge continuously for about 30 minute periods before it was necessary to refill the refrigerant chambers. This was actually a satisfactory technique since the normal synthesis for these runs required only about 1 - 1.5 hours.

This furnace arrangement was used quite successfully in the pyrolysis of the low temperature oxygen fluoride, O_2F_2, which permitted the detection and investigation of the O_2F free radical. It is particularly notable that withdrawing the exit of the furnace less than 6 mm from the edge of the electron beam resulted in such a decrease in the intensity of the O_2F^+ radical ion that it was barely detectable. This arrangement has also been used to observe the pyrolysis of OF_2 and the formation of BH_3 from the pyrolysis of B_2H_6.

Hot Filament Inlet System

A second arrangement is shown in Fig. 9 in which reaction products from the reactor-inlet system can be pyrolyzed directly in the electron beam of the spectrometer. A heated coiled wire filament is stretched directly across the exit port of the inlet system. With the extension piece of the inlet system positioned directly in the ion source as described earlier, the species can be passed directly over the hot filament. This permits detection of pyrolysis products formed by a single collision with the filament and with no subsequent gaseous collisions before analysis. It has been demonstrated that the filament can actually be immersed directly into the electron beam. This appears to represent the very optimum arrangement for this type of study and apparently has not been attained in any other similar experiments.

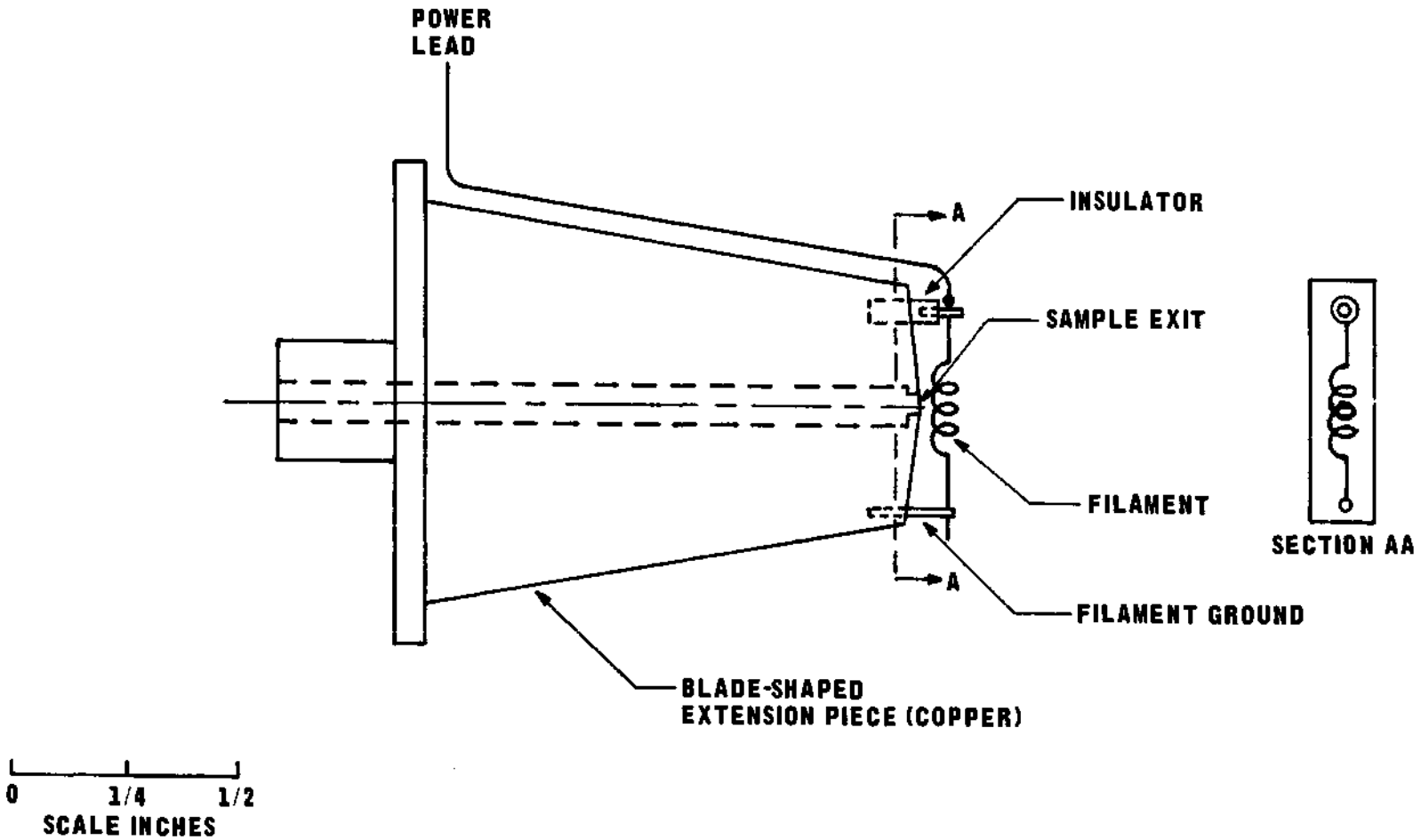

Figure 9. Schematic Diagram of Hot Filament Arrangement on the Extension Piece of the Cryogenic Reactor-Inlet System.

61

Numerous filaments were used in the investigation of the pyrolysis products of OF_2 at temperatures of 650°-1000°C. The temperature of the filament was determined by sighting through the observation port (13) with a Leeds and Northrup Model 8622-C optical pyrometer. It is interesting to note that these pyrolysis experiments varied markedly with various filaments which suggest that this might well be a suitable arrangement for the study of surface chemistry and catalysis.

Radio Frequency Discharge Tube Inlet System

In attempts to observe the formation of the OF free radical, a radio frequency electrodeless discharge was used to decompose the OF_2 molecule. In these experiments the OF_2 gas was injected through a Granville-Phillips leak valve into a 0.635 cm I.D. quartz or alumina discharge tube. The discharge was generated with a 50 turn, 2.5 cm, diameter coil powered by a Hallicrafter's BC-610 radio transmitter.

The gaseous products passed from the discharge region, around a 90° turn, and directly into the mass spectrometer through the header of the coaxial entrance to the ion source. The backing plate of the ion source was removed so that the end of the inlet tube could be inserted directly into the edge of the electron beam. The total length of the tube from the discharge region to the electron beam was 12.5 cm. The 90° elbow proved to be necessary to remove ions formed by the electrical discharge.

Mass Spectrum as a Function of Temperature

Positive Ion Spectra

Several hundred traces of the mass spectrum were made over the temperature range of 77° - 200°K in most of the low temperature oxygen

fluoride experiments. In addition, mass spectra as a function of temperature were obtained for the unreacted feed gas mixture of O_2 and F_2. The mass spectra of OF_2, SiF_4, CF_4, and C_2F_6 were also obtained since they turned out to be particularly troublesome impurities in the product mixtures. The Bendix machine permits the scanning and recording of the mass range of $12 \leq m/e \leq 130$ in approximately one minute. Several traces were made at each temperature with various electrometer index settings. Hence, the relative intensities of all ion currents were obtained and tabulated at each temperature.

The limitations of the spectrometer and complicated features of the spectra combined to necessitate much care in making mass assignments for the observed ions. Mass scales were prepared for each scan rate using $m/e = 16$ (O^+ ion) and $m/e = 69$ (CF_3^+ ion) as reference masses. Using only the measured distance between the reference masses as verified from several traces, the distance from $m/e = 16$ to all other masses out to $m/e = 130$ was calculated and plotted to yield completely unbiased scales. These scales were then checked by making traces for species that gave known fragments throughout the mass range. That is, traces for CF_3I, SiF_4, C_2F_6, OF_2, and CO_2 were obtained which combined gave major ion currents at m/e = 16, 19, 28, 31, 35, 44, 47, 50, 54, 66, 69, 85, 100, 104, 119, 126, and 127 which made it possible to verify that the mass scales were definitely correct. The use of these scales resulted in consistent and unambiguous mass assignments for $12 \leq m/e \leq 130$ for more than 98 per cent of all traces. Occasional fluctuations in the scan rate or recorder speed resulted in a shift of the larger masses for a few traces and, consequently, these traces were ignored.

The identification of all the ions in the mass spectrum was very difficult due to several impurities that were in the feed gas and others that were formed during the synthesis operation. The source of each ion was determined from the observed relative intensities, known cracking patterns of the impurities, the temperature at which each was first observed (which depends on the vapor pressure of the parent species), and their appearance potentials. In order to identify each impurity present in the O_2 and F_2 feed gas and to determine the volatility, and hence, the temperature dependence of the mass spectra, the unreacted feed gas was pumped through the system with both coolant chambers, (17) and (22), at 77°K, whereupon all significant impurities were condensed and concentrated. Spectra were then recorded at 2° - 3°K intervals as this condensate was warmed over the temperature range of 77° - 200°K. From the temperature required for the observation of the various condensed impurities, it was possible to determine what vapor pressure a species had to exert before it could be detected in the spectrometer, and, therefore, a fundamental calibration of the inlet arrangement was obtained.

The mass spectrum was normally obtained with an electron energy of 70 ev. However, near the decomposition temperature of O_3F_2, traces were made over a wide range of electron energies, 15-70 ev, in order to investigate the possibility that higher electron energies might result in excess fragmentation of some unstable species. The mass spectrum was also observed continuously on a Tektronix Type 543A oscilloscope during the warming process in order to detect any unusual changes between traces.

Negative Ion Spectra

The possibility that the oxygen fluorides might well yield negative ions in the mass spectrometer was considered very likely. Consequently,

several experiments were run in which both positive and negative ions were observed over the temperature range of 77° - 150°K. Unfortunately, the Bendix machine is not equipped to record negative ion currents. However, they can be observed on an oscilloscope output. Therefore, it was possible to see the negative ion spectra on the oscilloscope, to estimate the relative intensities of the various ions, and to determine the electron energies at which each was first observed and the energy at which it had a maximum intensity. The positive ion spectrum was recorded before and after a measurement of the negative ion spectrum at a given temperature. This permitted a determination of the relative abundances of all species present at that temperature and greatly facilitated the determination of the sources of the negative ion currents.

A negative ion mass scale that could be placed directly on the oscilloscope was prepared in the same manner as that for the positive ion scale, using CF_3I as a calibrating gas which gave ions at m/e = 19 (F^-), 69 (CF_3^-), and 126 (I^-). This scale was checked by observation of the negative ions from OF_2, CF_4, C_2F_6, and SiF_4 which appeared at m/e = 16, 19, 35, 69, and 85. The fact that negative ion currents could not be recorded made it impossible to calibrate the electron energy scale accurately.

Energy Measurements

The appearance potentials of the ions of interest observed in the spectrometer were usually determined using the retarding potential difference (RPD) method,[68] with the energy scale calibrated immediately before and after each energy measurement using argon and/or nitrogen. In some

experiments the ion current from the species of interest was so small that it was impossible to use the RPD method. Hence, the linear intercept and semilog matching methods were used in those tests. These latter methods were also used in most of the energy measurements that were confirmatory tests of values reported in the literature, as well as when only approximate values were desired. The RPD and linear intercept methods are discussed in some detail in Martin's thesis[3] and the variations of the semilog matching method are discussed in numerous papers.[69,70] Since this thesis was not concerned with the development or investigation of these various experimental techniques for measuring appearance potentials by electron impact methods, they will not be discussed in this work. In making the energy measurements on the highly reactive fluorine compounds, it was necessary for the ion source to become partially passivated before the spectrometer would stabilize enough to make accurate and reproducible measurements. The energy scale was calibrated before and after the spectrometer was conditioned by the oxygen fluorides to determine if there was an appreciable drift during that period. These studies showed that the energy scale moved upward by 1-2 ev during the conditioning period. A particularly troublesome problem was encountered in these energy measurements of the low temperature oxygen fluorides. That is, after several hours injection of the sample into the spectrometer, with the cryogenic inlet system in analytical position (see Fig. 4), an electric arc apparently occurred between the extension piece of the inlet system and the ion grids of the spectrometer. This changed the energy scale calibration and made it necessary to recondition the ion source and to then recalibrate the energy scale. With continuous injection of the fluoride samples, the trap current decreased to an inoperable level after 12-20 hours.

CHAPTER III

RESULTS AND DISCUSSION

Introduction

The true molecular consistency of the reported low temperature oxygen fluorides has been a question of interest to many investigators for several years. In addition, the question concerning the existence of oxygen-fluorine free radicals has been the object of much investigation as was pointed out earlier. The mass spectrometric results reported in this chapter were obtained in an effort to answer, in as much depth as possible, questions concerning both of these rather broad and complex problems. Hence, these results are very diverse in nature and will be discussed as essentially separate topics. That is, the mass spectrometric investigations of the low temperature oxygen fluorides, O_2F_2 and O_3F_2, which were carried out over a broad temperature range will be the object of one topic, while the investigations of the O_2F and OF radicals will be the subject of another rather different topic. However, it will be shown that the development of the energetics of the O_2F_2 molecule and O_2F free radical are dependent on both of these studies.

Mass Spectrometric Studies of the Low Temperature Oxygen Fluoride Molecules

The mass spectrum as a function of temperature was obtained in the manner described in Chapter II over the temperature range of 77° - 200°K

in sixteen O_3F_2 syntheses and four O_2F_2 syntheses. The fact that O_3F_2 decomposes to O_2F_2 and O_2 at about 115°K made it possible to study both species in each experiment. This was considered a fortunate situation since the synthesis operation and recording of the mass spectra over the temperature range of 77° - 150°K required from 12 - 20 hours for each experiment. However, the four O_2F_2 synthesis experiments were necessary in order to determine, by difference, the actual contribution of O_3F_2 to the mass spectra in the region of 77° - 120°K.

The effect of glass walls in contrast to metal walls on the mass spectra was investigated using both the in situ and external generator syntheses. No significant differences were noted in the mass spectra from these experiments. Therefore, the results will be discussed with no distinction between the experiments in which the reactor was glass lined and when it was not.

Mass Spectrum as a Function of Temperature

Positive Ion Spectra (In Situ Synthesis). Figs. 10 and 11 illustrate the general variation of the more interesting ion currents with temperature for the experiments in which O_3F_2 was the principal reaction product when using the in situ synthesis technique. Four temperature ranges are apparent (80° - 90°K, 90° - 102°K, 105° - 122°K, and 122° - 135°K) within which significant changes in the mass spectra occur. These temperature ranges coincide with the melting point of O_3F_2 (83° - 84°K); the temperature at which ozone has a vapor pressure of one torr (94°K); the temperature at which O_3F_2 has a vapor pressure of one torr (110°K), at which O_2F_2 decomposes (110° - 120°K), and at which O_2F_2 melts (109°K); and the temperature region (120° - 135°K) in

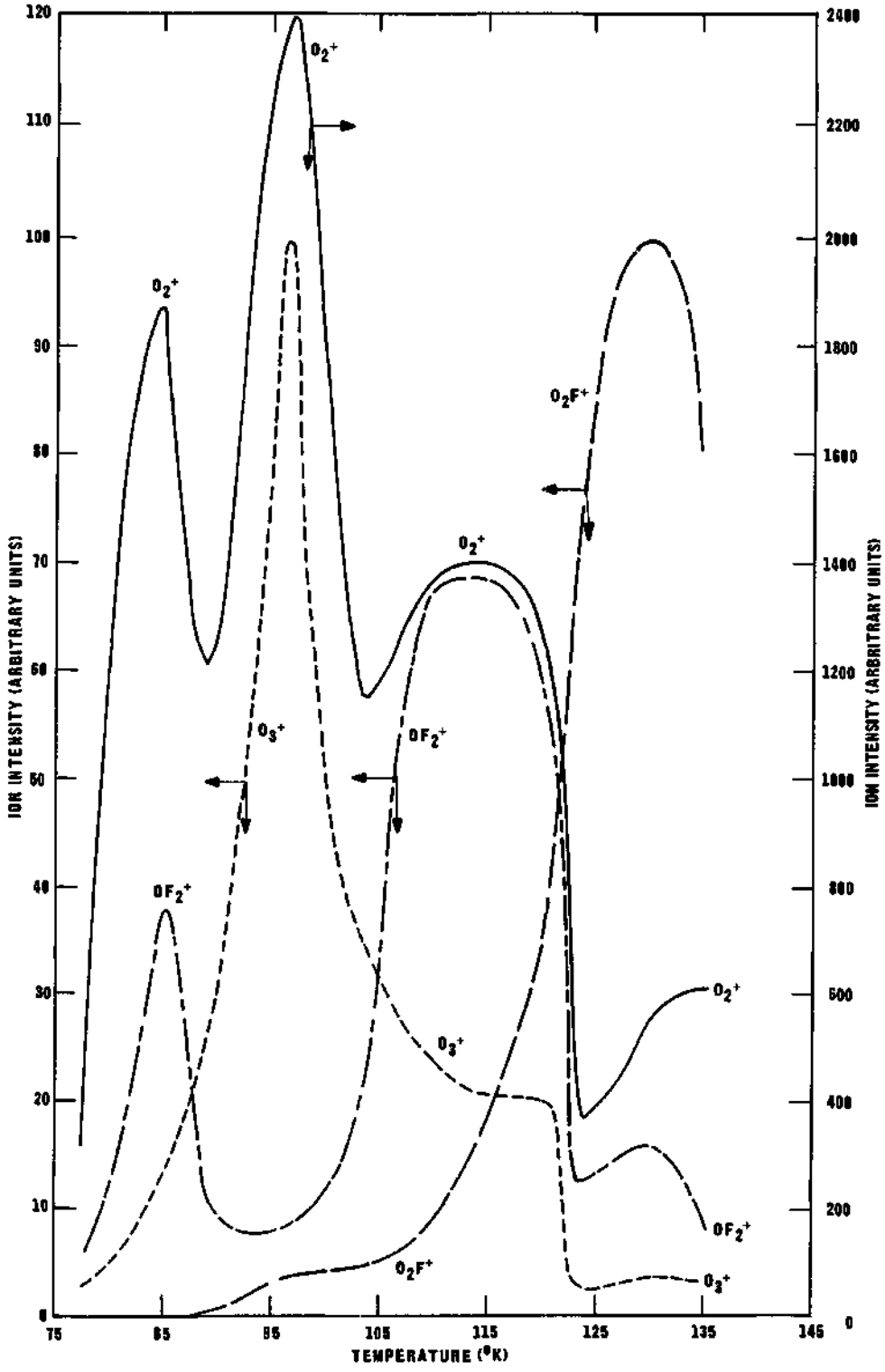

Figure 10. Representative Variation of Ion Current Intensities with Temperature of Some of the Most Interesting Ions Observed in the O_3F_2 Synthesis Experiments. The Reactor was Pumped Continuously during Warmup.

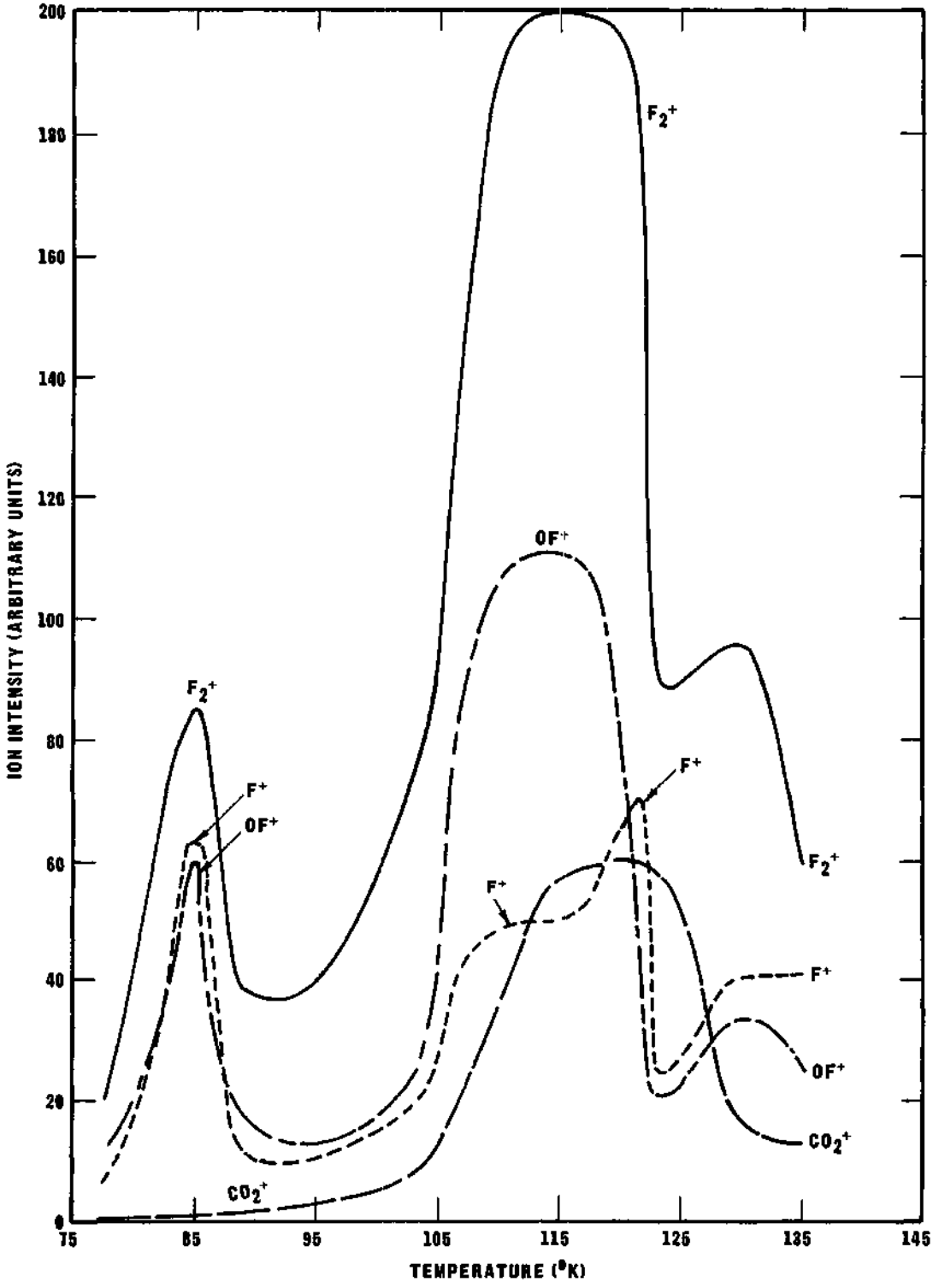

Figure 11. Representative Variation Ion Current Intensities with Temperature of Some of the Most Interesting Ions Observed in the O_3F_2 Synthesis Experiments. The Reactor was pumped During Warmup.

which O_2F_2, as a stable reagent, exerts a smoothly rising vapor pressure. The vapor pressure of O_2F_2 is one torr at approximately 130°K. In the experiments in which the principal synthesis product was O_2F_2, the mass spectra as a function of temperature from 77° - 150°K were essentially the same as for the O_3F_2 experiments except that the maximum ion currents at 80° - 90°K, 90°-102°K, and 105° - 122°K were much smaller. It would be expected that at least a small amount of O_3F_2 would also have been prepared in these O_2F_2 experiments.

In Figs. 10 and 11 it can be seen that the ratio of the ion current due to OF^+ to that due to OF_2^+ is about 1.7 - 2.4 over the entire temperature range, which is the ratio that was obtained for free OF_2 (see Appendix C). From the initial O_3F_2 experiments, illustrated by Fig. 12, in which only a small amount of OF_2 was present at 110° - 116°K, it appeared that an excess amount of OF^+ was observed at those temperatures. However, a detailed analysis of the mass spectra showed that the excess OF^+ (m/e = 35) current was due to an overlap of the extremely large O_2^+ ion current (m/e = 32).

There was considerable difference in the mass spectra from 90° - 120°K shown in Figs. 10 and 11 from that obtained in the earlier experiments. The major difference is that there are very large OF_2^+ and F_2^+ ion currents at 105° - 120°K in the more recent experiments, whereas these ion currents were very small in the earlier experiments. The only difference in procedure used in these experiments was that the condensation-transfer tube was pumped from its lower end (1) continuously during the warmup process for these later experiments while this pumpout was omitted during the earlier experiments.

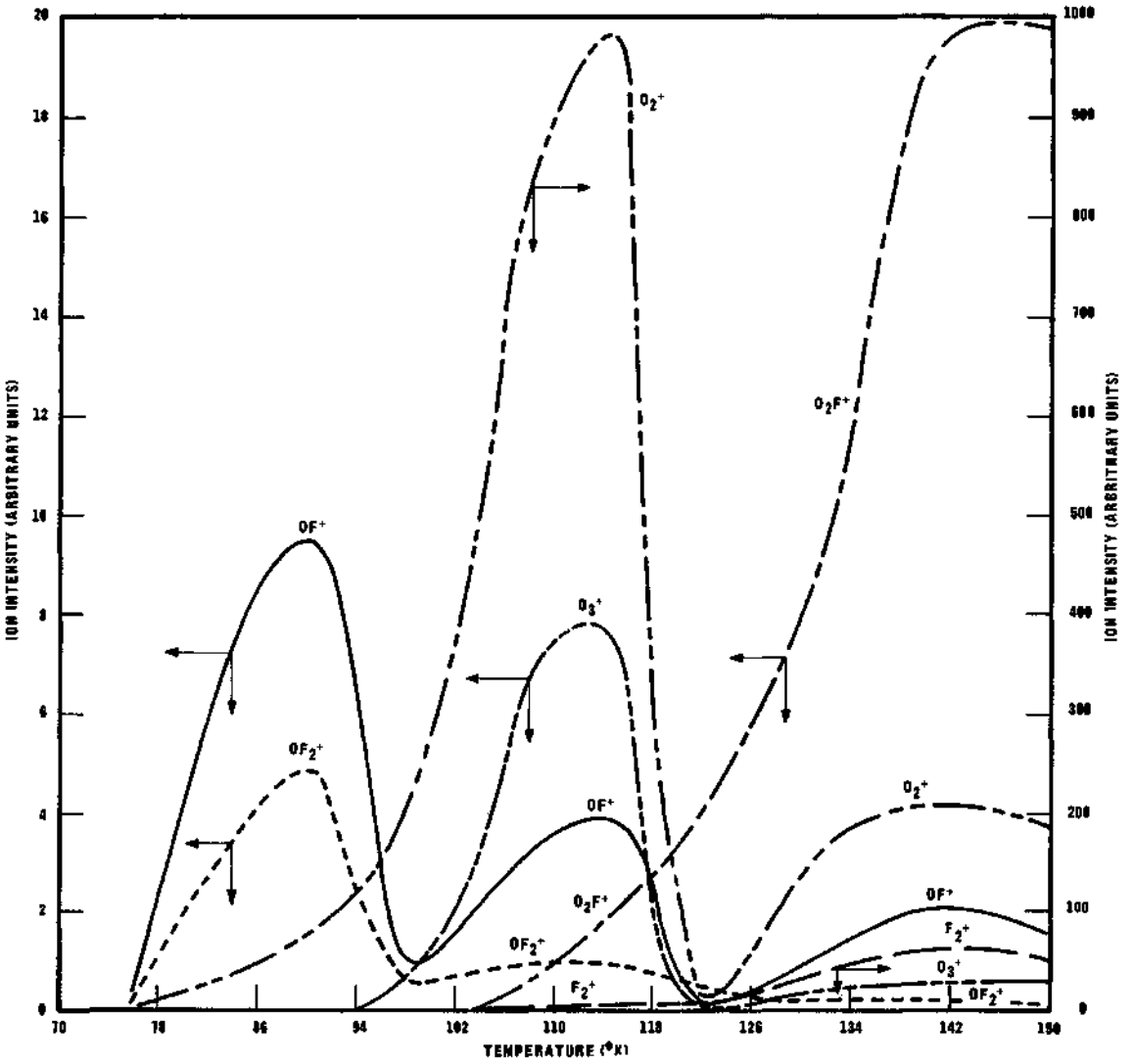

Figure 12. Representative Variation of Ion Current Intensities with Temperature of Some of the Most Interesting Ions Observed in the O_3F_2 Synthesis Experiments. The Reactor was not Pumped During Warmup.

In the earlier experiments the reactor was not pumped because it was feared that the more volatile reaction products might be pumped away so rapidly that very little sample would get into the mass spectrometer. However, the fact that very little F_2 or oxygen-fluorine species were observed at 105° - 120°K in these earlier experiments indicated that the vapor of O_3F_2 was not being transferred into the mass spectrometer. Experiments with CO_2 indicated that the transfer from the reactor space (4) along the gradient tube (19) and into the mass spectrometer was very slow unless there was continuous pumping at the lower end (1). Therefore, it was concluded that the O_3F_2 was decomposing, liberating large amounts of O_2, and the resulting partial pressures of the several oxygen-fluorine species in the vapor phase were very small. Hence, it was decided that continuous pumping of the reactor space to remove excess O_2 would result in a more rapid transfer of the sample along the gradient tube and a much larger partial pressure of O_3F_2 in the vapor phase. Using this technique, the quite different results shown in Figs. 10 and 11 were obtained, which supported the above arguments.

The presence of small amounts of impurities in the feed gas (i.e., OF_2, CF_4, C_2F_6, N_2, HF, NF_3, CO_2, H_2S, SF_6, and SiF_4), as well as others formed during the synthesis (i.e., N_2F_2, N_2F_4, COF_2, O_3, SO_2F_2, and additional SiF_4 and OF_2), made the interpretation of the mass spectra relatively difficult. The presence of ion currents at m/e = 66, 69, 85, and 104 due to SiF_2^+, $N_2F_2^+$, and COF_2^+; CF_3^+; SiF_3^+ and $N_2F_3^+$; and SiF_4^+ and $N_2F_4^+$, respectively, made the unprejudiced procedure described in Chapter II for making mass assignments definitely necessary. From the temperature required for the observation of the condensed impurities

of known vapor pressure, it was determined that a species exerted a vapor pressure of 10^{-4} - 10^{-5} torr when it was first detected in the spectrometer and gave a maximum intensity when its vapor pressure was about 0.1 - 1.0 torr. These facts proved particularly valuable in determining the parent species of the ion currents that were observed.

The parent ion of O_2F_2 (m/e = 70) was not observed even when the inlet system was raised above 150°K. A very small signal at m/e = 70 was observed only when a very large ion current was present at m/e = 69 due to CF_3^+ from CF_4 or C_2F_6, and was evidently due to the isotope $C^{13}F_3^+$. This heavier ion was determined (see Appendix C) to represent approximately one per cent of the $C^{12}F_3^+$ current. In addition, no ion currents due to O_4 (m/e = 64), O_3F (m/e = 67), O_4F (m/e = 83), O_3F_2 (m/e = 86), or O_4F_2 (m/e = 102), were observed in either the O_2F_2 or O_3F_2 experiments. The only time that an ion current at m/e = 86 was detected occurred when a relatively large current was present at m/e = 85 due to SiF_3^+. The ratio of the m/e = 85 and 86 ion currents was the same as that obtained for SiF_4 (see Appendix C) which indicated that only the isotope $Si^{29}F_3^+$ was present at m/e = 86. There were very small ion currents at m/e = 67, 83, and 102 due to SOF^+, SO_2F^+, and $SO_2F_2^+$, respectively, from a small amount of sulfuryl fluoride formed during the synthesis operation. This was apparently formed as a result of the presence of SF_6 in the feed gas. The assignment of these ion currents to the fragments of SO_2F_2 was based on their relative intensities and the temperature at which they exerted a maximum intensity (~ 140°K). It was obvious that they were not due to O_3F_2 and O_4F_2 since they both decompose at temperatures below 120°K. However, Nielsen[32]

reported that he had observed O_3F_2 and O_4F_2 in a mass spectrometer, as was discussed in Chapter I, at temperatures above about 140°K. In view of the facts that SO_2F_2 is apparently formed in the synthesis of the low temperature oxygen fluorides and give ion currents above about 140°K that would correspond to ion currents that might be expected from O_3F_2 and O_4F_2, it seems quite likely that Nielsen incorrectly assigned the ion currents from SO_2F_2 to the higher oxygen fluorides.

Appearance potentials were measured at several temperatures for the most interesting fragments in the mass spectrum from the O_3F_2 experiments. The appearance potential of O_2^+ was measured at 77°, 90°, 112° (O_3F_2 decomposition temperature), and 130°K. It was found that $A(O_2^+)$ at each of these temperatures was equal to $I(O_2)$. The large amount of molecular O_2 present as background interfered with the measurement of the appearance potential of O_2^+ from the fragmented oxygen fluorides, for, under the usual assumptions, it is clear that $A(O_2^+)$ from these species is greater than $I(O_2)$.

The appearance potential of OF^+ at 85°K was measured (see Fig. 13) to be 15.8 ± 0.2 ev, which is the value reported by Dibeler, et al.,[6] and verified in this work, for $A(OF^+)$ from OF_2. Attempts to measure the appearance potential of the OF^+ ion at the decomposition temperature of O_3F_2 (110° - 120°K) have been unsuccessful using the RPD or linear intercept methods due to the instability of the spectrometer as a result of the extremely large amounts of O_2 and F_2 that seem to be unavoidably present. However, using the diminishing current method, a value approximately equal to $A(OF^+)$ from OF_2 was obtained. This would only indicate that the appearance potential of OF^+ from the vapor phase of O_3F_2 is equal to or greater than that of OF^+ from OF_2

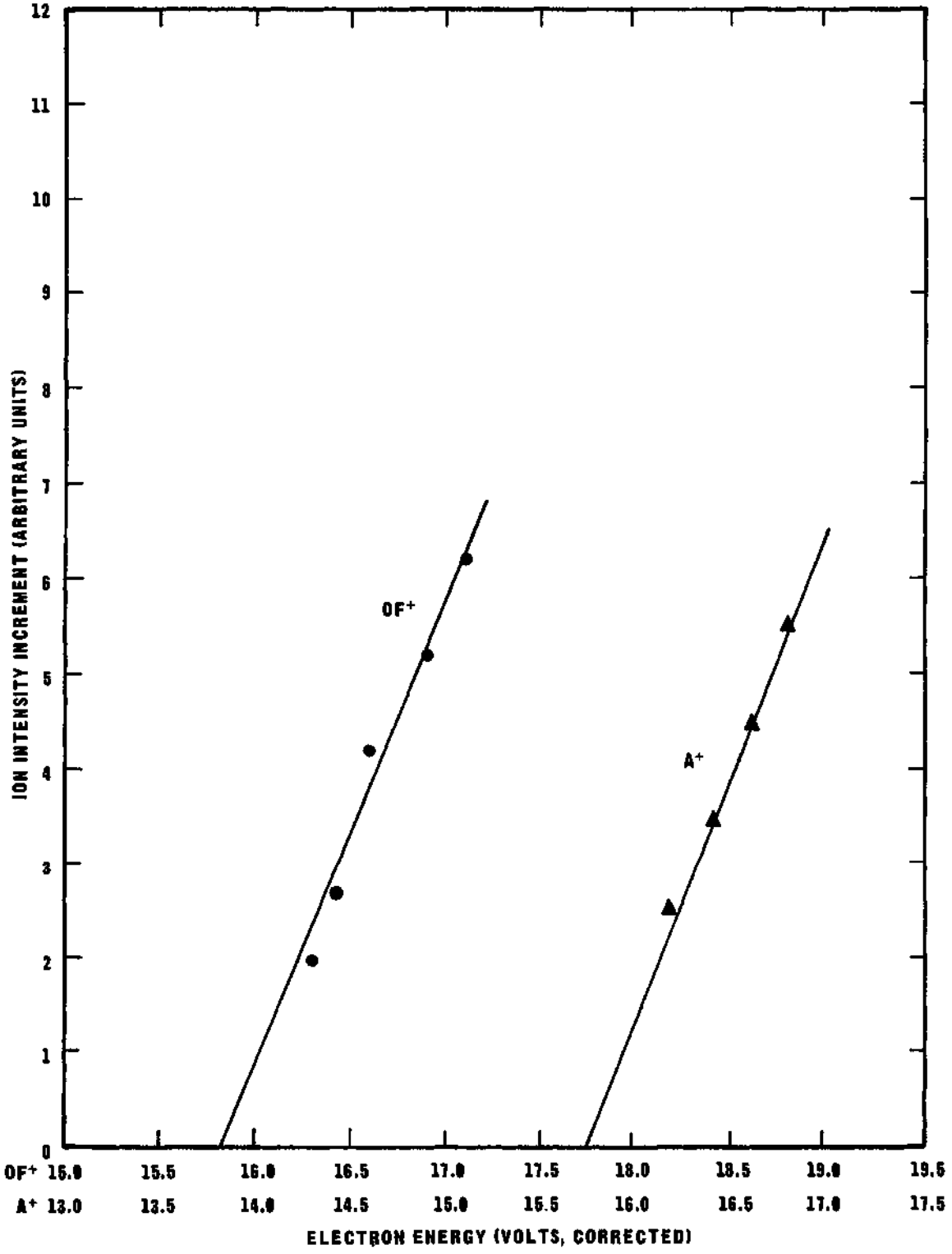

Figure 13. Ionization Efficiency Data by the RPD Method for OF^+ Observed at 80°-90°K in the O_3F_2 Synthesis Experiments Illustrated by Fig. 11. Argon is the Standard.

since there was at least a small amount of free OF_2 present at that temperature. In addition, the $A(OF_2^+)$ at 110° - 120°K was determined to be about 13.7 ev using the same technique, which is the value measured for the ionization potential of OF_2. The appearance potential of the O_3^+ ion was measured at 93°K, using the linear intercept method (see Fig. 14). A value of $A(O_3^+)$ = 12.8 ± 0.2 ev was obtained which is in excellent agreement with the value reported by Herron and Schiff[71] of 12.80 ± 0.05 ev for the ionization potential of ozone.

At 130°K, $A(O_2F^+)$ and $A(OF^+)$, were measured to be 14.0 ± 0.1 ev and 17.5 ± 0.2 ev, respectively, and these values were found to be the same for both the O_2F_2 and O_3F_2 experiments. The larger possible error in $A(OF^+)$ is due to the fact that the OF^+ current was small, and it was much more difficult to make accurate measurements. This measurement was further complicated by the fact that some OF_2 was present even at 130°K. The $A(OF^+)$ from OF_2 of 15.8 ev is nearly two volts below the $A(OF^+)$ from O_2F_2. This problem was apparently solved by pumping on the sample continuously until no OF_2^+ could be observed on the oscilloscope before attempting to measure $A(OF^+)$. This step usually required 1.5 - 3.0 hours of pumping to remove all the OF_2. $A(O_2F^+)$ was measured ten times in a total of four synthesis experiments with an average deviation of ±0.05 ev from 14.0 ev, and with a maximum deviation of 0.15 ev. These measurements will be discussed in detail later in this chapter.

Positive Ion Spectra (External Generator Synthesis). The fact that no direct evidence for molecular O_3F_2 was obtained using the in situ synthesis technique raised the question as to whether any O_3F_2 was actually being formed using that technique. Since O_3F_2 is a liquid at

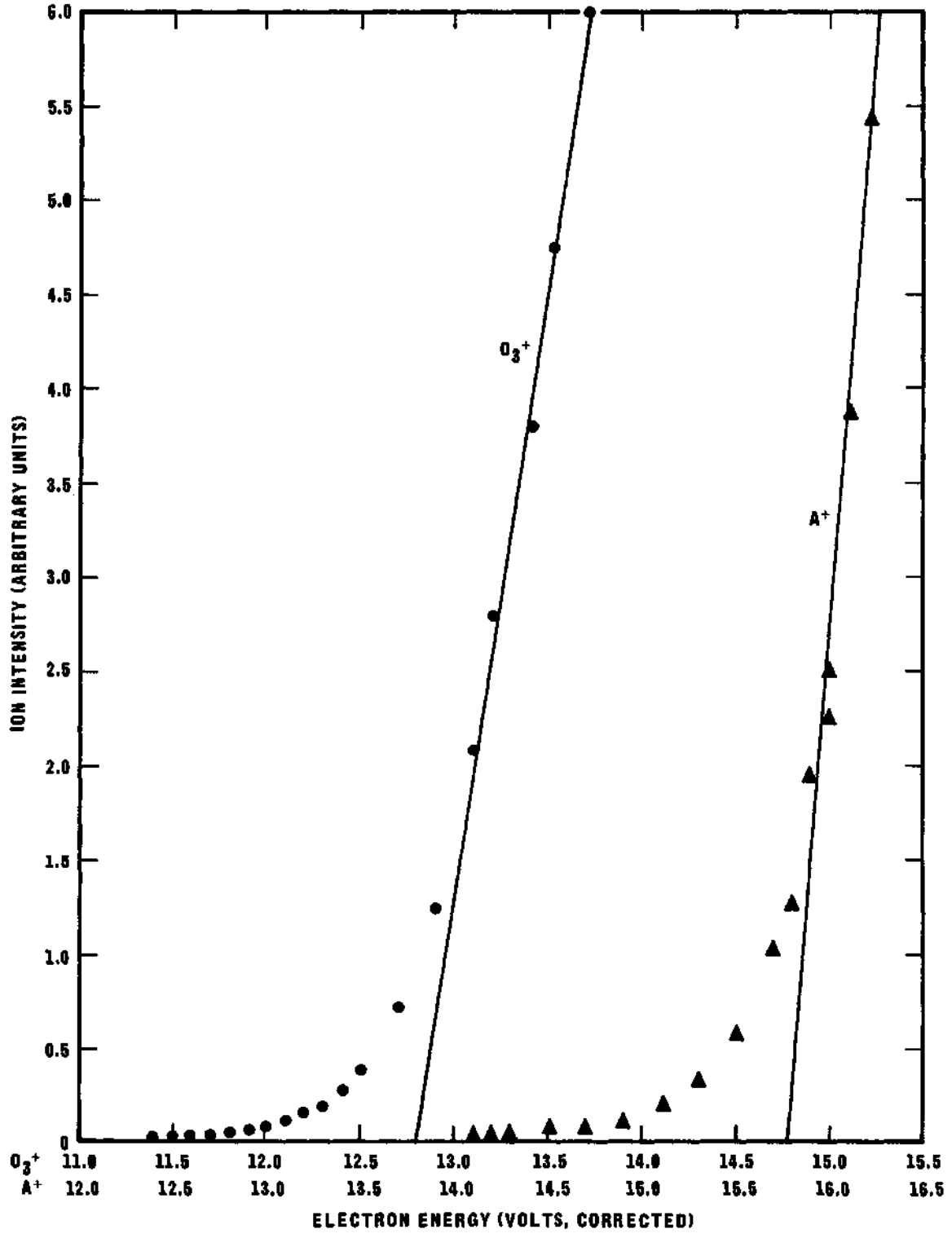

Figure 14. Ionization Efficiency Data for O_3^+ Observed at 90°-100°K in the O_3F_2 Synthesis Experiments Illustrated by Fig. 10. Argon is the Standard.

liquid oxygen temperature (90°K) where O_2F_2 is a solid, an obvious way of being certain that O_3F_2 was in the inlet system was to prepare it in glassware in an external system and transfer it directly into the inlet system at 90°K. Therefore, six O_3F_2 synthesis experiments were performed using the pyrex external generator described in Chapter II. In these experiments usually about 1 - 2 grams of O_3F_2 was synthesized at 90°K. Since O_3F_2 is quite viscous at that temperature, it was necessary to distill the sample into the inlet system. This was accomplished by permitting the liquid O_2 refrigerant to slowly boil off while pumping continuously on the lower end (1) of the condensation tube, as was described in Chapter II. The inlet system was maintained at 77°K and was in analytical position (see Fig. 4) to permit detection of any high vapor pressure species during this transfer operation. As the liquid O_2 coolant boiled away, the dark red O_3F_2 could be seen slowly moving along the reactor drain line directly into the cryogenic inlet system. In one experiment in which a relatively large sample of O_3F_2 was synthesized (3 - 5 grams) there were several flashes of light in the drain line as the sample was being transferred. After the sample was transferred into the inlet system, the mass spectrum as a function of temperature was obtained as in the <u>in situ</u> synthesis experiments.

During the transfer operation of the O_3F_2 samples into the inlet system, relatively large amounts of O_2, F_2, and OF_2 were observed in the mass spectrometer. This indicated that some decomposition was occurring during the transfer, which would be expected according to Solomon.[22] The mass spectrum as a function of temperature for these experiments was essentially the same as for the <u>in situ</u> synthesis

experiments, which indicated that O_3F_2 really was being prepared using the single electrode in situ arrangement.

In two of these experiments in which the inlet system was glass-lined, there was a violent explosion shortly after the temperature of the outer chamber (22) was raised slightly. The explosion "powdered" the glass liner in the inlet system in both cases. It has been reported[4] that a mixture of O_2F_2 and O_3 explodes violently at 125°K. Operation of the inlet system immediately before the explosions in this work indicated that heat was being generated in the reactor space at such a rate that the outer chamber (22) could not be cooled back down even with the maximum liquid N_2 refrigerant input rate. Hence, it was concluded that the sample was probably heated excessively as a result of the heat liberated by the combined action of the decomposition of O_3F_2 and the poor heat transfer between the glass liner and the cooled metal walls. This could result in an explosion due to the presence of O_3 in the sample. A similar explosion has occurred in a glass lined inlet system similar to the one used in this work during an experiment in which pure ozone was being transferred into the mass spectrometer. In later O_3F_2 experiments, using a glass liner, the inlet system was warmed extremely slowly (~ 5°K/hr) and no explosion occurred.

Negative Ion Spectra. The failure to detect positive ions of O_2F_2, O_3F, O_3F_2, O_4F, or O_4F_2 in the spectrometer made the interpretation of the mass spectra difficult. It was hoped that a simultaneous examination of the positive and negative ion spectra would permit a more definite interpretation of the data. That is, it seemed that the negative ions of some of the above species might well be produced and be

stable in the mass spectrometer for the required time of about 50 microseconds, which would thereby permit a more definite determination of the parent species of the positive ions that were observed (i.e., OF^+, OF_2^+, and O_2F^+). In addition, if O_3F^- or $O_3F_2^-$ could be detected, it would indicate that O_3F_2 is actually a molecular entity in the vapor phase. The same would be true for O_4F_2 if O_4F^- or $O_4F_2^-$ could be observed. Unfortunately, the Bendix mass spectrometer is not equipped to record negative ion currents. However, the relative intensities of the several ions were estimated for these experiments by scaling from a display of the spectrum on the oscilloscope.

Table 2 gives the relative intensities of the negative ion currents, the energies at which they are first observed on the oscilloscope, and the electron energies at which they are at a maximum for an O_3F_2 synthesis experiment in which the reactor was pumped continuously during the warmup. These data were obtained simultaneously with the positive ion data shown in Table 21 in Appendix C. The mass assignments for the various negative ion currents were relatively difficult to make since a trace of the spectrum could not be made. However, a mass scale was constructed as discussed in Chapter II, and, in addition, gases giving known negative ions were added simultaneously when there was some question as to a particular mass assignment. For instance, it was very difficult to determine from the mass scale whether or not the ion currents assigned to CF_3^- (m/e = 69) and SiF_3^- (m/e = 85) might possibly be $O_2F_2^-$ (m/e = 70) and $O_3F_2^-$ (m/e = 86). This question was answered by injecting C_2F_6 and SiF_4 (which gave ion currents at CF_3^- and SiF_3^-) into the mass spectrometer and noting that both observed ion currents

Table 2. Relative Abundances, Appearance Potentials,[a] and Energies for Maximum Ion Currents of Negative Ions in an Ozone Difluoride Synthesis Experiment. The Reactor Space was Pumped Continuously During Warmup

Temperature (°K)		Relative Intensities and Energies[d]								
IC[b]	OC[c]	O^-	F^-	O_2^-	OF^-	F_2^-	O_3^-	CF_3^-	SO_2F^-	SiF_3^-
77	77	100 (2.3) (4.4)	100 (2.3) (5)	-	-	-	-	-	-	-
88	92	100 (0) (6)	100 (0.5) (20[e])	1 (5)	3 (9)	< 1 (15)	-	-	-	1 (15)
92	97	100 (0) (5.5)	75 (3.6)	3 (4)	1 (8.7)	< 1 (16)	-	< 1 (5.3)	-	1 (13.6)
96	104	100 (0)	75 (0.3)	4 (1.5)	3 (4.5)	< 1 (5.7)	< 1 (50)	< 1 (3)	-	3 (5.5)
106	112	95 (0) (25[e])	100 (0) (15)	4 (2.7)	10 (3.2) (24)	4 (5.3)	-	< 1 (3.5)	-	10 (4.5) (24)
114	118	90 (0) (8[e])	100 (0) (8[e])	5 (0.4) (8.7[e])	20 (2.7) (17)	5 (4)	-	< 1 (3.7)	1 (15)	10 (3.7)
121	125	50 (0) (8[e])	100 (0) (3.8)	5 (0) (8[e])	10 (0)	5 (4)	-	< 1 (4) (8)	<1 (19)	5 (4) (8)
130	126	30 (0) (8[e])	100 (0) (3.2)	35 (0) (8[e])	10 (0) (8)	7	-	< 1 (6)	< 1 (18)	2 (6)

[a] Approximate values since energy scale was not calibrated.

[b] Inner chamber.

[c] Outer chamber.

[d] The first number gives the estimated relative intensity of ions for that temperature. There is no relation between the intensities at different temperatures. The first number in parentheses is the energy at which the ion current can first be detected on the oscilloscope. The second number in parentheses is the energy at which the ion current is a maximum.

[e] No sharp maximum was observed. Either the maximum was very broad or the ion current merely continued to increase with increasing electron energy. The value shown simply indicates that the signal is quite intense at that energy.

increased and no adjacent peaks were detected. This definitely proved that the mass assignments were correct.

The electron energy scale could not be calibrated for negative ions. However, it seems reasonable to assume that the scale is accurate within ±1 ev since the correction factor for the positive ion scale has been shown to almost always fall within this range. In any case, it can be seen from Table 2 that O^-, F^-, O_2^-, and OF^- are all observed on the oscilloscope at the lowest obtainable electron energies. This indicates that either the ions are formed on the surface of the ion source filament, which seems unlikely, or they are formed by thermal electrons from the filament. The behavior of the OF^- ion with varying electron energy at 85°K and 116°K was essentially the same as that obtained with OF_2 (see Appendix C).

Discussion of the Mass Spectrum of the Low Temperature Oxygen Fluorides

The intense OF^+ and OF_2^+ ion currents observed at 82° - 90°K in the O_3F_2 synthesis experiments were evidently arising from free OF_2 since the measured $A(OF^+)$ of 15.8 ev, using the RPD method, was the same as reported from an earlier electron impact study of OF_2. Further evidence that this was free OF_2 is that the ratio of OF^+ and OF_2^+ was the same as that obtained for a sample of OF_2. There is also a maximum in the O_2^+ and F_2^+ ion currents at this same temperature region. It seems probable that OF_2, O_2, and F_2 were adsorbed in the solid O_3F_2 at 77°K and were evolved rapidly as the sample melted at 83° - 84°K. Otherwise, all three of these species would be pumped away at 77°K since OF_2, O_2, and F_2 have vapor pressures of about 1, 100,

and 400 torr, respectively, at that temperature. In one experiment the sample was pumped continuously for about four hours before the warmup process was begun. However, the maximum ion currents at 82° - 90°K were still obtained. Another possible explanation for these maximum ion currents could be that a small amount of O_4F_2 is formed during the synthesis and decomposes in that temperature range. Since no ions were observed that could be definitely attributed to O_4F_2, it appears that the significance of this last explanation cannot be established using the mass spectrometer.

The very large maximum in the O_3^+ ion current at 90° - 98°K was evidently due to free ozone formed during the synthesis operation. There are two very good reasons for this conclusion. First, the measured $A(O_3^+)$ was, using the linear intercept method, essentially the same as the reported[71] ionization potential of ozone. Second, the O_3^+ current had a maximum at a temperature at which ozone has a vapor pressure of approximately one torr (93°K). From Fig. 11 it can be seen that CO_2 also had a maximum where its vapor pressure is about 0.1 torr. In addition, the other impurities SF_6, SiF_4, H_2S, CF_4, and C_2F_6 all had maximum intensities at temperatures where their vapor pressures were in the range of 0.1 - 1.0 torr. The fact that ozone has a maximum at the upper end of this range is probably due to the fact that it is completely soluble in both O_2F_2 and O_3F_2, which would reduce its partial pressure in the vapor phase.

The mass spectrum in the temperature range of 105° - 122°K was the object of considerable investigation since this is the region in which O_3F_2 should be distilled into the mass spectrometer (the vapor pressure

of O_3F_2 has been reported[9] to be 1.0 torr at 110°K), and where O_3F_2 begins to decompose fairly rapidly into O_2F_2 and O_2. Actually, O_3F_2 should be detectable well below 94°K where it has a vapor pressure of about 0.1 torr. In the initial experiments (Fig. 12) there was a very small maximum in the OF_2^+ and O_3^+ currents and an extremely large O_2^+ current in this temperature region. It was assumed that the OF^+ and O_3^+ maxima were probably due to free OF_2 and O_3 which had been matrix trapped in the solid O_2F_2 which melts at 109°K. The O_2^+ ion current was about ten times greater than the amount that could be attributed to the small amount of ozone.

In the more recent experiments illustrated by Figs. 10 and 11 in which the reactor was pumped continuously, there were very large OF_2^+, OF^+, and F_2^+ currents in addition to the very large O_2^+ current, with all having maxima at about 114°K. The measured $A(OF^+)$ and $A(OF_2^+)$, using the diminishing current method, indicated that there was some free OF_2 present. In addition, the ratio of OF^+ and OF_2^+ was the same as that for free OF_2. It does not appear that these ions could be due to free OF_2 formed in the synthesis reaction since it has a vapor pressure of about 300 torr at 114°K and would have been pumped away at a much lower temperature. For instance, Solomon[22] has reported that free OF_2 can be essentially completely pumped away from samples of O_2F_2 below 90°K. Ozone has a vapor pressure of about 15 torr at 114°K, which is considerably lower than that of OF_2 at that temperature, and, in addition, both OF_2 and O_3 are completely soluble in O_2F_2 and O_3F_2. However, the O_3^+ ion from ozone has a maximum at a much lower temperature (95°K) than this temperature of 114°K. Therefore, it would appear

that OF_2 would have appeared with maximum ion currents at a temperature lower than 95°K. These facts indicate that the OF^+ and OF_2^+ were probably resulting from free OF_2 arising from the decomposition of O_3F_2 and not from OF_2 present from the synthesis. Similarly, the large F_2^+ current could not be due to excess F_2 from the synthesis. It has a vapor pressure of about 400 torr at 77°K and is essentially insoluble in both O_2F_2 and O_3F_2, which certainly indicates that it would have been pumped away at 77°K.

There was an appreciable amount of O_2F^+ in the temperature region of 105° - 122°K, but it appears that most of it is probably due to the initial vapors of O_2F_2 which has a vapor pressure of 0.1 torr at 117°K. In addition, the $A(O_2F^+)$ was measured to be about 14.0 ev, using the diminishing current method, which is the same value obtained for O_2F^+ from O_2F_2. However, the variation of the O_2F^+ current with temperature (see Fig. 10) indicated that at least a small fraction of it was due to the vapor phase of O_3F_2. The sharp maximum in the F^+ ion current at 118° - 122°K was probably due to an overlap of F^+ resulting from the large amount of F_2 at 105° - 122°K (apparently due to decomposition of O_3F_2) and F^+ resulting from the initially vaporizing O_2F_2.

The large O^+, O_2^+, F^+, F_2^+, OF^+, and O_2F^+ ion currents at 122° - 135°K are evidently due to fragmentation and thermal decomposition of O_2F_2 in the mass spectrometer. The fact that the parent ion, $O_2F_2^+$, was not observed resulted in consideration that the O_2F^+ and OF^+ ions were produced from the O_2F free radical. However, energy measurements showed that this was not the case, and these results will be discussed in the next section of this chapter. Without regard to the energy measurements,

it would be expected that these ions were due to O_2F_2 since it has a vapor pressure of about 1.0 torr at 130°K and should give maximum ion currents at about that temperature as was discussed earlier.

From the above discussion it seems obvious that the presence of the large amounts of O^+, F^+, OF^+, O_2^+, F_2^+, and OF_2^+ at 105° - 122°K could only be due to (a) the fragmentation of O_3F_2 or a branched isomer of O_2F_2 in the mass spectrometer, or (b) the thermal decomposition of O_3F_2 in the inlet system forming O_2, F_2, and OF_2. If the OF_2 was due to fragmentation of O_3F_2 or $O{=}{=}OF_2$, due to electron bombardment, it seems that there would probably be a much larger amount of O_2F. This would certainly be expected since the epr studies have indicated the presence of a fairly large percentage (5 - 10 per cent) of the O_2F radical in liquid O_3F_2. The fact that no positive or negative ions were detected that would indicate the presence of molecular O_3F_2 certainly suggests the possibility that it does not vaporize as a molecular species. That is, the species could possibly vaporize as O_2F and OF radicals. This would be analogous to the N_2O_3 species which vaporizes as NO_2 and NO. However, if this were the case, the appearance potentials of O_2F^+ and OF^+ would be equal to the ionization potentials of these radicals, but this did not seem to be in fact the situation as was indicated by the energy measurements using the diminishing current method. Another explanation for the failure to detect molecular O_3F_2 could be that none of the ions of the larger fragments of the species, i.e., $O_3F_2^+$, O_3F^+, $O_3F_2^-$, and O_3F^-, are stable for the 50 microseconds required for detection by the Bendix TOF machine. Since it has been reported[11,22] that O_3F_2 can be distilled at temperatures of 100° - 110°K

and no evidence for free O_2F or OF was obtained, it seems that the possibility that the larger ions are not sufficiently stable for detection is the most reasonable one.

The large amount of OF_2 at 105° - 122°K suggests the two possibilities, (a) O_3F_2 has both fluorine atoms on the same oxygen atom, or (b) O_3F_2 decomposes forming at least small amounts of OF_2. The spectrum could arise from the thermal decomposition of an appreciable amount of a branched isomer of dioxygen difluoride, $O{=}OF_2$, as was mentioned above. However, from the proposed electronic structure of this isomer of O_2F_2 (see Appendix A), one would predict that $O{=}OF_2$ would not decompose to OF_2 and O_2 since that would require a breaking of the strong O-O bond that the structure implies. In any case, there seems to be no strong basis for assuming that this branched isomer is present.

Over the past 6 - 8 years there have been many investigations of O_3F_2 as were summarized in Chapter I. However, there has been no direct determination of the structure of this species. In fact, there have been no proposed structures of this species except that of Siegel and Schieler,[72] who suggested that O_3F_2 and O_4F_2 might be O_2F_2 with one and two O atoms, respectively, loosely bonded to the O atoms of O_2F_2. The major reason for this proposal was apparently due to the fact that it would offer an easy path for decomposition into O_2F_2 and O_2 which did not appear available for other structures, such as the chain arrangement. It is obvious that the mass spectral data discussed above did not permit a definite solution to this problem. However, it seems that an attempt should be made to propose a structure for O_3F_2 and a mechanism for its thermal decomposition that would agree with the mass

spectrometric, electron paramagnetic resonance, infrared, and nuclear magnetic resonance data that are available, as well as the physical and chemical properties of the species.

A systematic analysis of the possible electronic structures of known and unknown molecules, radicals, and ions that are composed of oxygen and fluorine is presented in Appendix A of this thesis. The conclusions of this analysis will be incorporated into the following discussion without a detailed explanation. Justification for the conclusions concerning the electronic structures of the various species can be obtained from that appendix.

Since the O_3F_2 species has a well defined melting point and other characteristic physical and chemical properties, it seems quite likely that it is a molecular entity in the liquid and solid phase and possibly in the vapor phase as discussed above. Assuming that this was the case, the most likely electronic structure of this species has been concluded to be a combination of,

(A) (B)

using the description of the double quartet modification of the octet rule (see Appendix A). All four possible arrangements of the atoms were considered, and several other electronic structures appeared acceptable but not as favorable as the above two. This conclusion is quite interesting because it will be shown now that structures (A) and (B) will agree with essentially all the data available for O_3F_2. The most

important data that the model must satisfy are that (a) the liquid phase contains the O_2F free radical in concentrations of 5 - 10 per cent, (b) it decomposes primarily into O_2F_2 and O_2 but also into O_2 and OF_2 to some extent, and (c) mixtures of O_2F_2 and O_3F_2 give only a single F^{19} nmr signal and that signal simply shifts its position as the relative concentrations of O_2F_2 and O_3F_2 are changed.

Examination of the electronic structures (A) and (B) show that they both have the basic electronic features of the OF and O_2F radicals (which were discussed in Chapter I and Appendix A) joined by a single electron bond which would be expected to be quite weak. This indicated weak bond between the two oxygen-fluorine radicals should not be considered unusual in view of the fact that there are several species reported in the literature which contain relatively weakly bonded oxygen-fluorine radicals. Some examples of such species are $NO_2{\cdot}OF$, $ClO_3{\cdot}OF$, $SF_5{\cdot}OF$, $FSO_2{\cdot}OF$, and $FSO_2{\cdot}O_2F$.[37,72] Infrared studies[73] of $SF_5{\cdot}OF$ have indicated that the S-O bond in that species has a relatively low fundamental stretching frequency, being 614 cm^{-1} or 585 cm^{-1}, and that the O-F bond has a relatively high fundamental stretching frequency of 888 cm^{-1}. This would indicate that the S-O bond energy is near that of the O-F bond energy in O_2F_2 and O_2F, which have O-F fundamental stretching frequencies of 615 cm^{-1} and 584 cm^{-1}, respectively.[25] Since it has been proposed[16,19] that the O-F bonds of O_2F_2 and O_2F are single electron bonds, it might be assumed that a single electron bond between the OF and SF_5 radicals is a reasonable description of the $SF_5{\cdot}OF$ molecule. This description would certainly be analogous to the structure proposed above for O_3F_2. Epr studies[37] of the uv

irradiation products of $FSO_2 \cdot O_2F$ have shown that the FSO_2 and O_2F radicals are formed, which indicates that the S-O bond in this molecule is probably its weakest bond. This species, $FSO_2 \cdot O_2F$, would appear to be quite similar to O_4F_2, which has been shown by ir studies to have the basic features of two very loosely bonded O_2F radicals. In addition, it appears that the electronic structure of O_4F_2 seems to be reasonably well represented by two O_2F radicals joined by a single electron bond (see Appendix A).

In view of these several instances of oxygen-fluorine radicals being weakly bonded to other radicals, it seems reasonable to assume that the description of structures (A) and (B) for $FO_2 \cdot OF$ is qualitatively reasonable and that a thermal decomposition into O_2F and OF would definitely be favorable. The free radicals could then react in one of two ways, forming either O_2F_2 and O_2 or OF_2 and O_2. The entire decomposition could be represented by the following equations.

$$2FO_2 \cdot OF \overset{(I)}{\rightleftharpoons} 2FO_2 \cdot + 2FO \cdot \begin{cases} \xrightarrow[\text{fast}]{(II)} O_2F_2 + 2FO_2 \cdot \xrightarrow[\text{slow}]{(III)} 2O_2F_2 + O_2 \\ \xrightarrow{(IV)} 2OF_2 + 2O_2 \end{cases} \qquad (1)$$

Reaction II would be expected to be quite rapid since all investigations have indicated that the OF radical is extremely reactive. This dimerization of OF to O_2F_2 would certainly be energetically favorable, being exothermic by about 100 Kcal and would probably have an activation energy of zero as indicated by ir studies of the radical. Reaction III represents an abstraction of a fluorine atom from an O_2F radical by a second

O_2F radical, giving O_2F_2 and O_2. It would be expected that this would be a rather slow reaction at low temperatures in view of epr studies which indicate that O_2F is relatively long lived at 90°K. This conclusion would be further supported by the fact that the reaction of two O_2F radicals to give O_2F_2 and O_2 would be exothermic by only about 2.3 Kcal, which certainly does not represent an appreciable decrease in the energy of the system. Reaction IV represents the abstraction of a F atom from the O_2F radical by the OF radical. This reaction would certainly appear to be energetically favorable (exothermic by about 49 Kcal), but it would not seem any more favorable than the simple dimerization of OF as indicated by reaction II. Actually, it would be expected that II would possibly be much more rapid than III, since essentially every collision of two OF radicals would be expected to result in dimerization (reaction II), whereas a collision of O_2F and OF could result either in abstraction of an F atom from O_2F (reaction IV) or the reformation of $FO_2{\cdot}OF$ (reverse of reaction I).

In view of the above statements it certainly seems plausible that formation of O_2F_2 and O_2 from $FO_2{\cdot}OF$ by way of reactions I, II, and III would predominate over the formation of OF_2 and O_2 by way of reactions I and IV. This would account for the fact that other investigators have reported that O_3F_2 decomposes into O_2F_2 and O_2, but have not detected the simultaneous formation of OF_2 as indicated by the maximum ion currents that were observed in the mass spectrometer in this work at the decomposition temperature of 110° - 120°K. The fact that relatively large concentrations of the O_2F radical occur in the liquid phase of $FO_2{\cdot}OF$ would also be accounted for by the above mechanism. That is, once

an O_3F_2 molecule dissociates into FO_2 and OF and the OF radical is removed by reaction II, the O_2F radical has no favorable path for reaction except as given by reaction III which would be expected to be relatively slow.

The investigation of O_3F_2 in these studies required the distillation of the sample a distance of 40 cm from the reactor space (4) to the inlet port (10) of the mass spectrometer. During this distillation O_3F_2 would be decomposing according to the reactions I through IV, forming copious quantities of O_2, O_2F_2, and OF_2. In addition, it would be expected that some F_2 would be formed during the transfer, as well as in the spectrometer, due to decomposition of O_2F_2 into O_2 and F_2. As O_2F_2 was formed it would be condensed on the walls of the transfer tube, but the O_2, F_2, and OF_2 would not. Consequently, large quantities of these gaseous species would be emitted into the spectrometer, and the partial pressure of other species would be expected to be quite small. This would account for the relatively small O_2F^+ current that was observed.

The nmr results from a study of a mixture of O_3F_2 and O_2F_2, discussed in Chapter I, were considered rather unusual in that it would be expected that there would be two F^{19} signals, one characteristic of O_2F_2 and the other characteristic of O_3F_2, but only one signal was observed. However, the presence of a single signal would be accounted for if the exchange rate of the F atoms on the various species was very rapid; that is, if the F atoms are quite mobile. This certainly does not seem impossible in view of the very weak O-F bonds in these species. The location of the nmr signal for such a situation would depend on the

relative concentrations of O_3F_2 and O_2F_2. That is, as the concentration of the O_3F_2 was decreased and the concentration of O_2F_2 was increased, the single signal would shift in the direction of the characteristic signal of O_2F_2. When all the O_3F_2 was decomposed, only the characteristic signal of O_2F_2 would be observed. This would explain the observation of a single nmr signal from the O_3F_2 - O_2F_2 mixture and and the shift of this signal as a result of the decomposition of O_3F_2 into O_2F_2 and O_2 as the sample was warmed.

Finally, Arkell[25] has made the interesting observation that when $O^{18}F_2$ was photolyzed in an O_2^{16} matrix at 4°K, $O^{16}F_2$ was formed and $O^{18}F_2$ decreased, as was discussed in Chapter I. He suggested the following exchange mechanism involving O_3F_2 as an explanation for the formation of $O^{16}F_2$.

$$O^{18}F_2 + O_2^{16} \rightleftharpoons FO^{18}O^{16}O^{16}F \rightarrow O^{16}F_2 + O^{16}O^{18} \qquad (2)$$

He also reported that there was a simultaneous formation of the O_2F_2 molecule and the O_2F radical during this photolysis. It is obvious that the formation of the $O^{16}F_2$, as well as the O_2F and O_2F_2, would be explained by the model involving reactions I-IV for the decomposition of O_3F_2. However, there are certainly other mechanisms by which these species could be formed.

The electronic structures of O_3F_2 and its mechanism for thermal decomposition that is proposed here certainly does not represent the final word on this unusual species. However, it is interesting that a new and relatively simple qualitative theoretical analysis (the double quartet approach) of the species has led to the conclusion that O_3F_2

would be expected to have a chain structure, having the basic features of an O_2F radical and OF radical loosely bonded together, and that description seems to agree quite well with the mass spectrometric, epr, ir, and nmr data that are available, as well as the physical and chemical properties of the species. Add to that the fact that similar instances of molecules containing loosely bonded oxygen-fluorine free radicals are already known, and it seems that the proposed electronic structure and mechanism for decomposition for O_3F_2 should be considered reasonably satisfactory until more definitive data can be obtained.

Energetics of Dioxygen Difluoride

The appearance potentials of the OF^+ and O_2F^+ ions were measured at 130°K using the retarding potential difference (RPD) method[68] and linear intercept method. In addition, $A(O_2F^+)$ was measured using the semilog matching method[69] and it will be discussed later along with the energy measurements on the O_2F free radical. Figs. 15 and 16 show the ionization efficiency curves of the OF^+ and O_2F^+ ions which gave $A(OF^+) = 17.5 \pm 0.2$ ev and $A(O_2F^+) = 14.0 \pm 0.1$ ev using the RPD method. For the measurement of $A(O_2F^+)$ both argon and nitrogen were used to calibrate the energy scale, but only argon was used in the measurement of $A(OF^+)$. Figs. 17 and 18 show the ionization efficiency curves for OF^+ and O_2F^+ which gave $A(OF^+) = 17.6 \pm 0.3$ ev and $A(O_2F^+) = 14.0 \pm 0.2$ ev using the linear intercept method. In the following discussion the two values for $A(OF^+)$ and $A(O_2F^+)$ determined by the RPD method will be used to develop the energetics of the O_2F_2 molecule. This development was completed and published[74] before initiation of the O_2F free radical investigations. These latter investigations substantiated the earlier

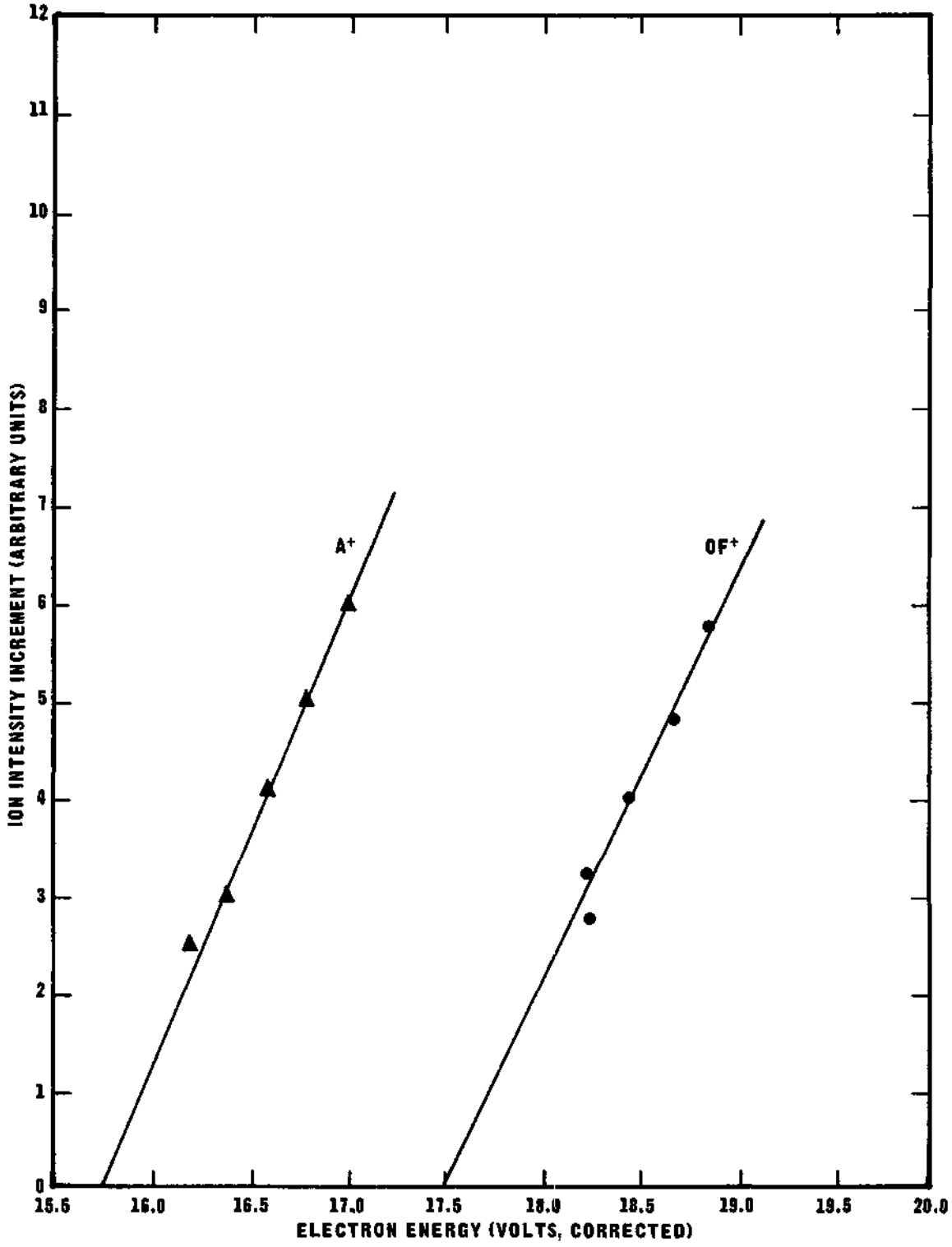

Figure 15. Ionization Efficiency Data for OF^+ from O_2F_2 Using the RPD Method with Argon as the Standard.

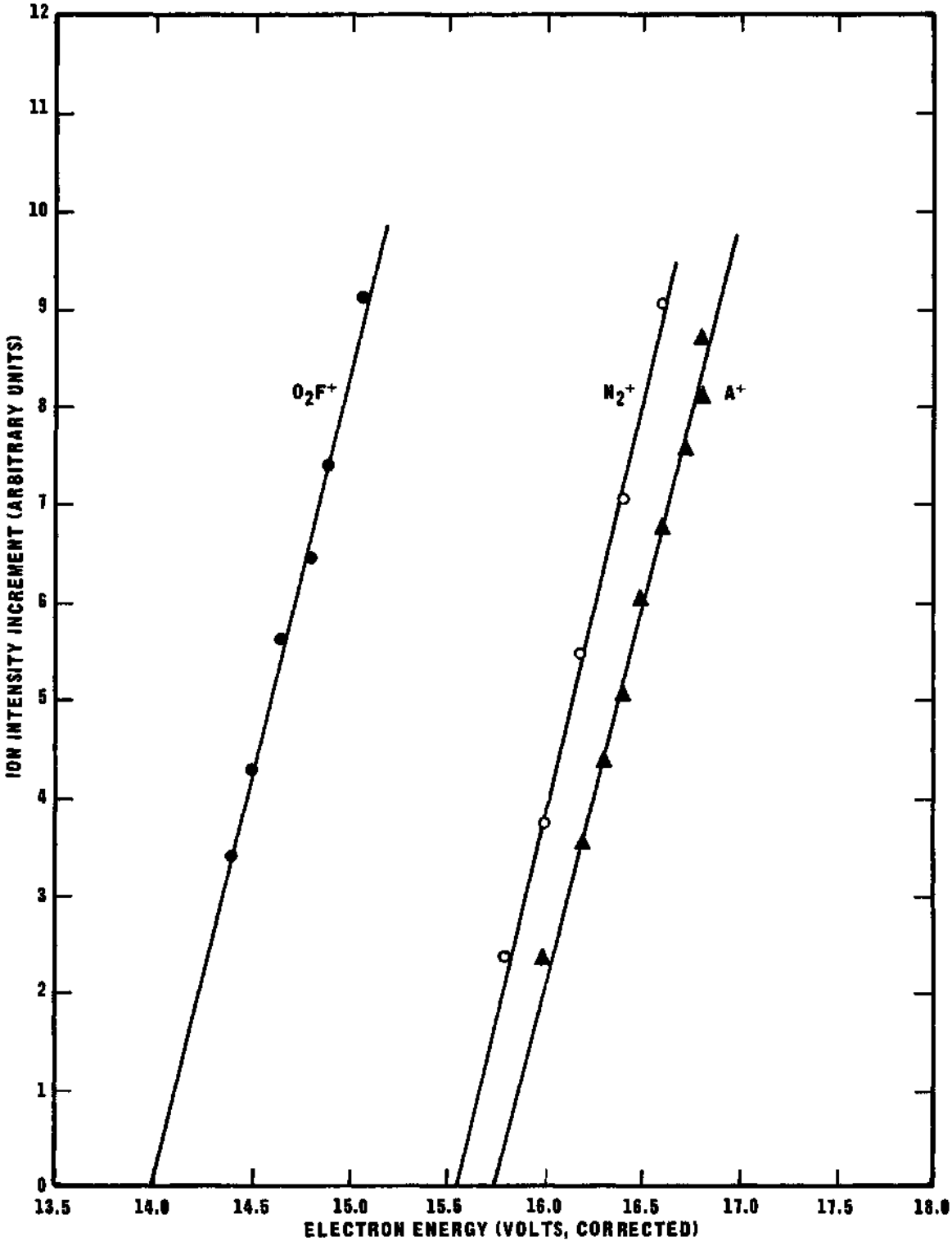

Figure 16. Ionization Efficiency Data for O_2F^+ from O_2F_2 using the RPD Method with Argon and Nitrogen as the Standards.

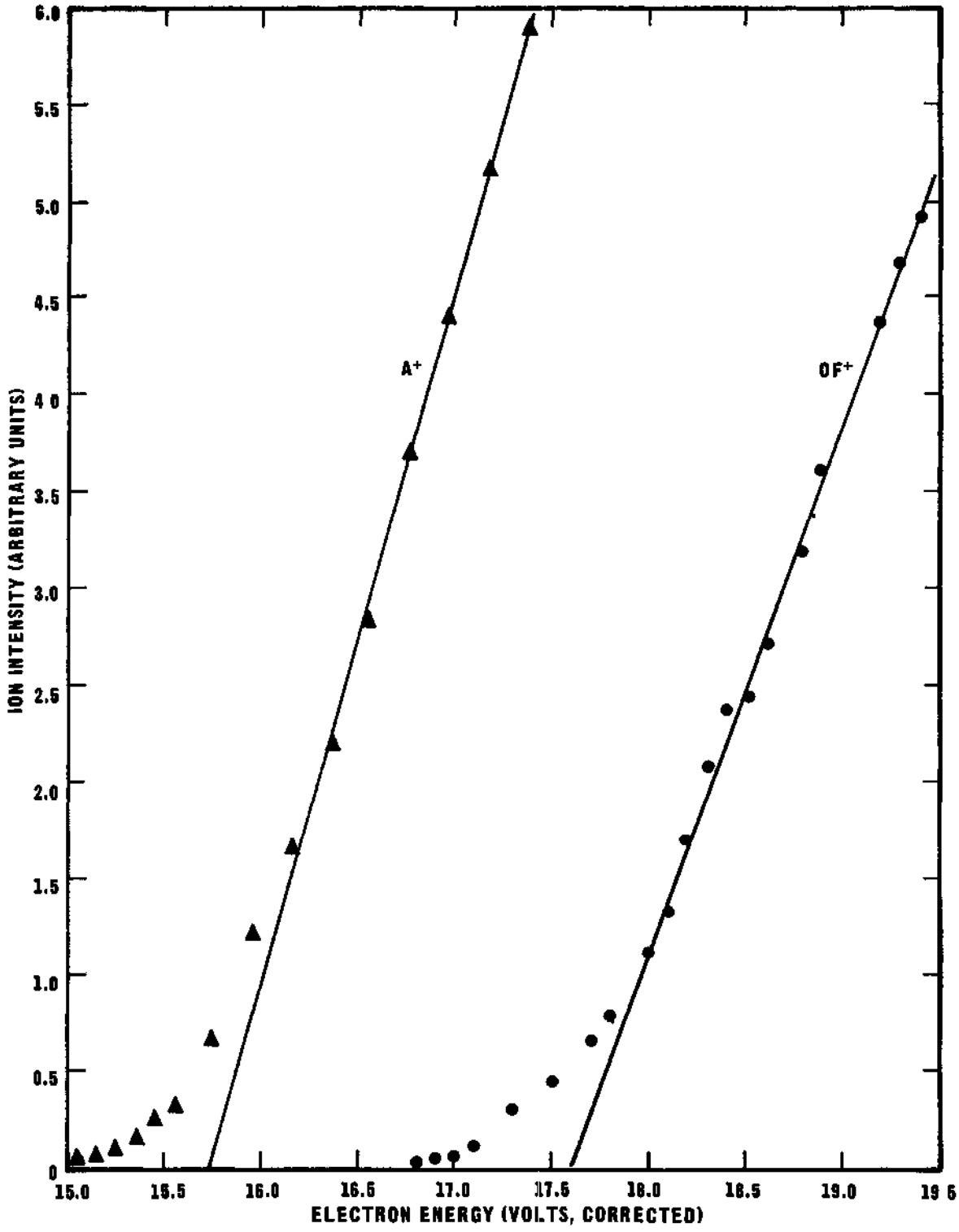

Figure 17. Ionization Efficiency Data for OF^+ from O_2F_2 With Argon as the Standard.

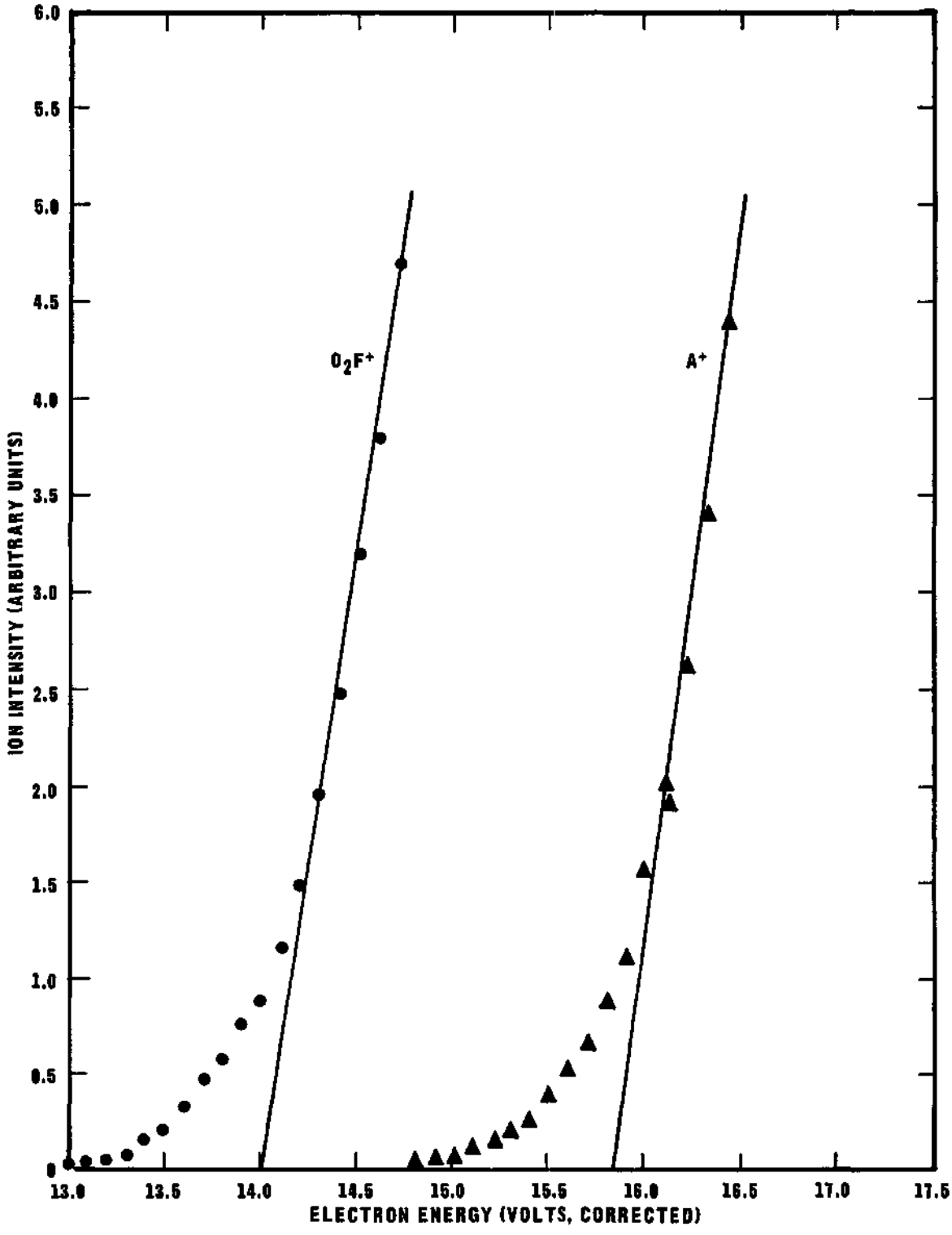

Figure 18. Ionization Efficiency Data for O_2F^+ from O_2F_2 With Argon as the Standard.

results as will be shown in the next section of this chapter. Therefore, the O_2F_2 energetics will be discussed without use of the later data on the O_2F radical, to illustrate the reasonableness of the results.

In determining the source of the O_2F^+ and OF^+ ions for which the appearance potentials were measured, several possibilities were considered, including ion pair production. However, all possibilities except the following three were easily eliminated on the basis of energetic arguments.

Case I:

$$O_2F_2 + e \rightarrow O_2F^+ + F + 2e \qquad (3)$$

and

$$O_2F_2 + e \rightarrow OF^+ + OF + 2e \qquad (4)$$

Case II:

$$O_2F_2 + e \rightarrow O_2F^+ + F + 2e \qquad (5)$$

and

$$O_2F_2 + e \rightarrow OF^+ + O + F + 2e \qquad (6)$$

Case III (Free O_2F as the Source):

$$O_2F + e \rightarrow O_2F^+ + 2e \qquad (7)$$

and

$$O_2F + e \rightarrow OF^+ + O + 2e \qquad (8)$$

For instance, assuming ion pair production for Equation (3) above, results in $D(O_2^+ - F) = -3.9$ ev which is obviously not reasonable. Dibeler, et al.,[6] made electron impact studies on the OF_2 molecule and reported

$A(OF^+)_{DRF}$ = 15.8 ev, I(OF) = 13.0 ev, and D(OF) = 1.1 ev. In the following discussion it will be shown that these energetics for OF_2 and the appearance potentials of the O_2F^+ and OF^+ ions from O_2F_2 measured in these experiments at 130°K are mutually consistent and indicate rather conclusively that these ions are fragments of the O_2F_2 molecule formed by the processes represented by Equations (3) and (4) in Case I. Therefore, this case will be discussed first, and justification for elimination of Cases II and III will be discussed last. In view of the fact that Arkell,[56] et al., have estimated that D(O-F) might be as high as 2.4 ev from their infrared studies and kinetic data[47,49] have indicated it is about 2.1 ev, the effect on the energetics of O_2F_2 using this larger value will be discussed; but it will be shown that the results are not consistent with existing thermochemical and microwave data.

Case I. Neglecting any excess kinetic energy or internal excitation, the appearance potentials are given by

$$A(O_2F^+)_I = D(F\text{-}O_2F) + I(O_2F) \qquad (9)$$

and

$$A(OF^+)_I = D(FO\text{-}OF) + I(OF) \qquad (10)$$

From our measured $A(OF^+)_I$ of 17.5 ev and Equation (10), the O-O bond energy in O_2F_2 can be calculated directly. D(FO-OF) = 17.5 - 13.0 = 4.5 ± 0.2 ev or 103.5 ± 5 Kcal. This results in an experimental energy of atomization for O_2F_2, $E_a(O_2F_2)_E$, of 103.5 + 2(25.4) = 154.3 Kcal = 6.7 ev, for the process $O_2F_2 \rightarrow 2(OF) - 2(O) + 2(F)$. Since the the heat of formation of O_2F_2 has been measured calorimetrically,[12] the energy of atomization can also be calculated thermodynamically using

$\Delta H_f^o(O_2F_2)$ = 4.7 Kcal/mole, $\Delta H_f^o(O)$ = 59.2 Kcal/mole and $\Delta H_f^o(F)$ = 18.9 Kcal/mole to give a heat of atomization at 298°K of 6.55 ev. Calculations have shown that this value is equal to the thermochemical energy of atomization, $E_a(O_2F_2)_T$, at 130°K within the experimental error, and it is seen to agree very well with the value obtained from our low temperature electron impact data.

The consistency of the $A(OF^+)$ from O_2F_2 obtained in our experiments and the data reported by Dibeler, et al.,[6] (DRF) in their investigation of OF_2 can be better illustrated by the following equation,

$$E_a(O_2F_2)_E = A(OF^+)_I - A(OF^+)_{DRF} - A(F^-) - EA(F) + K.E. + 2E_a(OF_2)_T \quad (11)$$

where $A(F^-)$ = 1.2 ev and K.E. = 2.0 ev are the appearance potential of the negative fluorine atom and the excess kinetic energy respectively measured by DRF for the process $OF_2 + e \sim OF + F^- + K.E.$ EA(F) = 3.6 ev is the electron affinity of the fluorine atom and $E_a(OF_2)_T$ = 3.9 ev is the thermochemical energy of atomization of OF_2 calculated from its heat of formation of 7.6 Kcal. Substituting these values into Equation (11) gives $E_a(O_2F_2)_E = 17.5 - 15.8 - 1.2 - 3.6 + 2.0 + 2(3.9) = 6.7$ ev which is in very good agreement with $E_a(O_2F_2)_T$ = 6.55 ev.

This excellent agreement between $E_a(O_2F_2)_T$ and $E_a(O_2F_2)_E$ indicates that the experimental values obtained by DRF and our measured $A(OF^+)_I$ are reasonably accurate and the process given by Equation (4) really does occur without any significant excess kinetic energy. This in turn would indicate that the resulting D(FO-OF) = 4.5 ev is a good value. The fact that this bond energy is nearly as large as that of O_2, $D(O_2)$ = 5.08 ev, also agrees qualitatively with the microwave data of

Jackson[2] who reported a very short O=O bond length in O_2F_2 of 1.22 Å which is nearly equal to the bond length in O_2 of 1.21 Å. It also agrees with the following electronic structures proposed for FOOF

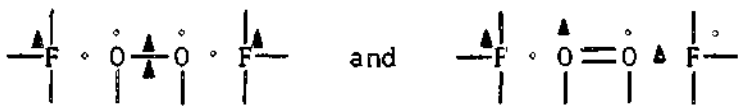

(C) (D)

(see Appendix A) in which the O - O bond is a four electron bond.

Since the energy of atomization of a molecule is independent of the path followed, we can write

$$E_a(O_2F_2)_E = 6.7 \text{ ev} = D(F\text{-}O_2F) + D(O_2\text{-}F) + D(O_2) \quad (12)$$

$$= D(F\text{-}O_2F) + D(O\text{-}OF) + D(OF) \quad (13)$$

From the known bond energy of oxygen, $D(O_2) = 5.1$ ev, and Equation (12)

$$D(F\text{-}O_2F) + D(O_2\text{-}F) = 6.7 - 5.1 = 1.6 \text{ ev} \quad (14)$$

and from Equation (13)

$$D(F\text{-}O_2F) + D(O\text{-}OF) = 6.7 - 1.1 = 5.6 \text{ ev} \quad (15)$$

Equation (14) shows that the O-F bonds in O_2F_2 are unusually weak. This also agrees qualitatively with the microwave results which indicated an unusually long O-F bond length of 1.58 Å for this molecule, as well as the proposed structures (C) and (D) in which the O-F bonds are single electron bonds.

In order to calculate D(O - OF) from Equation (15), it is

necessary to estimate the relative values of $D(F-O_2F)$ and $D(O_2-F)$. A reasonable assumption would be that these two bond energies are equal. This would give $D(F-O_2F) = D(O_2-F) = 0.8$ ev. Actually, we might expect $D(F-O_2F)$ to be 10-15 per cent greater than $D(O_2-F)$, but this would result in an error of only ~ 0.1 ev in the estimated value of 0.8 ev. Levy and Wesley[60] have estimated that $D(O_2-F) = 15$ Kcal = 0.7 ev from kinetic data[61] on the thermal decomposition of O_2F_2.

Using the estimated value of $D(F-O_2F) = 0.8$ ev, Equation (15) gives $D(O-OF) = 5.6-0.8 = 4.8$ ev = 110 Kcal. This appears qualitatively in the right range since we would expect $D(O-OF)$ to be greater than $D(FO-OF)$ which was found to be 4.5 ev, and it would certainly be less than $D(O_2)$ of 5.08 ev. In view of this last statement, we would also have predicted from Equation (15) that $D(F-O_2F)$ would be less than $5.6-4.5 = 1.1$ ev and certainly greater than $5.6-5.1 = 0.5$ ev. Using these extreme limits we would say that $D(F-O_2F) = 0.8 \pm 0.3$ ev which is the value obtained above by simply assuming that $D(F-O_2F) = D(O_2-F)$.

We have not needed our measured appearance potential of the O_2F^+ ion, $A(O_2F^+) = 14.0 \pm 0.1$ ev, to obtain any of the above results, but it is needed to estimate the ionization potential of the O_2F free radical. In order to qualitatively check the consistency of the measured $A(O_2F^+)$ and the assumption that no excess kinetic energy is formed in the process given by Equation (3), the energy of atomization can be written as

$$E_a(O_2F_2)_E = A(O_2F^+)_I + D(O_2^+-F) + D(O_2^+) - I(O) \qquad (16)$$

Using the known values of $D(O_2^+) = 6.48$ ev and $I(O) = 13.6$ ev, Equation (16) gives $D(O_2^+ - F) = 6.7 - 14.0 - 6.48 + 13.6 = -0.18$ ev. This would indicate that the O_2F^+ ion is unstable, but we know that it is stable for at least 50 microseconds since it is observed in the mass spectrometer. The most reasonable explanation of this observation is that the formation of the O_2F^+ ion is actually accompanied by at least a small amount of excess kinetic energy. Without actually measuring the excess kinetic energy, an accurate value for $I(O_2F)$ cannot be calculated. However, using the observed $A(O_2F^+)_I = 14.0$ ev gives an upper limit from Equation (9) of $I(O_2F) \leq 14.0 - 0.8 = 13.2$ ev. A reasonable estimate of the excess kinetic energy can be made from an analogy with the hydrogen peroxide molecule. The dissociation energies of the analogous species from H_2O_2 have been measured[95] by electron impact methods to be $D(H - O_2) = 2.0$ ev and $D(H - O_2^+) = 1.9$ ev, or the dissociation energies of the free radical and the ion are essentially equal. If we assume that this is the case for the O_2F_2 molecule, then $D(O_2^+ - F) = D(O_2 - F) = 0.8$ ev. Then we can calculate a probable upper limit of the excess kinetic energy from the following equation,

$$E_a(O_2F_2)_E = 6.7 = A(O_2F^+)_I - K.E. + D(O_2^+ - F) + D(O_2^+) - I(O) \quad (17)$$

This gives $K.E. = 14.0 + 0.8 + 6.48 - 13.6 - 6.7 = 1.0$ ev. Making a correction for this excess energy of 1.0 ev in Equation (9) gives an approximate value of $I(O_2F) = 14.0 - 1.0 - 0.8 = 12.2$ ev. This seems like a reasonable value in view of the fact that $I(O_2) = 12.2$ ev and $I(HO_2) = 11.5$ ev.[70] The fact that this estimated value of $I(O_2F)$ is equal to $I(O_2)$ is coincidental, but we would expect that it would probably be

between $I(O_2)$ and $I(HO_2)$ since the fluorine atom is only loosely bonded to O_2 in O_2F.

Since the parent peak of O_2F_2 was not observed, it is impossible to measure the $I(O_2F_2)$ directly, but we can say that $I(O_2F_2) \leq A(O_2F^+) = 14.0$ ev. This gives a maximum for $I(O_2F_2)$, but a more reasonable value would be nearer 13.0 ev, which takes into account the estimated excess kinetic energy of 1.0 ev.

Case II. The appearance potential of the O_2F^+ ion is the same as in Case I and is given by Equation (9). The appearance potential of the OF^+ ion is given by

$$A(OF^+)_{II} = D(F - O_2F) + D(O - OF) + I(OF) \qquad (18)$$

The $A(OF^+)_{II}$ required for this process can be readily calculated from Equation (18) using $D(F - O_2F) + D(O - OF) = E_a(O_2F_2)_T - D(OF) = 6.6 - 1.1 = 5.5$ ev. This gives $A(OF^+)_{II} = 5.5 + 13.0 = 18.5$ ev, which is 1.0 ev greater than the measured value of 17.5 ev which means that the process of Equation (6) is not correct.

Case III. In this case it is assumed that the O_2F^+ and OF^+ ions are arising from the O_2F free radical. Therefore, $A(O_2F^+)_{III} = I(O_2F) = 14.0$ ev and the appearance potential of the OF^+ ion is given by

$$A(OF^+)_{III} = I(O_2F) + D(O - OF^+) \qquad (19)$$

Equation (19) gives $D(O - OF^+) = 17.5 - 14.0 = 3.5$ ev. From the relation

$$D(O - OF^+) + D(O^+ - F) = D(O_2^+ - F) + D(O_2^+) \qquad (20)$$

and the dissociation energy of the OF^+ ion, $D(OF^+) = 1.7$ ev, reported

by DRF,[6] a value of $D(O_2^+ - F) = 3.5 + 1.7 - 6.48 = -1.3$ ev is obtained. This is an unlikely value and indicates that the observed appearance potentials are not consistent for the assumption of a free O_2F radical.

Since there are no other processes that are energetically reasonable and the results obtained for Case I are consistent with both the available thermochemical and microwave data, it seems evident that the O_2F^+ and OF^+ ions are formed by the processes given by Equations (3) and (4).

If the dissociation energy of OF is equal to about 2.1 ev as indicated by kinetic[47,49] and infrared studies,[56] rather than 1.1 ev, as measured by DRF, then it appears that the ionization potential of OF of 13.0 ev would also be 1.0 ev too low. This would certainly seem to be the case since the $A(OF^+) = 15.8$ ev from OF_2 reported by DRF was verified in this work, so $I(OF) = A(OF^+) - D(F - OF) = A(OF^+) - E_a(OF_2)_T + D(O - F) = 15.8 - 3.9 + 2.1 = 14.0$ ev. In addition, the appearance potential of OF^+ from O_2F_2 measured in this work would be too high for the mechanism given by Equation (4). As shown earlier from thermochemical data, $E_a(O_2F_2) = 6.6$ ev $= D(FO - OF) + 2D(O - F)$. Therefore, for $D(O - F) = 2.1$ ev, $D(FO - OF) = 2.4$ ev, so $A(OF^+)$ for Equation (1) can be calculated from Equation (20) to be 16.4 ev which is 1.1 ev lower than the measured value of 17.5 ev. This certainly does not seem possible since it would be expected that the measured $A(OF^+)$ would be too low, if any thing, as a result of small amounts of free OF_2 that might be present. This indicates that mechanisms other than Equation (4) for the formation of OF^+ should be considered. If the mechanism were given by Equation (6), then $A(OF^+)$ can be calculated to be 18.8 ev which does not

seem reasonable since it is 1.3 ev higher than the measured value. If the mechanism involved ion pair production as follows,

$$O_2F_2 + e \rightarrow OF^+ + OF^- + e \qquad (21)$$

the $A(OF^+)$ should be about equal to 16.4 - EA(OF) which is certainly not reasonable. If the process

$$O_2F_2 + e \rightarrow OF^+ + O + F^- + e \qquad (22)$$

were occurring, then $A(OF^+)$ should be 18.8 - EA(F) = 18.8 - 3.6 = 15.2 ev which is definitely too low. Therefore, it appears that there is no mechanism for formation of OF^+ that would be consistent with its measured appearance potential of 17.5 ev and a OF bond energy of 2.1 ev. Regardless of these facts, the O - O bond energy of 2.4 ev calculated above for O_2F_2 using only thermochemical data[12] seems too low in view of the microwave data[2] which indicated that its bond length was essentially equal to the bond length of O_2. In addition, the infrared studies have indicated that the O - O force constant in these higher oxygen fluorides is very close to that of O_2. Both of these studies, as well as the proposed electronic structures, (C) and (D), would indicate a very strong O - O bond in O_2F_2 relative to that in H_2O_2. However, Foner and Hudson[70] have reported the D(HO - OH) = 2.2 ev which is essentially equal to D(FO - OF) = 2.4 ev obtained for the case where D(O - F) is taken to be the high value of 2.1 ev. Using D(O-F) = 2.4 ev as suggested by Arkell from his infrared studies, D(FO - OF) = 1.8 ev is obtained which is even lower than D(HO - OH). It should also be noted that the O - O bond energy in the O_2F radical can also be calculated from

thermochemical data, using $D(O - F) = 2.1$ ev, to be 3.7 ev which also appears too low in view of the infrared data for this species reported by Arkell. He calculated an $O - O$ force constant of 10.45 mdynes/Å for O_2F as compared to 11.8 for O_2. The electronic structures proposed for O_2F (see Appendix A) also indicate a very strong $O - O$ bond. In view of the above facts, it seems necessary to assume that the energetics of O_2F_2 obtained using $D(O - F) = 1.1$ ev, are reasonably correct. However, it is obvious that an accurate measurement of $I(OF)$ or $D(O - F)$ is highly desirable in that it would remove any doubt associated with the above arguments.

Synthesis and Energetics of the Dioxygen Fluoride Free Radical

In the previous section in which the energetics of the O_2F_2 molecule were developed, the bond energies of the O_2F radical were also determined. In addition, the ionization potentials of O_2F and O_2F_2 were estimated using an excess kinetic energy of 1.0 ev for the process given by Equation (3). This excess kinetic energy was calculated assuming that $D(O_2 - F) = D(O_2^+ - F) = 0.8$ ev. From these results it is obvious that a direct measurement of the ionization potential of O_2F was certainly desirable. This served as an added incentive for synthesizing the O_2F radical as a free species for this thesis. Obviously, the most intriguing reasons for preparing this species was to prove the existence of a free radical of oxygen and fluorine and, in particular, to show that O_2F really did exist as predicted using the theoretical arguments of the double quartet modification of the octet rule.[19]

In this investigation, O_2F_2 was synthesized in the cryogenic

reactor-inlet system with the extension piece (16) replaced by the furnace attachment described in Chapter II. By vaporizing the sample through the heated alumina tube which extended directly into the ionizing electron beam of the spectrometer, the O_2F free radical was formed by pyrolysis and permitted a direct measurement of $I(O_2F)$ and calculation of $I(O_2F_2)$.

The optimum position of the furnace in the electron beam was determined by setting the energy of the ionizing electrons about 2.0 ev above $A(O_2F^+)$ from O_2F_2 and then moving the furnace in and out of the beam until the position corresponding to a maximum O_2F^+ current was obtained. With the electron energy decreased to a level at which no O_2F^+ was formed from O_2F_2, the temperature of the furnace was slowly increased while monitoring the O_2F^+ current. A maximum value of this ion current was obtained when the pyrolysis was conducted at approximately 250°K. It is notable that the position of the furnace in the electron beam was very critical, in that moving it either into the beam or withdrawing it from the beam by less than 6 mm from the point at which the maximum O_2F^+ ion current was obtained, resulted in such a decrease in ion intensity that the O_2F radical was barely detectable. This was certainly to be expected from the earlier sensitivity calculations that are discussed in Appendix B and summarized in Chapter II. The ionization potential of O_2F was determined using the semilog matching method[69] with argon as the reference species. In addition, the appearance potential of O_2F^+ from O_2F_2 was obtained using this same technique and was compared with the value obtained by the retarding potential difference (RPD) method[68] which was used in the initial work. The energy scale was calibrated with the heater on and off using argon as the standard, and the results were identical.

The ionization potential of O_2F was determined to be 12.6 ± 0.2 ev, while the appearance potential of O_2F^+ from O_2F_2 was 14.0 ± 0.1 ev which is the same value that was reported earlier using the RPD method.[74] Figs. 19 and 20 show the semilogarithmic plot of the data used to determine these values for the O_2F radical and O_2F fragment from O_2F_2, respectively. The excess kinetic energy for the process of Equation (3) is given by K.E. = $A(O_2F^+)$ - $I(O_2F)$ - $D(F - O_2F)$. Using an estimated $D(F - O_2F)$ = 0.8 ev and the above measured values for $I(O_2F)$ and $A(O_2F^+)$, the kinetic energy is calculated to be 14.0 - 12.6 - 0.8 = 0.6 ev, and therefore, $I(O_2F_2) + D(F - O_2F^+) = A(O_2F^+) - K.E. = 14.0 - 0.6 = 13.4$ ev. In view of the fact that the $O_2F_2^+$ ion is not observed in the mass spectrometer, it could be assumed that $D(F - O_2F^+) = 0$, and hence $I(O_2F_2)$ = 13.4 ev. However, since it could well be that $D(F - O_2F^+) \neq 0$, the value of $D(O_2F_2)$ = 13.4 ev is best considered to be the maximum possible value. The bond energies of the O_2F^+ ion can also be calculated directly to be $D(O_2^+ - F) = D(O_2 - F) + I(O_2) - I(O_2F) = 0.8 + 12.2 - 12.6$ = 0.4 ev, and $D(O - OF^+) = D(O_2^+ - F) + D(O_2^+) - D(OF^+) = 0.4 + 6.5 - 1.7^6$ = 5.2 ev. Both of these values seem reasonable in view of the bond energies of the O_2F radical of $D(O_2 - F)$ = 0.8 ev and $D(O - OF)$ = 4.8 ev that were previously obtained. They also agree quite well with the electronic structure proposed for O_2F^+ in Appendix A.

It is obvious that the energetics of O_2F determined in this investigation is quite consistent with the independent development of the energetics of O_2F_2. In summary it appears that the bond energies obtained for these two species, using the electron impact data on O_2F_2 and O_2F from this work and the data for OF_2 reported by DRF, are quite

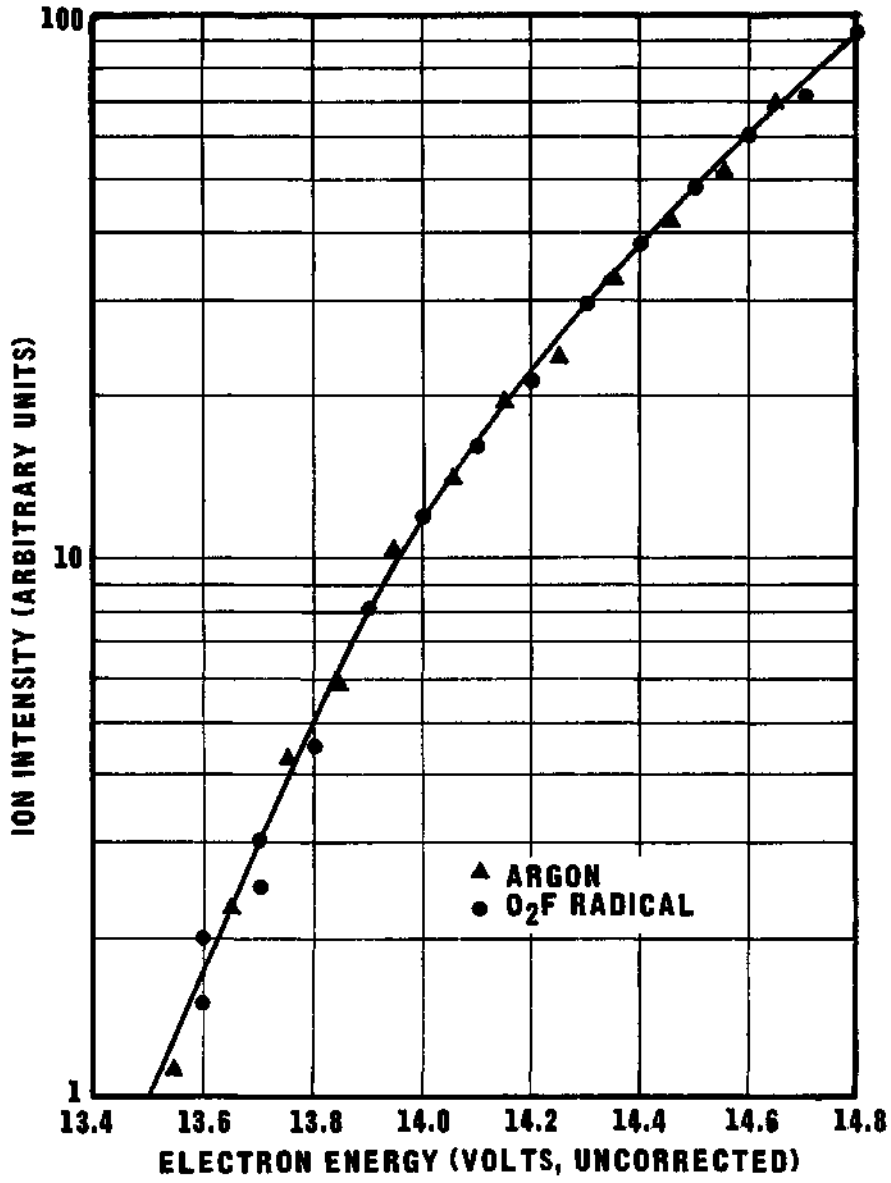

Figure 19. Ionization Efficiency Data for O_2F^+ from the O_2F Free Radical Using the Semilog Matching Method. Argon is the Standard and the O_2F Scale has been Shifted 3.15 ev to Yield the Indicated Superposition.

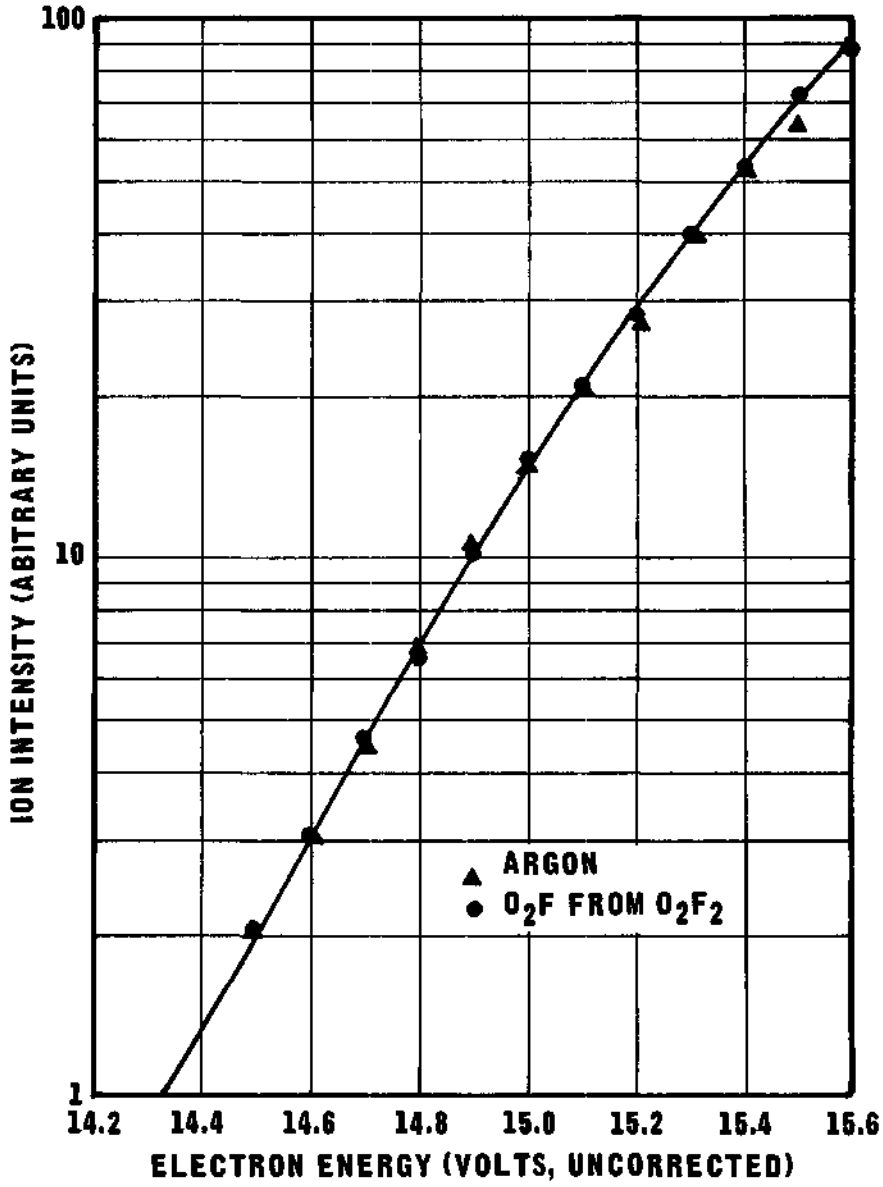

Figure 20. Ionization Efficiency Data for O_2F^+ from O_2F_2 Using the Semilog Matching Method. Argon is the Standard and the O_2F Scale has been Shifted 1.78 ev. to Yield the Indicated Superposition.

consistent with the microwave, kinetic, and infrared data for them, as well as their electronic structures that have been proposed using the double quartet description. Hence, it seems that these results should be considered reasonably accurate, despite the controversy concerning the bond energy of OF. These energetics for O_2F and O_2F_2, along with the mass spectrometric cracking pattern of O_2F_2, are summarized in Table 3.

It should be pointed out that attempts were made to synthesize the O_2F radical by subjecting gaseous $O_2 - F_2$ mixtures and $O_2 - OF_2$ mixtures to an electrodeless radio frequency discharge using the arrangement described in Chapter II. In these experiments a large excess of oxygen was normally used. Similar experiments have been performed successfully by Foner and Hudson[69] in their production of the HO_2 free radical. In addition, they showed that a confined electrodeless low-power glow discharge in a rapidly flowing stream of H_2O_2 vapor was an excellent source of HO_2 radicals. They also formed HO_2 by several other techniques such as reacting H atoms with O_2. Similar experiments with $O_2 - F_2$ mixtures and $O_2 - OF_2$ mixtures were conducted in this work over broad pressure and discharge power input ranges, but there was no evidence for formation of the O_2F radical. An exhaustive study of this technique for preparing O_2F was not conducted since the pyrolysis technique had already been proved to be quite successful. However, this approach might be considered further for future investigations of O_2F since it would not require synthesis of O_2F_2 which must be prepared and handled at cryogenic temperatures.

These investigations of O_2F were particularly satisfying in that

Table 3. Relative Abundance and Appearance Potentials of Positive Ions in the Mass Spectrum of O_2F_2: Energetics of the O_2F_2 Molecule and O_2F Radical

Ion	Relative Abundance (%)	Appearance Potential (ev)	Energetics
$O_2F_2^+$	-	-	$I(O_2F_2) \leq 13.4$ ev
O_2F^+	100	14.0 ± 0.1	$I(O_2F) = 12.6 \pm 0.2$ ev
OF^+	10.1	17.5 ± 0.2	$I(OF) = 13.0$ ev[b]
O_2^+	$(1020)_a$	-	$D(F - O_2F) = 0.8$ ev
O^+	$(305)_a$	-	$D(FO - OF) = 4.5 \pm 0.2$ ev
			$D(O_2 - F) = 0.8$ ev
F_2^+	$(300)_a$	-	$D(O - OF) = 4.8$ ev
F^+	$(120)_a$	-	$D(OF) = 1.1$ ev[b]
			$D(O - OF^+) = 5.2$ ev
			$D(O_2^+ - F) = 0.4$ ev

[a] Includes large background due to decomposition of O_2F_2 in the spectrometer.

[b] From Dibeler, et al.[6]

they represented the synthesis of an oxygen-fluorine free radical that had been predicted to be stable by theoretical arguments; they demonstrated the usefulness of the cryogenic reactor-inlet system for synthesizing and investigating the initial pyrolysis products of thermally unstable species; and they supported the validity of the sensitivity calculations discussed earlier which indicated that detection of extremely unstable or reactive species would require their synthesis almost directly in the electron beam of the mass spectrometer.

Investigation of the OF Free Radical

In the previous two sections it was pointed out that there was considerable controversy regarding the bond energy of the OF radical. Since the development of the energetics of all of the other oxygen fluorides depends, at least partially, on the ionization potential or the bond energy of this radical, it is obvious that a direct measurement of one of these values is highly desirable. However, the only reported direct identification of this species was from infrared studies[56] in which OF_2 was irradiated at 4°K in a solid matrix (see Chapter I), and hence no direct study of the energetics of the species has been possible. In view of the numerous indirect evidences as well as the great interest in this radical, several techniques were used in this work in an attempt to synthesize and investigate it.

Several kinetic studies have indicated that pyrolysis and photolysis of OF_2 results in the formation of OF as a short-lived intermediate. Hence, it seemed that a pyrolysis of OF_2 directly in the electron beam of the mass spectrometer could well result in detection of the OF radical.

Pyrolysis experiments of OF_2 in a mass spectrometer reported by Dauerman, Salser, and Tajima[49] were discussed in Chapter I. In these experiments in which a nickel furnace was used, no evidence for free OF was obtained. However, the exit of their furnace was about 1.9 cm from the electron beam. According to the sensitivity calculations discussed earlier and summarized in Appendix B, the sensitivity for such an arrangement would be expected to be a factor of about 65 - 95 less than an arrangement in which the electron beam is in grazing incidence with the furnace exit. Since the concentration of OF formed in this type of experiment would possibly be quite small, it is obvious that the unfavorable arrangement used by Dauerman, et al., could have prevented its detection.

In this work OF_2 was pyrolyzed using several different filaments and furnaces using the optimum arrangement of the filament or the furnace relative to the electron beam. For the experiments using hot filaments, the arrangement and techniques described in Chapter II were used. Filaments of niobium, tantalum, platinum, titanium, molybdenum, zirconium, tungsten, and nichrome were used and the results are summarized in Table 4. From this table it can be seen that the nature of the OF_2 pyrolysis differed considerably with some choices of filaments.

Molybdenum and nichrome both gave very small yields of F_2, but the OF_2 molecule was not cracked to any appreciable extent on these filaments even at 900°C. In these experiments the electron energy was set at an energy (14 - 15 ev) such that only a very small OF^+ current from OF_2 could be detected with the filament off. Then the ratio of the OF_2^+ to OF^+ was measured as the temperature of the filament was increased. For both the molybdenum and nichrome filaments the OF_2^+/OF^+

Table 4. Results of Hot Filament Pyrolyses of OF_2

Filament	Decomposition Temperature, °C	Approximate Per Cent Decomposition	Decomposition Products	Comments
Niobium	600 - 700	90 - 95	Very large F_2 yield; Small O_2 yield; No OF detected.	--
Tantalum	550 - 750	70 - 80	Very large F_2 yield; Small O_2 yield; No OF detected.	Very high noise level above 750°C.
Platinum	700	70 - 80	No OF detected	Extremely high noise level, even below 700°C.
Titanium	650 - 750	50 - 60	Very large F_2 yield; Small O_2 yield; No OF detected.	Very high noise level above 750°C.
Molybdenum	800	15 - 25	Very small F_2 yield; No O_2 detected; Evidence of small OF yield.	Noise level low below 800°C, but was fairly high above 900°C.
Zirconium	650 - 750	70 - 80	Very large F_2 yield; Small O_2 detected; No OF detected.	--
Tungsten	750	10	--	Extremely high noise level at 700°C.
Nichrome	800 - 900	10 - 20	Very small F_2 yield; Small O_2 yield; Evidence of small OF yield.	Noise level was quite high above 900°C.

ratio decreased from 20 at room temperature to about 10 at 800° - 900°C for an electron energy of about 14 ev (energy scale was not calibrated). The OF_2^+ current decreased with increasing temperature while the OF^+ current increased. The decrease in the OF_2^+/OF^+ ratio indicates the possible formation of small amounts of free OF, but variation of the filament temperature and OF_2 flow rate failed to increase its yield significantly. There still was not enough OF^+ at 900°C to permit a measurement of its appearance potential, and above 900°C the noise level was too high to operate.

Niobium, tantalum, titanium, and zirconium all gave very large amounts of F_2, very small amounts of O_2, and no evidence at all for free OF. It is interesting to note that an appreciable F_2^+ ion current was observed in these experiments even when the energy of the ionizing electron beam was reduced to zero. This, as well as the fact that essentially no O_2 was observed, indicated that the OF_2 molecule was decomposing directly into O and F_2 on the surface of the hot filament and the F_2 was in turn ionized on the hot surface. This conclusion that F_2^+ was formed by surface ionization is further supported by the fact that it gave a broad and poorly resolved peak which would be expected since there would be a relatively broad spatial distribution of the ions in the source. This spatial distribution would result in a broadening of the F_2^+ peak since all the ions would not arrive at the mass analyzer at the same time.

The apparent direct formation of F_2 on the surface of these latter filaments is quite interesting in view of the kinetic data for the pyrolysis of OF_2. Several investigators have proposed that OF_2 decomposes

first to F and OF. Assuming this mechanism, they have calculated a critical energy for the process, presumably D(F - OF), of about 40 Kcal/mole which results in an estimated D(O - F) of about 50 Kcal/mole. It has already been shown that this value for D(O - F) appears too high in view of the O - O bond energy that it would require for O_2F_2. This suggests the possibility that the critical energy measured in the kinetic experiments is for some process other than the formation of F and OF. In view of the large amount of F_2 and small amount of O_2 occurring from a single collision with a hot filament as indicated by the above mass spectrometric experiments, it seems reasonable to consider the reaction,

$$OF_2 \rightarrow O + F_2 \qquad (23)$$

as the initial step in the thermal decomposition of OF_2. In fact, it has already been pointed out[46] that the energetics of Equation (23) would also agree with the kinetic data, but the mechanism involving the formation of OF was considered more likely since OF_2 has been shown to react with various species by adding an OF group.

The formation of large amounts of F_2 on the surface of the hot filaments in the above experiments also suggested the possibility that the decomposition was catalyzed by the metal surface. Consequently, OF_2 was pyrolyzed using an alumina furnace and the same technique as was employed in the pyrolysis of O_2F_2 to form O_2F. In these experiments the OF_2 was 50 - 75 per cent cracked at temperatures of 450° - 600°C, but there was no evidence for formation of OF. Only very large amounts of O_2 and F_2, as well as possibly some O and F, were observed. In

a similar experiment using a bundle of four 0.050 cm ID x 1.3 cm long monel tubes inside a 0.635 ID monel tube for the furnace, essentially the same results were obtained, but the decomposition occurred at a somewhat lower temperature than in the alumina furnace. There was only slight decomposition of the OF_2 below 368°C using this monel furnace, but above that temperature there was an extremely rapid decrease in the OF_2^+ ion current. For instance at 373°C, only 5°C above the temperature at which OF_2 began to decompose rapidly, essentially all the OF_2 was cracked, but no free OF was observed.

The failure to prepare an appreciable amount of OF by pyrolysis of OF_2, or even to prove conclusively that OF was formed at all, made it necessary to consider other possible techniques for its synthesis. Cracking of OF_2 with a low power electrodeless discharge was considered a likely possibility . Hence, several experiments were run in which OF_2 was cracked in a radio frequency discharge tube as described in Chapter II. In the initial experiments, wherein a quartz tube was used, the only products observed were very large amounts of O_2, F_2, and SiF_4. Essentially all the OF_2 was cracked when the glow of the discharge was bright enough to be observed, regardless of the energy input, reactor pressure, or OF_2 flow rate used. The large amount of SiF_4 that was formed in these experiments indicated that F atoms were reacting quite rapidly with the quartz reactor tube. This suggested the possibility that any OF radical that was formed was destroyed immediately on the quartz surface. Therefore, the quartz tube was replaced by an alumina tube and the experiments repeated. This eliminated the formation of SiF_4, but still no evidence was obtained for the presence of

free OF. Only large quantities of O_2 and F_2 were observed. In some of these experiments excess O_2 was added to the OF_2, but the results were essentially the same.

From the above results of the investigations of the possible existence of the OF radical in the vapor phase, it was concluded that this species is quite unstable and/or extremely reactive. This is exactly the conclusion that numerous other investigators have reached. The hot filament experiments described above, using molybdenum and nichrome, indicated the possible formation of very small amounts of OF. However, the other filaments, which cracked the OF_2 molecule much more readily, gave no evidence for the formation of OF. In view of the facts that this technique utilized the very best physical arrangement of the filament, i.e., directly in the electron beam, and the OF_2 molecule could experience only a single collision with the filament, it was concluded that synthesis and detection of the OF radical by mass spectrometry would be extremely difficult, if not impossible. Consequently, the investigation of this species for this thesis was discontinued.

CHAPTER IV

CONCLUSIONS AND RECOMMENDATIONS

The work described in the preceeding chapters has led to the following conclusions:

1) Mass spectrometer sensitivity calculations indicate that investigation of thermally unstable species requires injection of the gaseous labile samples essentially directly into the electron beam; this conclusion was strikingly verified in the investigation of the O_2F radical.

2) The multipurpose cryogenic reactor and mass spectrometer inlet assembly developed for this work allows detection of species at temperatures at which they exert a vapor pressure of only 10^{-6} torr; it also permits investigation of the synthesis, stability, energetics, and chemical reactivity over a broad temperature range of extremely unstable species as well as the initial decomposition products of these species.

3) $A(O_2F^+)$ and $A(OF^+)$ from O_2F_2 are 14.0 ± 0.1 ev and 17.5 ± 0.2 ev, respectively. These ions are formed by the following mechanisms

$$O_2F_2 + e \rightarrow O_2F^+ + F + 2e$$

and

$$O_2F_2 + e \rightarrow OF^+ + OF + 2e$$

Neither the positive nor negative ion of dioxygen difluoride, $O_2F_2^+$ or $O_2F_2^-$, was detected in the mass spectrometer.

4) The bond energies of the O_2F_2 molecule and O_2F free radical can

be developed from other available data and the measured appearance potentials of O_2F^+ and OF^+ from O_2F_2. These bond energies have been determined to be

$$D(F\text{-}O_2F) = 0.8 \text{ ev}$$

$$D(FO\text{-}OF) = 4.5 \text{ ev}$$

$$D(O\text{-}OF) = 4.8 \text{ ev}$$

$$D(O_2\text{-}F) = 0.8 \text{ ev}$$

which are consistent with microwave, thermochemical, infrared, and kinetic data that are available on O_2F_2 and O_2F. These energetics are also consistent with the proposed electronic structures of the species.

5) The method of appearance potential lowering permitted the first detection of the O_2F free radical (which had been predicted to possibly be a stable species) in the vapor phase. This radical was produced by the pyrolysis of O_2F_2 in a tubular alumina furnace at about 250°K. No evidence was obtained for the production of O_2F upon subjection of gaseous O_2-F_2 mixtures and O_2-OF_2 mixtures to an electrodeless radio frequency discharge.

6) The vertical ionization potential of O_2F was measured to be 12.6 ± 0.2 ev; the ionization potential of O_2F_2 was determined to be equal to or less than 13.4 ev.

7) There was some evidence for the formation of small amounts of the OF free radical in the pyrolysis of OF_2 on hot filaments of molybdenum and nichrome, but the evidence was not very conclusive.

8) There was no evidence for the formation of the OF radical in the pyrolysis of OF_2 on hot filaments of niobium, tantalum, platinum, titanium, zirconium, or tungsten; nor in tubular monel and alumina furnaces despite the fact that the very optimum mass spectrometric arrangement possible, i.e., pyrolysis directly in the electron beam, was employed. The only pyrolysis products detected were O, O_2, and large amounts of F_2, which suggested that OF_2 decomposes directly to O and F_2 on the hot surfaces.

9) No evidence was obtained for production of OF upon subjecting gaseous samples of OF_2 or O_2-OF_2 mixtures or O_2-F_2 mixtures to an electrodeless radio frequency discharge. Only O, F, O_2, and F_2 were detected.

10) No unequivocal evidence was obtained for the existence of O_3F_2 as a molecular entity in the vapor phase. That is, no positive or negative ions directly attributable to molecular O_3F_2, i.e., $O_3F_2^+$, $O_3F_2^-$, O_3F^+, or O_3F^-, were observed in the mass spectrometer. However, it seems likely that O_3F_2 is a molecular entity, but the above ions are not stable for the 50 microseconds required for detection by the TOF mass spectrometer.

11) The reported thermal decomposition of O_3F_2 to O_2F_2 and O_2 was verified, but very strong evidence for its simultaneous decomposition into OF_2 and O_2 was also obtained.

12) A qualitative theoretical analysis of the O_3F_2 molecule, using the double quartet modification of the octet rule, indicated that it might have a chain structure and that the following two electronic configurations

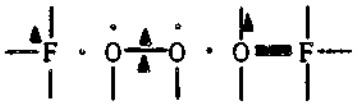 and 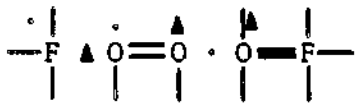

would be expected to be the major contributors to its overall electronic structure if it has this chain arrangement.

13) The following mechanism for decomposition of O_3F_2

$$2FO_2{\cdot}OF \rightleftharpoons 2FO_2{\cdot} + 2FO{\cdot} \xrightarrow{\text{fast}} O_2F_2 + 2FO_2{\cdot} \xrightarrow{\text{slow}} 2O_2F_2 + O_2$$

$$2FO{\cdot} \longrightarrow 2OF_2 + 2O_2$$

agrees with the mass spectrometric observations, as well as electron paramagnetic resonance, nuclear magnetic resonance, and infrared data. It also agrees with other physical and chemical properties reported for O_3F_2 and with its proposed electronic structure.

14) No direct evidence was obtained for the existence of O_4F_2, O_5F_2, or O_6F_2 as molecular entities in the vapor phase.

15) No evidence was obtained for the existence of an unsymmetrical isomer of dioxygen difluoride, $O{=}OF_2$.

Several extensions of the present work may be proposed.

Since the completion of the present experimental work for this thesis, the TOF mass spectrometer has been modified to permit "blanking out" of any portion of the mass spectrum that may not be desired. This adaptation would greatly facilitate the investigation of the mass spectrum of O_3F_2 at its decomposition temperature by permitting the blanking out of the very large O_2^+ ion current. In fact, it seems quite likely

that the $A(OF^+)$ could be determined at that temperature by blanking out all the mass spectrum except that from m/e = 33 to 37. A measurement of this appearance potential of OF^+ might permit the development of the energetics of O_3F_2.

The investigations of the OF radical were not extensive for this work. However, it was pointed out that a direct measurement of the ionization potential of this free radical is highly desirable in that it would settle the controversy concerning the value of D(O-F). In view of the fact that there was some indication of formation of OF upon pyrolysis of OF_2 on molybdenum and nichrome filaments, it seems reasonable to pursue the pyrolysis of OF_2 as a possible means of producing free OF. However, pyrolysis of other parent species such as $SF_5 \cdot OF$, $NO_2 \cdot OF$, and $FSO_2 \cdot OF$ might prove to be more satisfactory. In any case, it seems that a continued investigation of the existence of the OF radical seems worthy of consideration.

An obvious extension of this work is the study of the chemical reactivity of the low temperature oxygen fluorides with a broad range of species. Several reports discussing the reactions of these compounds state that unstable and highly reactive products were produced at the low temperature but were lost upon warming, and hence no identification was possible. However, it seems that the cryogenic reactor-inlet system developed for this thesis research would be ideal for investigation of these unstable products at the low temperature. This type of study could well result in the identification and investigation of a host of unreported and unusual compounds.

A particular class of species that would be of interest to investigate, using these cryogenic techniques, would be the N-O-F compounds.

Several N-O-F compounds have been reported, and it seems quite likely that more unusual and energetic species of this type might be stabilized at low temperatures. An interesting approach to this problem would be to make a systematic analysis of all N-O-F molecules and radicals that might seem feasible, using the double quartet modification of the octet rule approach. On the basis of that analysis, it might be possible to predict the existence and molecular parameters of some unreported species, as was done with the oxygen fluorine species for this thesis. This would offer a systematic approach to the investigation of the N-O-F compounds, and subsequent synthesis of species predicted to be stable by the qualitative theoretical analysis would be particularly exciting. This same approach might later be extended further to compounds of C-N-O-F since the double quartet description seems quite satisfactory for species containing these elements, and it seems quite possible that unknown molecules of this type might be stable at low temperatures.

APPENDICES

APPENDIX A

ELECTRONIC STRUCTURES OF THE OXYGEN FLUORIDES AND THEIR POSITIVE AND NEGATIVE IONS

Introduction

The unusual and interesting physical and chemical properties exhibited by the low temperature oxygen fluorides have been the subject of much discussion and investigation in the past few years. As a result, a rapidly growing store of information concerning their synthesis, stability, molecular structure, physical properties, and chemical reactivity is accumulating and is permitting a much better understanding of their unusual nature. However, from the discussions in Chapter I and III of this thesis, it is obvious that there is still a considerable amount of missing information concerning the structures and properties of some of these species, and even the existence of some others. This is particularly true for the oxygen-fluoride free radicals and higher oxygen fluorides, O_3F_2, O_4F_2, O_5F_2, and O_6F_2.

In this appendix a systematic discussion of the possible electronic structures of the reported oxygen fluorides, as well as unreported molecules, radicals, and ions of oxygen and fluorine, will be presented. The double quartet modification of the octet rule, which was recently proposed by Linnett,[17] will be used extensively for describing these structures. This method of formulating the electronic structures of molecules is based on the use of fundamental physical characteristics such as electrostatic repulsion of electrons, the attraction of electrons

by nuclei, the consequent tendency to achieve a fairly uniform charge distribution of electrons, and similar physical effects, to account for the electronic structures in molecular systems and to explain the resulting molecular properties. This approach to chemical bonding is essentially qualitative, but it seems to accomplish its stated purpose of "extending the understanding of the variation in properties in groups of related molecules and ions." Linnett has also pointed out that it provides a means of constructing wave functions, and hence numerical calculations are possible. However, this will not be done in this thesis.

The primary purpose of this discussion is to describe the most likely electronic structures of the oxygen fluorides that are reasonably well understood, based on their known physical and chemical properties. With the understanding and intuitive feeling gained in explaining the known properties of the known oxygen fluorides as a basis, the same arguments will be extended to the compounds, radicals, and ions which have not been observed or for which little is known. This should lead to a better understanding of the structures and properties of these other species.

Linnett has pointed out that the double quartet approach is a particular method of describing electronic structures of molecules and is not intended to provide a comparison with others such as those employing molecular orbitals. However, in this discussion explanations of molecular properties using other successful methods, such as the molecular orbital and valence bond approaches, will be presented for comparison of the different arguments for arriving at the same conclusions. In the assessment of his book, Linnett stated that

> "the double quartet model is based on a localized approach, but, instead of dealing always with electrons in pairs, one of each spin, the space is divided into one set of regions

> for the electrons of one spin, and into another set of regions for the electrons of the other spin. If the two sets of regions are the same as each other then the electrons occupy the regions in pairs but, if they are not, and this is permitted, then the disposition of the electrons of one spin is different from that of the electrons of the other spin. It is this modification that makes this method different from the ordinary valence bond method. However, it resembles the valence bond method in employing as its basis a localized approach and, in this, it differs from the molecular orbital method."

The formal approach and criteria for selecting the major contributors to the overall electronic structure of a given species are presented in Linnett's book and will not be discussed here, but the arguments proposed for individual species in the following sections will illustrate most of them. Linnett does not discuss how he determines the maximum number of electronic configurations possible for a given compound, while adhering to the restrictions of the double quartet model. This definitely seemed desirable for a systematic approach to each compound and, as a result, the following technique was used. First, the number of bonding electrons, E_B, was calculated by subtracting the sum of the number of valence shell electrons, E_v, in each atom of the species from the product of eight times the number of atoms, N_A, in the compound. That is,

$$E_B = 8N_A - E_v \qquad (1)$$

This gives the number of necessary bonding electrons since it is required that there be eight electrons about each atom, four of each spin. After obtaining E_B, the maximum number of arrangements of these electrons in N_B bonds, $(N_A - 1)$ bonds for noncyclic compounds, can readily be calculated. The number of possible configurations, C, of E_B electrons

in N_B bonds with the restrictions that there be a minimum of one electron in each bond and a maximum of six electrons in any bond, is given by the following equations;

For $N_B \leq E_B < N_B + 6$

$$C = (E_B - 1)!/(N_B - 1)!(E_B - N_B)! \qquad (2)$$

For $N_B + 6 \leq E_B < N_B + 12$

$$C = (E_B - 1)!/(N_B - 1)!(E_B - N_B)! - N_B(E_B - 7)!/(N_B - 1)!(E_B - N_B - 6)! \qquad (3)$$

The equations applicable to the cases where $E_B \geq N_B + 12$ have also been developed, but they will not be presented here since no such case occurred for the oxygen-fluorine species discussed in this appendix. The total number of arrangements for molecules containing one to four bonds (all atoms are assumed different) has been calculated using the above approach and are given in Table 5. The actual number of configurations would usually be lower than the values in Table 5 for molecules that contain like atoms since mirror images and indistinguishable structures would occur. It should be noted, however, that the values given do not include additional configurations that would be possible due to rearrangement of the spins of the electrons in any four electron bond. That is, there is one additional configuration for each four electron bond since it can have either two electrons of each spin or three of one spin and one of the other.

Table 5. Number of Possible Electronic Configurations For Molecules Using the Double Quartet Description

Number of bonding electrons	Number of Possible Configurations			
Number of Bonds	1	2	3	4
1	1			
2	1	1		
3	1	2	1	
4	1	3	3	1
5	1	4	6	4
6	1	5	10	10
7		6	15	20
8		5	21	35
9		4	25	56
10		3	27	80
11		2	27	104
12		1	25	125
13			21	140
14			15	146
15			10	140
16			6	125
17			3	104
18			1	80
19				56
20				35
21				20
22				10
23				4
24				1

OF Radical, OF^- Ion, and OF^+ Ion

Linnett[17] has recently discussed the electronic configuration of OF. It has thirteen valence-shell electrons, six electrons of one spin and seven of the other, which would result in it being paramagnetic. Using the double quartet model, the only electronic structure would be

(I)

Since there are three bonding electrons and FOOF has six, it might be expected that the OF monomer would tend to be stable, as is NO. However, the formal charges for the F and O atoms are + 1/2 and - 1/2, respectively. This positive charge on the F atom is definitely objectionable according to the criteria of Linnett (A formal charge of -1 to + 1/3 is considered satisfactory for fluorine while a charge of + 1/2 is considered possible but somewhat objectionable. Similarly, a charge of - 1/2 to + 1/2 is satisfactory for oxygen and + 1 and - 1 are considered possible.). Apparently, this unfavorable charge distribution results in the dimerization of 2OF to O_2F_2 which decomposes into O_2 and F_2 at about 200°K. Linnett has proposed that F_2 and O_2 are stable relative to 2OF because the formal atomic charges are all zero in the former system, and in O_2 inter-electron repulsion is reduced. The adverse formal charge situation in OF does not exist in NO. Another reason for the stability of NO relative to that of OF has also been proposed by Green and Linnett.[59] They suggested that a reaction path is open to OF, over which NO cannot pass. They stated that the following four-center mechanism would satisfy this requirement:

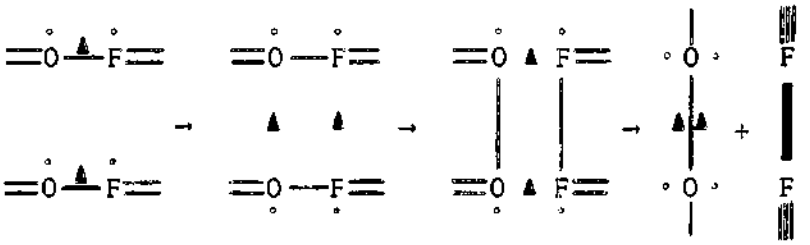

(4)

It was noted that the difference in order of individual links between the two transition states is only 1/2, so that a change from one to the other ought not to be difficult. In addition, there could be a resonance hybrid of the two forms, which would further lower the energy of activation. For a similar four-center mechanism involving NO, they showed that there is a large change in bond distribution during the transition and, consequently, the reaction would be unlikely.

The HO_2 radical is isoelectronic with OF and would be expected to have a structure

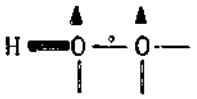

(II)

Studies of the reaction of hydrogen and oxygen have shown that this radical is an important participant in the sequence of processes that occur. It has recently been studied as a free species in a mass spectrometer by Foner and Hudson[70] and its bond energies were obtained. Using the data of Foner and Hudson, the $O-O$ bond energy for HO_2 is calculated to be about 76 Kcal/mole. This is very interesting because the corresponding bond in $HOOH$, which is a two electron bond, is 49 Kcal/mole and is 117 Kcal/mole for O_2, which is a four electron bond. Hence, the intermediate value of 76 Kcal/mole for the bond in

HO_2 would indicate that the above structure, which gives a three electron bond, is a satisfactory one.

A similar analysis of OF, which would also have a three electron bond, would indicate that it may have a bond strength somewhat greater than the average bond energy of OF_2 of 48 Kcal/mole. However, the unfavorable positive charge on the F atom could tend to reduce this bond strength considerably. The value of 25 Kcal/mole for the OF bond energy reported by Dibeler, et al.[6], from electron impact studies of OF_2, is considerably lower than would be predicted for a three electron bond as indicated by structure I. However, the relatively unfavorable + 1/2 formal charge on the F atom could possibly result in a weakening of the bond.

The O_2^- ion is also isoelectronic with OF and the structure is probably

(III)

which is identical to that of OF shown earlier. In this case, the formal charges on the two atoms are satisfactory, being -1/2 on both. In addition, Linnett has pointed out that the bond length in O_2^- is 1.28 Å, which is intermediate between the four electron bond in O_2 of 1.21 Å and the two electron bond in HO-OH of 1.48 Å. This would be expected for the three electron bond indicated above. The fact that oxygen exists in the crystal of KO_2 entirely as paramagnetic O_2^-, indicates that a three electron bond, as proposed for OF, can be stable

under the proper conditions. From these discussions it seems that OF might possibly be stable. However, there is still considerable doubt as to whether the failure to detect this species in the gas phase is due to its very high chemical reactivity or the fact that the bond is relatively weak as indicated by the electron impact studies.

The OF^- ion has fourteen valence-shell electrons and is isoelectronic with F_2 and $O_2^=$. The electronic structure would be

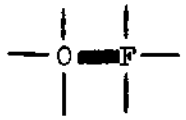

(IV)

where the formal charges of the O and F atoms are -1 and zero, respectively. The formal charge of -1 on the O atom is not altogether satisfactory, and Linnett[17] has pointed out that the process

$$2OF^- \rightarrow O_2 + 2F^- \qquad (5)$$

would be favored because the formal charge is transferred from the oxygen to the fluorine which is more suitable. In addition, the electrons of opposite spin are separated from one another in both O_2 and F^-, while there is a close pair of electrons in OF^- as indicated by the heavy line in IV. Consequently, the right-hand side of Equation (5) would also be favored by a reduction in inter-electron repulsion energy. This would account for the fact that it has only been observed in the mass spectrometer as reported in this work. Linnett stated that a possibility of stabilizing OF^- might be under the influence of the field provided by an array of positive charges in a crystal. The isoelectronic

species, $O_2^=$, does exist, though only when stabilized by an appropriate electric field such as in Li_2O_2, Na_2O_2, or RaO_2.

The OF^+ ion has twelve valence-shell electrons which is isoelectronic with NF and O_2. Its electronic structure would be given by either of the following structures or both.

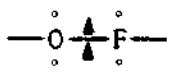

(V)

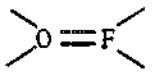

(VI)

Both structures give a formal charge of zero on the O atom and + 1 on the F atom. The electronic structures, V and VI, are identical to that of the ground state, VII, and first excited state, VIII, of O_2,

(VII)

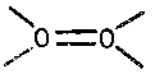

(VIII)

respectively, which were proposed by Linnett. It is obvious that V and VII would be paramagnetic while VI and VIII would not. It would be expected that V would give the lower energy for OF^+ and would indicate that it would be a paramagnetic species with a four electron bond which would probably be stronger than the bond in the OF radical. $D(O - F^+)$ has been reported by electron impact methods[6] to be 40 Kcal/mole which may be compared to 25 Kcal/mole for $D(O - F)$. This would appear to be qualitatively in the correct order, and the relatively small difference for the two can probably be accounted for by the presence of the very objectionable + 1 formal charge on the F atom in OF^+. This unfavorable charge distribution could also account for the fact

that the bond is much weaker than the O_2 bond. It is interesting to note that Price, Passmore, and Roessler[58] have estimated values for $D(O-F)$ and $D(O-F^+)$ of 52 and 87 Kcal/mole, respectively, from isoelectronic similarity curves of radicals and ions. These values are also qualitatively in the correct ratio according to the proposed structure but they seem much too high as discussed in Chapter III.

Green and Linnett[59] have stated that OF^+ might be more likely to be stable than NF because the differences in electronegativity of the two atoms in OF^+ is less than in NF. They proposed that the large difference in the electronegativity between the atoms in NF makes it likely that some localization of the unpaired electrons occurs on the fluorine atom which results in a decrease in bond order of the radical. Consequently, dimerization of the radical to form FNNF would be favored since it would result in an increase in bond order, which would not be the case if there was no localization of the electrons. This would account for the reluctance of O_2 to dimerize since there would be no rise in bond order in the dimer, O_4. The fact that the electronegativity difference in oxygen and fluorine is relatively small would indicate that OF^+ would have little localization of the unpaired electrons, and hence it might be stable under very unusual conditions. This has prompted Green and Linnett[59] to propose an investigation of the possible existence of OF^+ in some suitable solvent. It should be pointed out that OF^+ has been observed in the mass spectrometer during the investigation of both OF_2 and O_2F_2.

The above description of the electronic structures of the OF radical and its ions are based completely on the double quartet model.

However, it can be seen that the electronic structures described for these diatomic species are identical to those that would be obtained by a molecular orbital description. The relation between the double quartet and molecular orbital descriptions will certainly not be so obvious for the more complicated species that are to be discussed later.

Oxygen Difluoride (OF_2), OF_2^- Ion, and OF_2^+ Ion

The oxygen difluoride molecule contains twenty valence-shell electrons and is a stable species below about 250°C. It has four bonding electrons and, consequently, has a maximum of three possible electronic structures according to Table 5. Actually, there are only two possible structures since the molecule is symmetrical. One of these structures places a formal charge of + 1/2 on one of the F atoms and would not be considered very important. As a result the electronic structure is probably

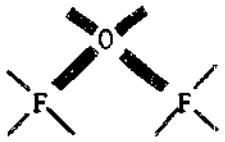

(IX)

which is identical to the valence bond description proposed by Pauling.[31] Structure IX indicates that OF_2 would be diamagnetic, which is the case. The electrons around the oxygen are spatially paired as a result of the tetrahedral arrangement of the electrons about each atom, but the unshared electrons on the fluorine atoms are not since the two sets can be staggered relative to one another. The formal charges on all the atoms are zero which is good. However, the fact that there are four close pairs

of electrons, i.e., four pairs of electrons occupying the same spatial orbitals, would mean that $2OF_2$ would be more energetic than would $O_2 + 2F_2$ in which there are no close pair electrons in O_2 and only one close pair in F_2. Linnett has pointed out that OF_2 is endothermic to the extent of only 7.6 Kcal/mole. Since there is no change in the number of shared electrons in OF_2 and $O_2 + 2F_2$, he has proposed that the increase in energy in forming OF_2 from $F_2 + 1/2\ O_2$ can be ascribed, at least in part, to an increase in inter-electron repulsion energy.

The OF_2^- ion contains 21 valence-shell electrons and would be paramagnetic. There are only two structures that this ion could have. They are

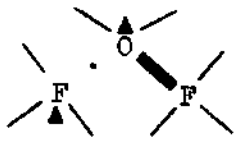

(X)

and its mirror image. This places formal charges of -1/2 on the O atom and one of the F atoms and a formal charge of zero on the other F atom. These are acceptable formal charges on all the atoms but would indicate a lower value for $D(F - OF^-)$ than for $D(F - \overset{\cdot\cdot}{O}F)$ which has been reported to be 40 - 65 Kcal/mole. It might be expected that OF_2^- could be unstable relative to $1/2\ O_2 + F_2^-$ since the number of bonding electrons is the same in both cases and there are no close pair electrons in the latter products while there is one close pair in OF_2^-. In addition, the -1/2 formal charge on the O atom in OF_2^- would be shifted to the other F atom in $1/2\ O_2 + F_2^-$. Actually, there would probably be little difference in the energies of the two systems, but, in any case, the OF_2^- ion has not been observed except in mass

spectrometry. The only reported observation of it is from the studies for this thesis in which an extremely small ion current due to OF_2^- was observed when very large samples of OF_2 were emitted into the spectrometer (see Appendix C).

The OF_2^+ ion, which is isoelectronic with both O_2F and NF_2, has 19 valence-shell electrons and actually has no electronic structure that would appear to be very satisfactory. The only structures that are somewhat reasonable are

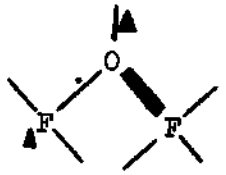

(XI)

and its mirror image. The formal charges are + 1/2, + 1/2, and zero for the left F atom, O atom, and right F atom, respectively. The + 1/2 charge on the F atom is not very satisfactory and this situation is even poorer due to the + 1/2 charge on the adjacent O atom. Structure XI would indicate that $D(F - OF^+)$ might possibly be slightly greater than $D(F - OF)$ which was reported to be 65 Kcal/mole from electron impact studies but only about 40 Kcal/mole from kinetic data. The electron impact studies also gave a $D(F - OF^+)$ of 48 Kcal/mole which is intermediate between the extremes reported for $D(F - OF)$. This value of 48 Kcal/mole is actually about equal to the average O - F bond energy of OF_2 of 45 Kcal/mole. This indicated low value for $D(F - OF^+)$ might well be partially due to the very unsatisfactory charges of + 1/2 on the adjacent O and F atoms. Values for $D(F - OF)$ and $D(F - OF^+)$

have been estimated as 40 and 7 Kcal/mole, respectively, by interpolating from isoelectronic similarity curves of radicals and ions.[59] However, it does not seem that $D(F - OF^+)$ could possibly be this low in view of the electron impact data for OF_2 of Dibeler, et al.[6] The only observation of OF_2^+ has been in mass spectrometry, and it probably will not be seen in a stable condensed species.

Dioxygen Difluoride: Chain Isomer (FOOF)

Dioxygen difluoride has been shown to be a stable species only below about 200°K, and microwave studies[2] indicate that it is a nonplanar, symmetrical chain molecule very similar to the hydrogen peroxide molecule except that it has unusually long O - F bonds and a surprisingly short O - O bond. In addition, it has been shown that it has a high barrier for internal rotation. Both of these facts indicate that there must be some multiple bonding between the two oxygen atoms which is quite different from that in the HOOH molecule.

There have been several attempts to explain the unusual molecular parameters in FOOF. Linnett[16] proposed an explanation using the double quartet approach which indicates that there are ten possible electronic structures if completely ionic structures are also considered. It seems that a presentation of all ten of these structures, along with arguments justifying the selection of the most likely configurations, will facilitate later discussions of the other oxygen fluorides and hence it will be given at this point. The ten structures are

(XII) (XIII) (XIV)

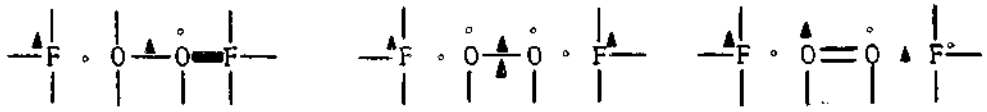

(XV) (XVI) (XVII)

(XVIII)

and the mirror images of XIII, XV, and XVIII.

The formal charges on the atoms and the number of close pairs of electrons for each of the above structures is given in Table 6.

Table 6. Formal Atomic Charges and Number of Close Pairs of Electrons for the Various Electronic Structures of FOOF

Structure	Formal charges on F	O	O	F	Number of close pairs
XII	0	0	0	0	7
XIII	-1	0	+1	0	6
XIV	-1	+1	+1	-1	2
XV	-1/2	0	+1/2	0	1
XVI	-1/2	+1/2	+1/2	-1/2	0
XVII	-1/2	+1/2	+1/2	-1/2	0
XVIII	-1	+1/2	+1	-1/2	0

Linnett stated that XIII, XIV, and XVIII are probably of low importance because of the existence of a formal charge of + 1 on at least one of

the oxygen atoms. Structure XII was considered as probably unimportant due to the high inter-electron repulsion energy resulting from the presence of seven close pairs. This leaves XV and its mirror image, XVI, and XVII, but XV has one close pair of electrons which would tend to reduce its importance. However, XV would be favored relative to XVI and XVII by the fact that only two atoms carry formal charges of 1/2 as opposed to four for XVI and XVII. Consequently, Linnett stated that all four structures, XV and its mirror image, XVI, and XVII should be given about equal weight. However, this would give an O - O bond that would be expected to have a length of about 1.24 Å (between 1.28 Å in O_2^- and 1.21 Å in O_2), and the observed length is 1.22 Å. Hence, Linnett concluded that XVI and XVII are the major contributors to the structure of FOOF. These structures indicate that the O - F bonds are single electron bonds while the O - O bond has four electrons. This would explain the unusual bond lengths in O_2F_2, as well as its high barrier to internal rotation. It is also interesting to note that arrangement of the electrons tetrahedrally about the atoms, as proposed by the double quartet model, would result in a dihedral angle of 90° for structure XVII which is very close to the actual value of 87.5° determined by Jackson.[2]

The fact that XVI and XVII give an O - O bond that contains four electrons would indicate that its bond strength would be essentially the same as that of O_2. However, the presence of a formal charge of + 1/2 on each of the O atoms would probably tend to reduce the bond strength somewhat. It was determined in this work (see Chapter III) that this is actually the case. The O - O bond in FOOF was determined to be 4.5 ev as compared to $D(O_2)$ = 5.1 ev. In addition, it was shown that the O - F

bond energy was only 0.8 ev which is very weak. Both of these facts would definitely support the proposed structures, XVI and XVII.

Jackson[2] has discussed the several differences between the FOOF and HOOH molecules and compared the OF_2 and FOOF system with the H_2O and HOOH system. He pointed out that in HOOH the O - O bond length (1.48 Å) is very similar to that in other peroxides and that the O - H bond (0.95 Å) is like that in H_2O(0.96 Å). In contrast, the O - O bond in FOOF (1.22 Å) is much shorter them in HOOH and the O - F bond (1.58 Å) is much longer than in F_2O (1.41 Å). In addition, the dipole moments indicate that the O - F bond moment in FOOF is four times as large in OF_2, whereas the bond moments in H_2O and HOOH are very nearly equal.

Using a valence bond approach for describing FOOF, Jackson[2] has proposed that there are considerable contributions from ionic structures of the type $F^- \; O{=}{=}O^+F$. He pointed but that this would lead to a shortening of the O - O bond and a lengthening of the O - F bond. The electronegative character of fluorine would tend to make these ionic contributions energetically favorable. In F_2O_2, contributions from structures of the form $F^- \; O^+F$ might be expected to be small because the two fluorine atoms are competing for electrons from only one oxygen. In H_2O_2, on the other hand, the ionic contributions are of the form $H^+ \; {}^-OOH$ and there is no tendency for double bond formation between the two oxygen atoms. Also, it would be expected that structures of the type $H^+ \; {}^-OH$ would contribute to the overall structure of water. These proposed differences in ionic structures would account for the large differences in the dipole moments of FOOF and HOOH, as well as for the high barrier for

internal rotation.

Libscomb[2] has proposed still another explanation for the unusual structure of FOOF using a molecular orbital description. He proposed that the 2py-orbital on one of the O atoms can overlap with the 2py-orbital on the second O atom to form the πy^* 2p-molecular orbital which has one electron in it. Hence, a fluorine atom can bond to the πy^*2p-orbital, adding an electron, to give a resultant electron pair in a three-center orbital. A similar situation would exist with the 2pz-orbitals and the second fluorine atom. The molecular orbitals for O_2 are represented in Fig. 21A and a diagrammatic representation of the proposed bonding molecular orbitals in O_2F_2 is given in Fig. 21B. It was pointed out that the three-center orbitals indicated do not have the full symmetry of the whole molecule. However, from the point of view of transferability to other similar molecules, Libscomb found it more convenient to consider them in that way rather than to consider the appropriate linear combination which would have the full symmetry of the molecule. Jackson stated that this description would certainly account qualitatively for the observed molecular parameters in FOOF. He pointed out that the dissociative energy of F_2 (36 Kcal/mole) is much lower than for the other halogens, and that this is normally ascribed to repulsion between pairs of non-bonding electrons on the fluorine atoms. He stated that a similar effect in FOOF would favor the bonding scheme above over the normal covalent bonding in HOOH. It was further pointed out that OF_2 cannot form the three-center orbital bonds and that the O - F bond is much weaker than the O - H bond in H_2O, which supports these arguments. He also stated that the three-center bond would also account qualitatively

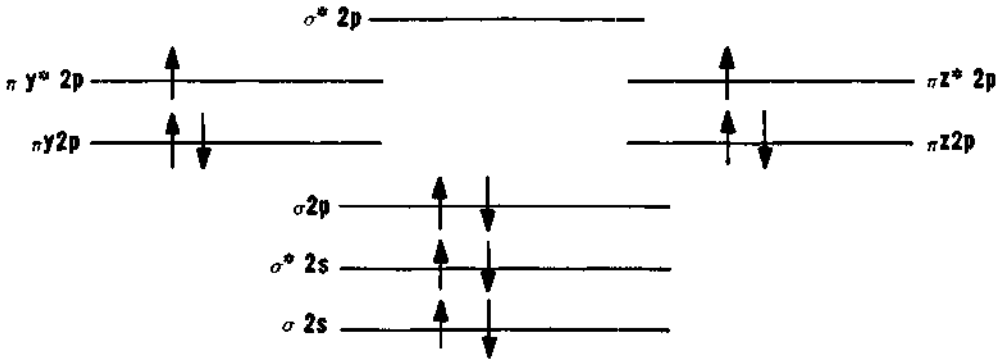

MOLECULAR ORBITALS IN O_2.

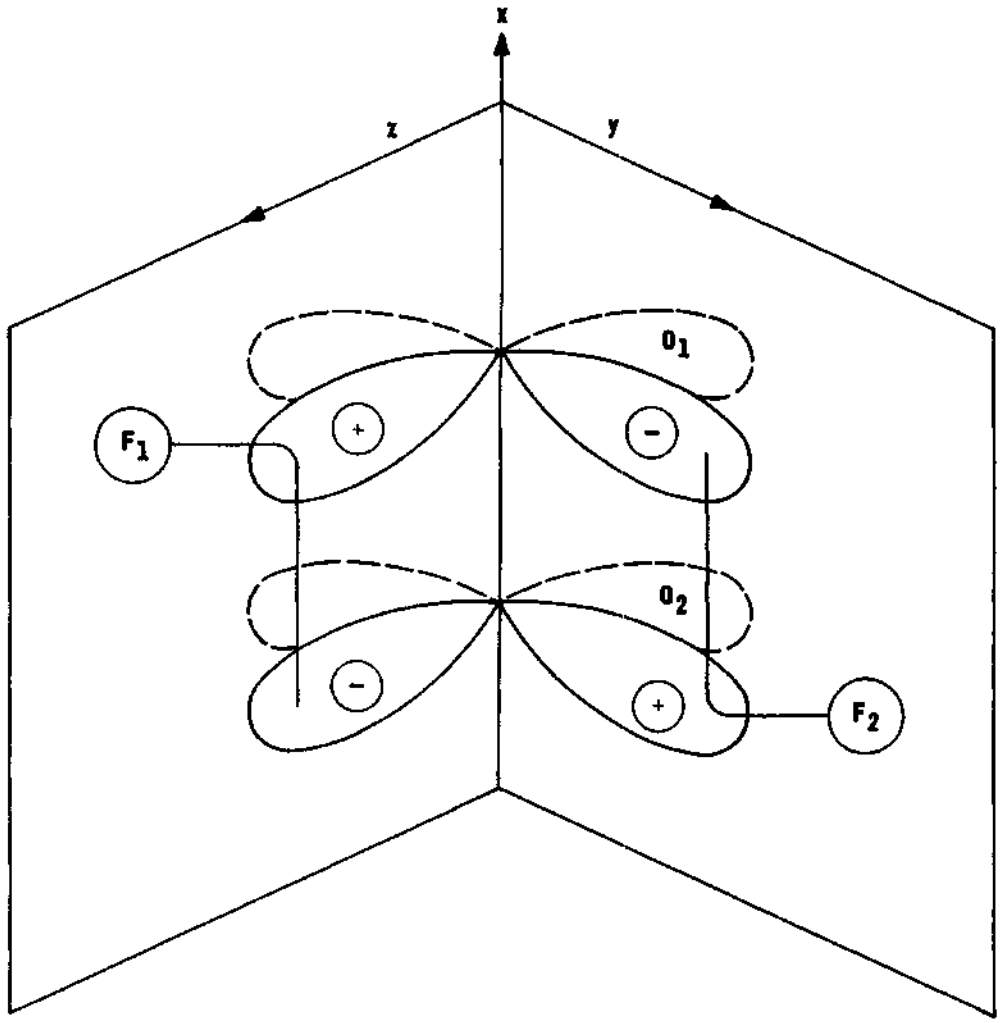

Figure 21. Molecular Orbitals in O_2 and Diagrammatic Representation of the Bonding Molecular Orbitals in O_2F_2.

for the fact that the barrier to internal rotation is considerably higher than that reported for HOOH.

Unusual bonds in other molecules similar to FOOF have been reported in the literature. Electron diffraction studies[13] of ClSSCl and BrSSBr have indicated that the S-S bond length in both species are shorter than is usually found for a singly bonded S-S link and that the S-Cl bond in ClSSCl is longer than that found in SCl_2. For instance, the normal single S-S bond is reported[76] to be 2.04 Å in S_8 and 2.05 Å in HSSH, while the S-S bond is only 1.89 Å in FSSF[77] which is identical to the value reported for S_2. Bauer[14] has also shown that the N-F bond in FNNF is longer than expected for a normal single bond.

From the above discussions it is quite obvious that the FOOF molecule has very unusual molecular parameters, as do several other similar species, and that a reasonable explanation of these properties is highly desirable. It seems that the three explanations presented, using the double quartet, valence bond, and molecular orbital approaches, are all reasonably acceptable for describing the situation. However, the double quartet approach permits a relatively simple description of the species compared to the molecular orbital approach and appears to permit a better qualitative feeling than the valence bond approach for the electronic repulsion and geometry resulting from the various electronic structures of the molecules. It is obvious that the double quartet approach does not offer the final word on the description of the electronic structures of species. However, it does seem reasonable, in view of its success in explaining the unusual nature of the simpler oxygen

fluorides, that it might offer some valuable insight to the question concerning the possible existence and structures of the other reported, but more complicated, molecules (i.e., O_3F_2 and O_4F_2) as well as other unreported species. Hence, this approach will be used almost exclusively in the remainder of these discussions. The general approach for each species will be very similar to that used for the FOOF molecule, but only the more reasonable electronic structures of each will be presented.

$FOOF^-$ Ion

The possible existence of negative ions of the oxygen fluorides was considered to be a strong possibility for the detection of these species for the cases where their positive ions were not detected. For instance, the positive ion of FOOF was not detected in the mass spectrometer, and this made the interpretation of the mass spectral data somewhat complicated. It was hoped that the negative ion of FOOF could be detected, which would have simplified the interpretation as was discussed in Chapter III. There would be five bonding electrons in this ion, which would give six possible structures according to Table 5. However, symmetry of the ion reduces this number to four, and the most reasonable structure is given by

(XIX)

which places formal charges of -1/2 on each F atom and zero on each O atom. This is certainly an acceptable charge distribution and would

indicate that it could possibly be somewhat stable, at least in a mass spectrometer. However, this ion was not detected in the spectrometer, and it could be that the Franck-Condon mechanism is not favorable for the formation of this ion from FOOF, which has a somewhat different electronic structure, according to XVI and XVII.

$FOOF^+$ Ion

The $FOOF^+$ ion has 25 valence-shell electrons, which result in seven bonding electrons. Therefore, Table 5 indicates that there would be 15 possible structures, but symmetry of the ion reduces the possibilities to ten. Of these ten possibilities, there is only one that appears acceptable. It is

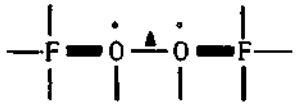

(XX)

which gives formal charges of zero on both F atoms and + 1/2 on each O atom. The positive formal charges on the adjacent oxygen atoms are not completely satisfactory, and, in addition, there would be two close pairs of electrons, which would result in a relatively high electronic repulsion energy. This would indicate that this ion would be relatively unstable if it exists at all. It would almost certainly be less stable than the FOOF molecule. This could be the reason that it was not detected in the mass spectrometer in these experiments. However, another explanation for this could be that the electronic structures of $FOOF^+$ and FOOF are quite different, as is indicated by their proposed structures, and the Franck-Condon mechanism might not favor the formation of

the ion from the molecule.

Dioxygen Difluoride: Branched Isomer ($O{=}OF_2$)

The possible existence of a branched isomer of O_2F_2 is of particular interest since two isomers of disulfur difluoride, FSSF and $S{=}SF_2$, have been observed. Seel and Budenz[15] have very recently reported that they have also observed a stable dimer of these isomers, $FSSF{\cdot}S{=}SF_2$. The FSSF isomer has very similar molecular parameters to FOOF, and it might be expected that the isomer, $O{=}OF_2$, might also exist and have molecular parameters similar to $S{=}SF_2$. The fact that early kinetic data indicated that O_2F_2 had a branched structure is added reason for considering its possible existence.

There are seven possible structures for $O{=}OF_2$, but only six of these merit consideration. They are

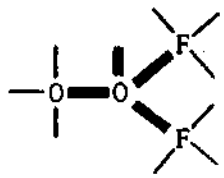

(XXI)

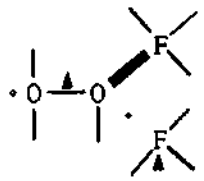

(XXII)

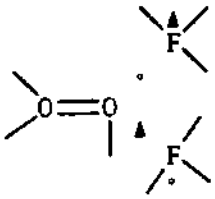

(XXIII)

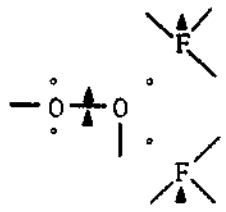

(XXIV)

and the mirror image of XXII. Structure XXI probably would be of little importance since it places formal charges of - 1 and + 1 on the terminal

and center O atoms, respectively. Structure XXII and its mirror image give a formal charge of -1/2 on the terminal O atom, + 1 on the center O atom, and -1/2 on one of the F atoms and zero on the other. These structures also require a close pair of electrons. Structures XXIII and XXIV both place formal charges of zero and + 1 on the terminal and center O atom, respectively, and -1/2 on each F atom. It seems likely that XXIII and XXIV would be more important than XXII and its mirror image since the formal charge of -1/2 on the O atom of the latter is shifted to the more suitable F atom in the former. In addition, there are no close pairs of electrons for XXIII and XXIV as there is for XXII and its mirror image. The positive formal charge of + 1 on the center O atom for these two structures is not considered very suitable, but not impossible. For example, the ozone molecule has formal charges of -1/2 on each of the terminal atoms and + 1 on the center atom, which is essentially the same situation as in XXIII and XXIV. Both XXIII and XXIV would give non-planar structures very similar to that of $S{=}SF_2$.

From the above analysis it might be expected that a branched isomer of O_2F_2 could possibly exist, and that it could possibly be stabilized at very low temperatures. However it would almost certainly be much less stable than the chain isomer, FOOF, which decomposes at about 200°K. If the unsymmetrical isomer is ever detected, it would be expected to have molecular parameters very similar to those of the $S{=}SF_2$ molecule. There has been no direct evidence reported for the existence of the $O{=}OF_2$ species, and no evidence was obtained in this work for its existence as was pointed out in Chapter III.

Dioxygen Fluoride Radical (O_2F)

The O_2F free radical contains 19 valence-shell electrons and is isoelectronic with NF_2 and OF_2^+. The possible existence of this species was a very interesting question prior to this work since no one had succeeded in detecting any free radicals of oxygen and fluorine. Using the double quartet approach, this species should have six bonding electrons and five possible electronic structures. However, the only three that seem reasonable are the following

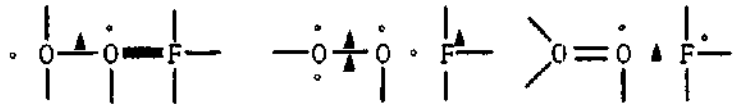

(XXV) (XXVI) (XXVII)

For structure XXV, the formal charges on the terminal O, center O, and F atoms would be - 1/2, + 1/2, and zero, respectively. These are quite acceptable, but a shortcoming of this structure is that is contains a set of close pair electrons which are indicated by the heavy black line. This would result in a relatively large interelectronic repulsion force and would be somewhat unfavorable energetically. The corresponding formal charges for both of the structures, XXVI and XXVII, are zero, + 1/2, and - 1/2, which is certainly acceptable. Actually, this formal charge distribution would be more favorable than that in XXV since the negative formal charge is shifted from the terminal O atom to the F atom which is more suitable. In addition, there are no close pairs of electrons in XXVI and XXVII as there are no close pairs of electrons in XXVI and XXVII as there is in XXV.

These qualitative arguments would indicate that structures XXVI

and XXVII would probably contribute most to the structure of the O_2F radical. Examination of the geometry of these structures, using the tetrahedral arrangement of the electrons about the atoms as proposed by the double quartet model, indicates that the species would be nonlinear. In fact, the arrangement would be essentially the same as that of the O_2F moeity in O_2F_2. It can be seen that the electronic configuration of structures, XXVI and XXVII, are identical to the structures of FOOF, XVII and XVIII, presented earlier, but with one of the fluorine atoms removed. Assuming that XXVI and XXVII are the major contributors to the structure of O_2F, it would be concluded that the O - O bond would be essentially double bond in character while the O - F bond would be very weak as was the case for the FOOF molecule. Actually, the O - O bond would probably be slightly stronger in O_2F than in O_2F_2 because both O atoms in O_2F_2 would have a positive formal charge of 1/2 which would tend to reduce their bonding energy.

On the basis of the above analysis, it was proposed[19] that this radical might well exist at low temperatures. Subsequent to this proposal, O_2F has been synthesized and investigated in the vapor phase as part of this thesis as was discussed in Chapter III. In addition, it has been trapped in a solid matrix at liquid helium temperatures and studied by infrared techniques. It has also been observed in the liquid phases of O_2F_2 and O_3F_2 by epr studies.[35,36,37] It is very interesting to note that the bond energies of O_2F measured in this work, as well the ir data,[25] supported the proposed structures, XXVI and XXVII. The O - O bond was measured to be 4.8 ev which is intermediate between the values of 4.5 ev and 5.1 ev for FOOF and O_2, respectively. In addition,

the O - F bond was calculated to be 0.8 ev, which agrees with a value of 0.7 ev estimated[60] from kinetic data and supports the proposed structures which indicate a single electron bond.

A valence bond description of O_2F would indicate a large contribution from the ionic form $F^- \; O{=}O^+$, which would result in a shortening of the O - O bond and a lengthening of the O - F bond. A molecular orbital description of O_2F has also been proposed by Kasai and Kirshenbaum.[36] They proposed that the main electronic features of FOOF, proposed in Jackson's paper,[2] are still maintained in O_2F, just as was indicated above in the double quartet description.

O_2F^- Ion

The O_2F^- ion has 20 valence-shell electrons and is isoelectronic with OF_2. There are three possible electronic configurations for this species, but only one of them seems reasonable. It is

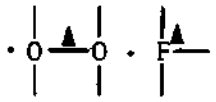

(XXVIII)

which gives formal charges of -1/2, zero, and -1/2 on the terminal O atom, center O atom, and F atom, respectively. Actually, these are quite acceptable formal charges, and it seems that this ion could possibly be stabilized under special conditions. It was not observed in the investigation of the negative ions of FOOF in this work, but, once again, it can be seen that the electronic configuration, XXVIII, is somewhat different from that of FOOF and O_2F and its formation in

the mass spectrometer may not be favored.

O_2F^+ Ion

The O_2F^+ ion has six bonding electrons and there are three electronic structures that seem reasonable. They are

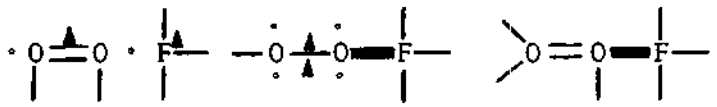

(XXIX) (XXX) (XXXI)

Structure XXIX gives formal charges of + 1/2, + 1, and -1/2 on the terminal O atom, center O atom, and F atom, respectively. The corresponding formal charges of XXX and XXXI are zero, + 1, and zero. The formal charge of + 1 on the center O atom for all these structures is not entirely satisfactory. Structures XXX and XXXI would be favored over XXIX in that there are formal charges on all the atoms in XXIX. However, XXIX would be favored over XXX and XXI in that the latter structures have a close pair of electrons. Consequently, it seems reasonable to assume that all three of these structures would contribute to the overall structure of O_2F. This would indicate that the bonds would be slightly greater than in O_2F, but the large formal charge on the center O atom would tend to weaken the bonds so that the difference would probably be small. These trends were shown to exist in this work, in which the O - O bond was determined to be 5.2 ev and the O - F bond was 0.4 ev. The corresponding bonds in O_2F were 4.8 ev and 0.8 ev.

Ozone Difluoride (O_3F_2)

Ozone difluoride has been reported for several years, but no direct

observation of it as a molecular entity has been made. Consequently, its structure is still unknown. However, epr and chemical studies of the liquid phase of this species, which were discussed in Chapter I, indicate the presence of a relatively high concentration (5 - 10 per cent) of the O_2F free radical. In addition, it is known that it decomposes at 110° - 120°K primarily into O_2F_2 and O_2. Further, the mass spectrometric data discussed in Chapter III indicated that it either had both F atoms on the same O atom or decomposed in some manner forming appreciable amounts of OF_2.

If this species is really a molecular entity, there are four possible arrangements of the atoms, omitting cyclic structures. They are

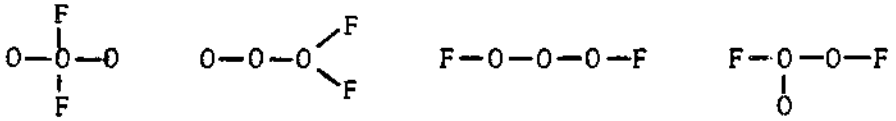

(A) (B) (C) (D)

The molecule would have to contain eight bonding electrons which would indicate that there are 35 different arrangements of the electrons in the four bonds for each type structure. However, symmetry in A, B, and C reduces the number of possibilities for these arrangements. Elimination of the structures that would place a positive charge of greater than +1/2 on either fluorine atom also reduces the number of possibilities. Since the mass spectra suggested the possibility that the structure of O_3F_2 might be like that of A or B, in which both fluorine atoms are on the same oxygen atom, they will be discussed first.

Arrangement A would correspond to the structure of sulfuryl fluoride,

SO_2F_2, which has a tetrahedral arrangement of the atoms. Of the large number of possible electronic structures, there are only eight that merit close consideration. They are

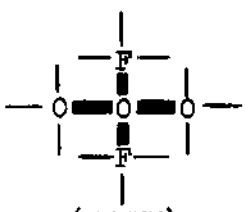

(XXXII)

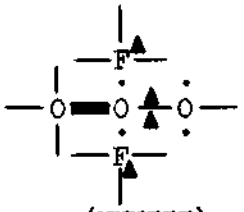

(XXXIII)

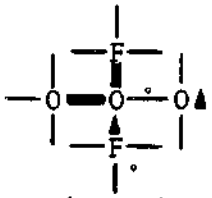

(XXXIV)

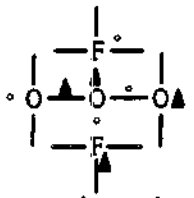

(XXXV)

the mirror image of XXXIII and three mirror images of XXXIV. All the possible configurations for this arrangement places a formal charge of + 2 on the center O atom which would definitely be considered prohibitive by the general arguments of Linnett. None of these electronic structures would be paramagnetic. Structure XXXII places a formal charge of -1 on each of the terminal O atoms and zero on both F atoms while XXXV has corresponding charges of -1/2 for all four of these atoms. Structure XXXIII and its mirror image place formal charges of -1/2 on each of the F atoms, -1 on one of the terminal O atoms, and zero on the other O atom. The formal charges for structure XXXIV and its three mirror images are -1/2 for one of the F atoms and one of the terminal O atoms, -1 for the other terminal O atom, and zero for the other F atom. There should not be a large difference in energy for any of these four electronic structures, but XXXII would probably be the least important since

it has four close pairs of electrons and a formal charge of -1 on both terminal O atoms. In addition, it would seem that XXXIII, XXXIV, and their mirror images would be less important than XXXV since they all have a formal charge of -1 on one terminal O atom as well as close pairs of electrons. Hence, it appears that structure XXXV would probably be the major contributor to the electronic structure of O_3F_2 if it has the tetrahedral type structure. The + 2 formal charge on the center O atom would definitely be considered prohibitive according to the arguments of Linnett, but the symmetrical distribution of negative charges on all the other atoms surrounding it could possibly offset this unfavorable situation, at least partially. In any case, there are a few isolated cases known in which an O atom is tetracovalent. For instance, there are a few donor-acceptor compounds in which the oxygen atom in an ether donates both lone pairs, as in the very unstable etherate of ethyl dichloroboron[78]

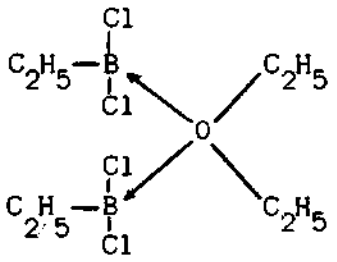

and in indium trimethyl etherate[78]

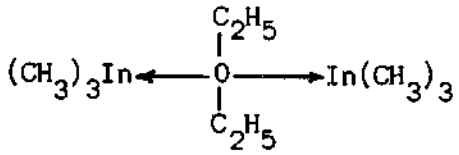

It would seem that this type of bonding might even be more favorable in O_3F_2 as a result of the strong oxidizing character of fluorine.

It is interesting to note that XXXV has essentially the same electronic configuration as ozone,

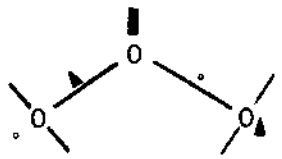

(XXXVI)

which was proposed by Linnett,[17] with the F atoms very loosely bonded to the center O atom. This would indicate that the fluorine atoms could be easily removed from O_3F_2 giving F_2 and O_3. However, it is known that the species decomposes primarily into O_2F_2 and O_2, apparently by way of the O_2F free radical. It hardly seems likely that any of the above structures would decompose very readily by way of the O_2F radical. In view of this, as well as the extremely unfavorable formal charge distribution, it seems fairly unlikely that O_3F_2 has the type of structure indicated by A.

Arrangement B has seven electronic structures in which the formal charge distributions are quite satisfactory. They are

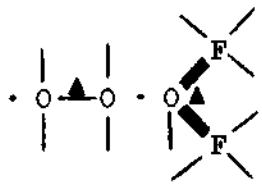

(XXXVII)

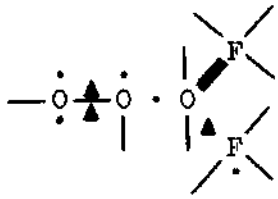

(XXXVIII)

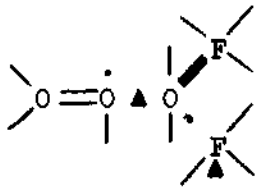

(XXXIX)

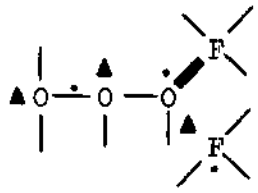

(XL)

and the mirror images of XXXVIII, XXXIX, and XL. The formal charges for the above structures can readily be calculated. However, there is no need to discuss them since none of the above electronic arrangements could be obtained without destroying the tetrahedral arrangements of the electrons as proposed by the double quartet model. Regardless of this fact, it does not seem that O_3F_2 could have this type of structure in that none of the above arrangements would appear to be favorable for the formation of the O_2F radical. It is interesting to note, however, that XXXVII, XXXVIII, and XXXIX would probably be quite favorable for a direct decomposition into $O_2 + OF_2$.

There are eleven chain structures, like C, that merit consideration. They are

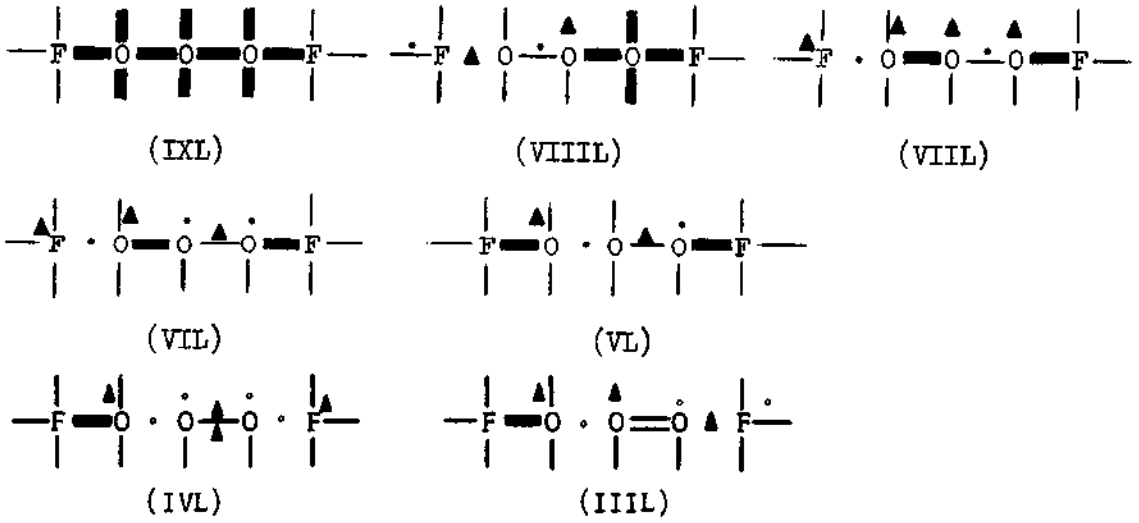

(IXL) (VIIIL) (VIIL)

(VIL) (VL)

(IVL) (IIIL)

and the mirror images of VIIIL, VIIL, VIL, VL, IVL, and IIIL. The formal charges on the atoms and the number of close pairs of electrons for each of these structures is given in Table 7. Structures IXL and VIIIL would probably be of little importance due to the large number

Table 7. Formal Atomic Charges and Number of Close Pairs of Electrons for the Various Electronic Structures of the Chain Isomer of FOOOF

Structure	Formal charges on F	O	O	O	F	Number of close pairs
IXL	0	0	0	0	0	10
VIIIL	-1/2	0	+1/2	0	0	4
VIIL	-1/2	-1/2	+1/2	+1/2	0	2
VIL	-1/2	-1/2	+1/2	+1/2	0	2
VL	0	-1/2	0	+1/2	0	2
IVL	0	-1/2	+1/2	+1/2	-1/2	0
IIIL	0	-1/2	+1/2	+1/2	-1/2	0

of close pairs. In addition, neither of them would seem to be particularly favorable for formation of the O_2F radical. Structures VIIL and VIL are essentially identical except VIIL is paramagnetic (it has two unpaired electrons) and VIL is not. The nonuniform charge distribution and presence of two close pairs would probably reduce their contribution to the overall structure considerably. Further, they do not appear to favor the formation of O_2F either. Structures VL, IVL, and IIIL all have quite acceptable formal charges and would seem to favor a decomposition by way of the O_2F radical due to the single electron bond between the OF and O_2F groups. However, the presence of two close pairs would tend to reduce the importance of VL relative to IVL and IIIL. Hence, these last two structures would appear to be the major contributors to the structure of O_3F_2 if it really has this chain structure. Actually, structures IVL and IIIL are essentially identical. It is interesting to note that these two structures have the basic features of the O_2F and OF

radicals joined by a very weak bond. In fact, the O_2F group in IVL and IIIL has essentially the same electronic configurations as do structures XXVIII and XXVII, respectively, of the O_2F radical that were proposed earlier. Several investigators have stated that it seems impossible for O_3F_2 to have a chain structure. The primary reason for this conclusion seems to be that no obvious mechanism appeared available for its decomposition into O_2F_2 and O_2. However, structures IVL and IIIL do seem to offer a favorable path for this decomposition as was discussed in Chapter III. It appears that, according to the qualitative criteria of the double quartet model, that these two structures would be quite favorable for O_3F_2, but the single electron bonds would result in it being a rather unstable species, which is the case. In addition, their electronic structures would account for the unusual physical and chemical behavior that it exhibits. Hence, it seems reasonable to conclude that the O_3F_2 molecule could well have a chain structure like C, and that IVL and IIIL would probably contribute about equally to its electronic structure.

Siegel and Schieler[72] have proposed that the electronic structure of O_3F_2 is probably of type D with an O atom loosely bonded to the O_2F_2 molecule. There are twelve structures like D that merit consideration and they are all nonparamagnetic. They are

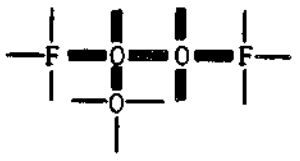

(IIL)

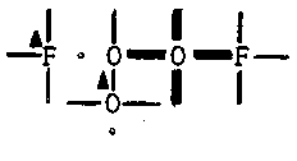

(IL)

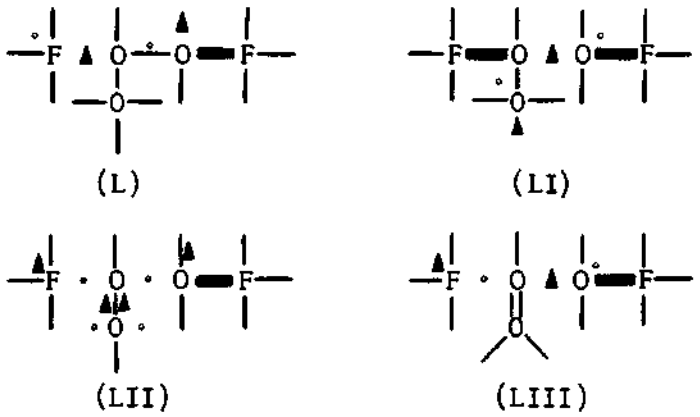

(L) (LI)

(LII) (LIII)

and the mirror image of each. Table 8 summarizes the important features of each of these structures. From Table 8 it can be seen that all of these structures place a + 1 formal charge on the tricovalent bonded O atom, which is not entirely satisfactory. The -1 charge on another O atom for IIL, as well as the large number of close pairs would probably render it unimportant. The presence of four close pairs in IL and the -1 charge on the O atom in L would probably make these two structures unimportant. Structure LI would probably be less important than LII

Table 8. Formal Atomic Charges and Number of Close Pairs of Electrons for the Various Electronic Structures of FO(O)OF.

Structure	Formal charges on					Number of close pairs
	F	O	(O)	O	F	
IIL	0	1	-1	0	0	7
IL	-1/2	1	-1/2	0	0	4
L	-1/2	1	-1	1/2	0	1
LI	0	1	-1/2	-1/2	0	2
LII	-1/2	1	0	-1/2	0	1
LIII	-1/2	1	0	-1/2	0	1

and LIII since it has two close pairs and the -1/2 charge on two O atoms, while the latter two have only one close pair and a -1/2 charge shifted to a fluorine atom which is more favorable. Therefore, on the basis of the formal charge distribution and number of close pairs, it would be expected that LII and LIII would be the major contributors to the structure of FO(O)OF. In addition, these are the only two structures of this type, except for LI, that would favor the formation of the O_2F radical. No structures of this type were considered acceptable in which the branched O atom was only loosely bonded (i.e., a single electron bond) since they would all require a + 1.5 formal charge on the O atom which is considered prohibitive. They also did not favor the formation of the O_2F radical. A comparison of LII and LIII with IVL and IIIL show that they have quite similar structures and might behave chemically in essentially the same manner. However, it seems that the chain structure, FOOOF, would be more favorable than the branched structure, FO(O)OF, since the + 1 formal charge on one of the O atoms in LII and LIII is not very satisfactory, whereas this situation does not exist in IVL and IIIL. In fact the charge distributions in IVL and IIIL are almost identical to those in XVI and XVII that were proposed by Linnett for O_2F_2. In view of these facts, it seems quite possible that the electronic structure of O_3F_2 is described satisfactorily by a combination of structures LII and LIII. This conclusion is certainly supported by the physical and chemical behavior of this species, as was discussed in Chapter III.

Tetraoxygen Difluoride (O_4F_2)

Tetraoxygen difluoride was first reported in 1961,[27,28] and very

little is known about it. It has been reported that it is fairly stable below 90°K but decomposes quite rapidly at 95° - 105°K into O_3F_2 and O_2. Epr studies[35] have indicated that it is very strongly paramagnetic, but that the epr signal is different from that obtained for O_2F_2 and O_3F_2. This would indicate that the epr signal is not due to the O_2F free radical. However, infrared studies by Arkell[25] have indicated that O_4F_2 consists of two very loosely bonded O_2F radicals. These studies indicated that the properties of the O_2F radical are essentially maintained in the O_2F moiety of O_4F_2.

Theoretically, there are numerous possible arrangements of the atoms and electrons in the bonds for this species. However, it seems that a reasonable approach for proposing the description of this species is to let its physical and chemical properties serve as guidelines. There are four chain structures in which the basic features of the O_2F radical are maintained as indicated by the ir studies.[25] They are

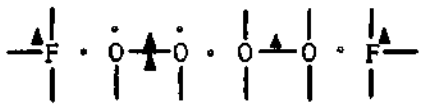

(LIV)

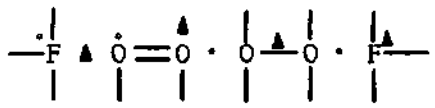

(LV)

and the mirror image of both. Both structures have formal charges on the atoms, starting at the left, of -1/2, +1/2, +1/2, zero, zero, and -1/2. These structures have the basic features of two O_2F radicals joined by a weak single electron bond. This would imply that there is a true chemical bond between the two radicals, despite the fact that it is quite weak. Arkell has suggested that the radicals might be bonded in a manner similar to the very weak bond between two oxygen

molecules in the dimer, O_4 ($D(O_2 - O_2)$ = 0.13 Kcal/mole[98] which is not considered in the region of a true chemical bond). Regardless of how the two radicals are bonded, it is not obvious how this structure would result in a decomposition into O_3F_2 and O_2. It would appear that a direct decomposition into O_2F_2 and O_2 would be favored.

Siegel and Schieler[72] have suggested that O_4F_2 might have a structure of the type

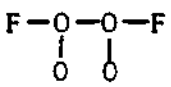

There does not appear to be a reasonable electronic structure, using the double quartet model, in which the branched O atoms are only weakly bonded as suggested by Siegel and Schieler. There are two structures for this type of arrangement which have the basic features of two O_2F radicals joined by a single electron bond. Neither of them would be paramagnetic and there charge distributions are not as favorable as for the case where the radicals are bonded between the terminal O atoms as in LIV and LV. Consequently, it seems that structures LIV and LV could possibly be a satisfactory description of the O_4F_2 molecule.

A short summary of the proposed structures of O_2, O_2F, FOOF, $O{=}OF_2$, O_3F_2, and O_4F_2 using the double quartet description, points out the close similarities in their electronic structures. There were two structures proposed for each of the species, and it can be seen that one set has essentially the same configuration as O_2 in its ground state as follows

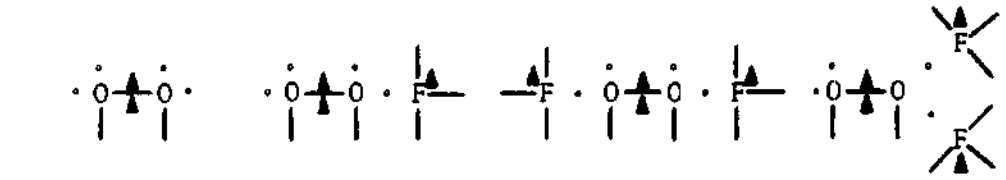

(VII) (XXVI) (XVI) (XXIV)

(IVL) (LIV)

while the other set has the features of O_2 in its first excited state (a $^1\Delta_g$)

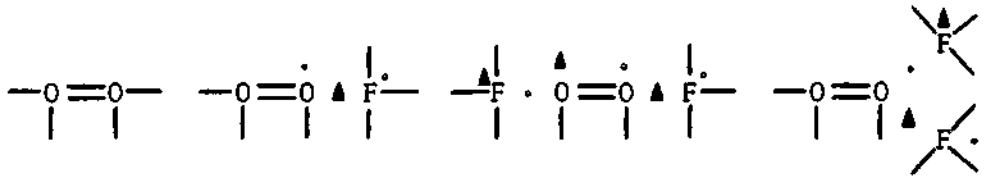

(VIII) (XXVII) (XVII) (XXIII)

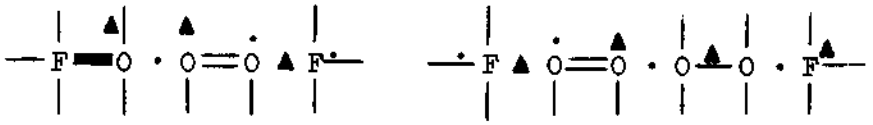

(IIIL) (LV)

As was indicated through the discussions to this point, it seems reasonable to assume that both structures for each of these species would contribute about equally to their overall structure.

APPENDIX B

DESIGN CONSIDERATIONS AND CALCULATIONS FOR THE CRYOGENIC REACTOR-INLET SYSTEM

The most important factors considered in the modification and rebuilding of the cryogenic reactor and inlet system designed and built by McGee and Martin[3] for the Bendix Time-of-Flight Mass Spectrometer were discussed in Chapter II. The major results of calculations indicating the relative sensitivity of coaxial and perpendicular inlet arrangements were also presented. Since these design considerations and calculations give insight into the importance of the physical arrangement of inlet systems for investigation of thermally unstable species, it seems that a more detailed discussion of the mechanical considerations and mathematical developments should be presented. That is the purpose of this appendix.

Perpendicular Versus Coaxial Entrance Inlet Systems

The original cryogenic inlet system was designed for a perpendicular entrance primarily for mechanical reasons, principally the following: (a) the ion source of the mass spectrometer is located in a cross with all its electrical connections entering through a header directly opposite the drift tube and hence coaxial with the drift tube, while the entrance perpendicular to the drift tube is completely unobstructed. Consequently, the size and flexibility of design of a coaxial entrance assembly would be greatly restricted while the perpendicular entrance permits insertion of an inlet system of almost any reasonable size or

design; (b) the geometry of the ion source permits insertion of a narrow metal extension piece between the ion grids to admit the sample directly into the ionizing electron beam when using the perpendicular entrance, whereas a coaxial inlet requires (without significant modification of the source structure) emission of the gas at a minimum distance of 3 mm from the electron beam; and (c) an extension piece for the perpendicular entrance assembly permits emission of the sample gas directly into the electron beam in a collision free manner and with the gas at essentially the same temperature as the inner chamber (see (17) of Fig. 2) of the cryogenic inlet system. The coaxial entrance would require passage of the gas through a small hole in the "backing plate" of the source structure which cannot be readily cooled below room temperature.*

Since the need for increased sensitivity was a primary reason for modification of the original inlet system, a major consideration in comparing the coaxial and perpendicular arrangements was the relative sensitivity of the two systems. A species exerting an equilibrium vapor pressure of 10^{-4}-10^{-5} torr in the inlet system results in a very slow flow rate through the exit channel into the spectrometer. Hence, gaseous species must be emitted almost directly into the electron beam to be detected while exerting such low vapor pressures. It was pointed out above that the perpendicular arrangement permits injection of the gas sample directly into the electron beam, but it views the narrow side (0.076 x 0.64 cm) of the rectangular beam. The coaxial arrangement views the

*In other related experiments the backing plate has been removed and the fast reaction inlet port in the bendix source has been enlarged, and hence the disadvantages of the coaxial arrangement included under items (b) and (c) above are somewhat reduced in importance.

broad side of the beam (0.50 x 0.64 cm), but the gas is emitted at a distance of 3 mm from the beam.

Since it was not obvious which system would give the greatest sensitivity, it was necessary to make calculations to determine if there was a significant difference in the two approaches. If the coaxial inlet was two or three orders of magnitude more sensitive than the perpendicular inlet, it almost certainly would have been desirable to build a front entrance assembly despite the several mechanical disadvantages discussed above.

Since it is necessary to detect and investigate the condensed species that we are interested in at the lowest possible temperatures, and hence also at the lowest possible vapor pressures (10^{-5}-10^{-6} torr), the flow of these species through the exit channel of the inlet system (hereafter this channel will be referred to as the inlet channel to the mass spectrometer) will certainly be molecular. Therefore, for an inlet channel of given cross-section, πr^2, and length to radius ratio, L/r, it is possible to calculate the number of molecules effusing per unit time from this channel into the vacuum space of the spectrometer.

The number of molecules, $N_{t\theta}$, emitted per unit time per unit solid angle in the direction θ with respect to the center line of the inlet channel (see Fig. 21),may be developed in the form of the usual cosine distribution function multiplied by a deviation factor, J, which is a complicated function of L/r and θ, i.e.,

$$N_{t\theta} = \frac{N_t}{\pi} \cdot J \cos\theta \qquad (1)$$

N_t is the rate at which molecules enter the sample inlet channel and is given by the product of the molecular number density in the sample reservoir, the average molecular velocity, and the sample inlet area, i.e., $PA/(2\pi mkT)^{1/2}$. As was originally developed by Clausing,[65] the deviation factor, J, in Equation (1) is given by one of two equations, depending on the value of $\frac{L\tan\theta}{2r} \equiv p$.

For $p \leq 1$

$$J = 1 - \frac{2}{\pi}(1 - \delta)(\sin^{-1}p + p\sqrt{1 - p^2}) + \frac{4}{3\pi}(1 - 2\delta)\frac{1 - \sqrt{1 - p^2}^3}{p} \tag{2}$$

or for $p \geq 1$

$$J = \delta + \frac{4}{3\pi}\frac{1 - 2\delta}{p} \tag{3}$$

where

$$\delta = \frac{(L^2 + 4\pi^2)^{1/2} - L}{2r + \frac{4r^2}{(L^2 + 4r^2)^{1/2}}} \tag{4}$$

J has a maximum value of 1.0 for an infinitely thin edge orifice and decreases with increasing $\frac{L}{r}$. Therefore, for a thin edge orifice the molecules effuse out of the inlet port in a simple cosine distribution of intensities; whereas replacement of the orifice with a long channel of the same cross-section would result in a reduced but more directed flow. The distribution of intensities for a thin edge orifice and a long channel

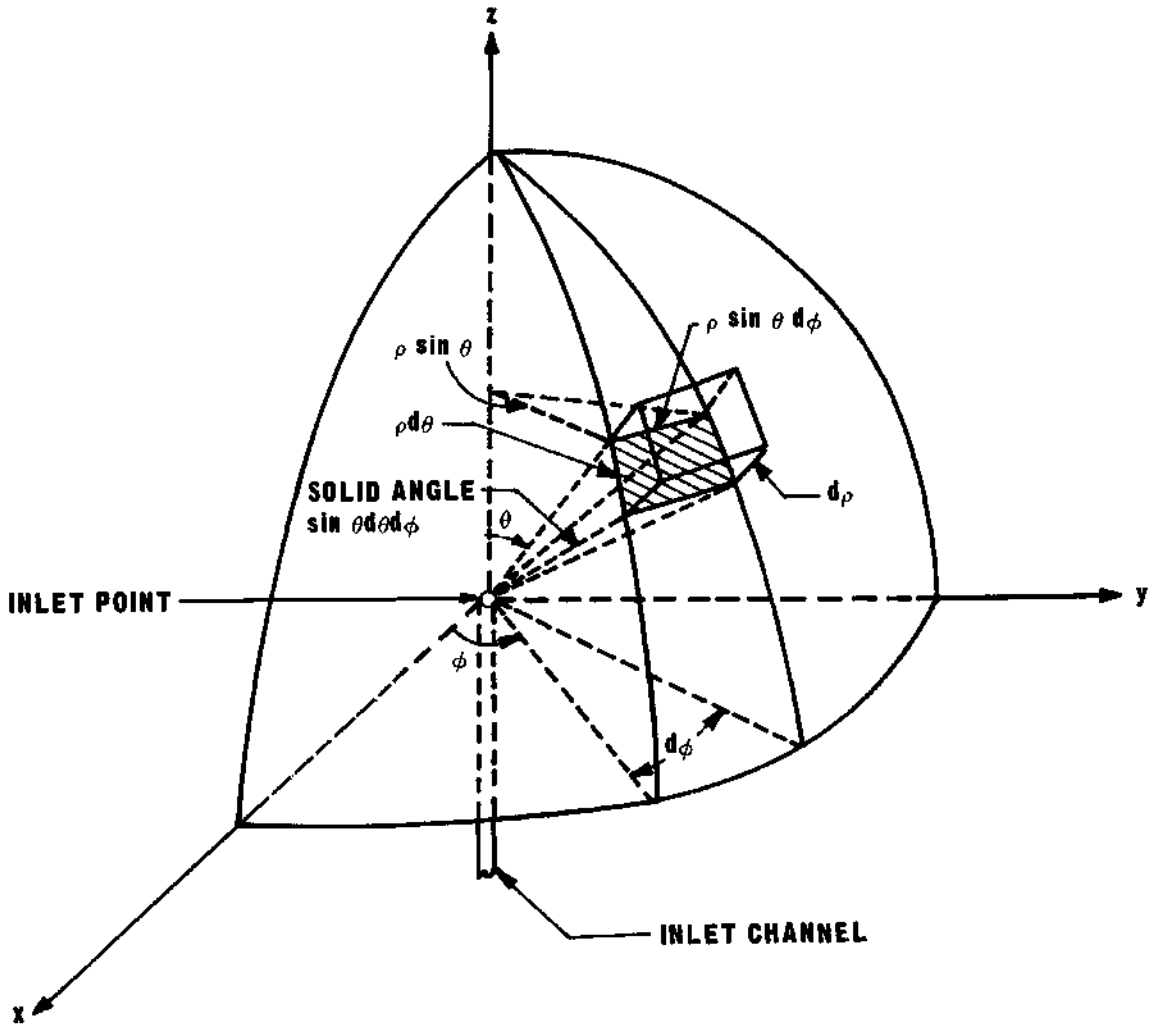

Figure 22. Spherical Coordinate System for Calculating the Number Density of Molecules at Any Point, (ρ, θ, ϕ), for the Efflux of a Gas Through a Hole in a Thin Edge Orifice.

are shown qualitatively in Fig. 23. From this Fig. 23 it is evident that for a fixed upstream pressure both the intensity at any angle and the total flow will be a maximum for a thin edge orifice for which case J has the value of unity. Hence, a thin edge orifice inlet port would correspond to the optimum design for the cryogenic inlet system.

Considering the case for which the cosine distribution of intensities is correct, i.e., J = 1, the number of molecules emitted per unit of time through the shaded solid angle, $d\omega$, shown in Fig. 22 is $N_{t\theta}d\omega$ where $d\omega = \sin\theta d\theta d\varphi$. Hence, the molecular flux at that point is given by $N_{t\theta}(d\omega/dA)$ where $dA = \rho^2 \sin\theta d\theta d\varphi$. The number density of molecules, $D(\rho,\theta)$, at any point is given by the molecular flux divided by the average molecular velocity,

$$D(\rho,\theta) = (N_{t\theta}\sin\theta d\theta d\varphi)/(\bar{v}\rho^2 \sin\theta d\theta d\varphi) \tag{5}$$

which reduces to

$$D(\rho,\theta) = \frac{N_{t\theta}}{\bar{v}\rho^2} \tag{6}$$

Substituting for $N_{t\theta}$ from Equation (1)

$$D(\rho,\theta) = \frac{N_t}{\pi\bar{v}\rho^2}\cos\theta \tag{7}$$

Equation (7) gives the number density of molecules at any point in spherical coordinates and corresponds to Equation (1) of Chapter II. Transforming Equation (7) into rectangular coordinates yields the expression

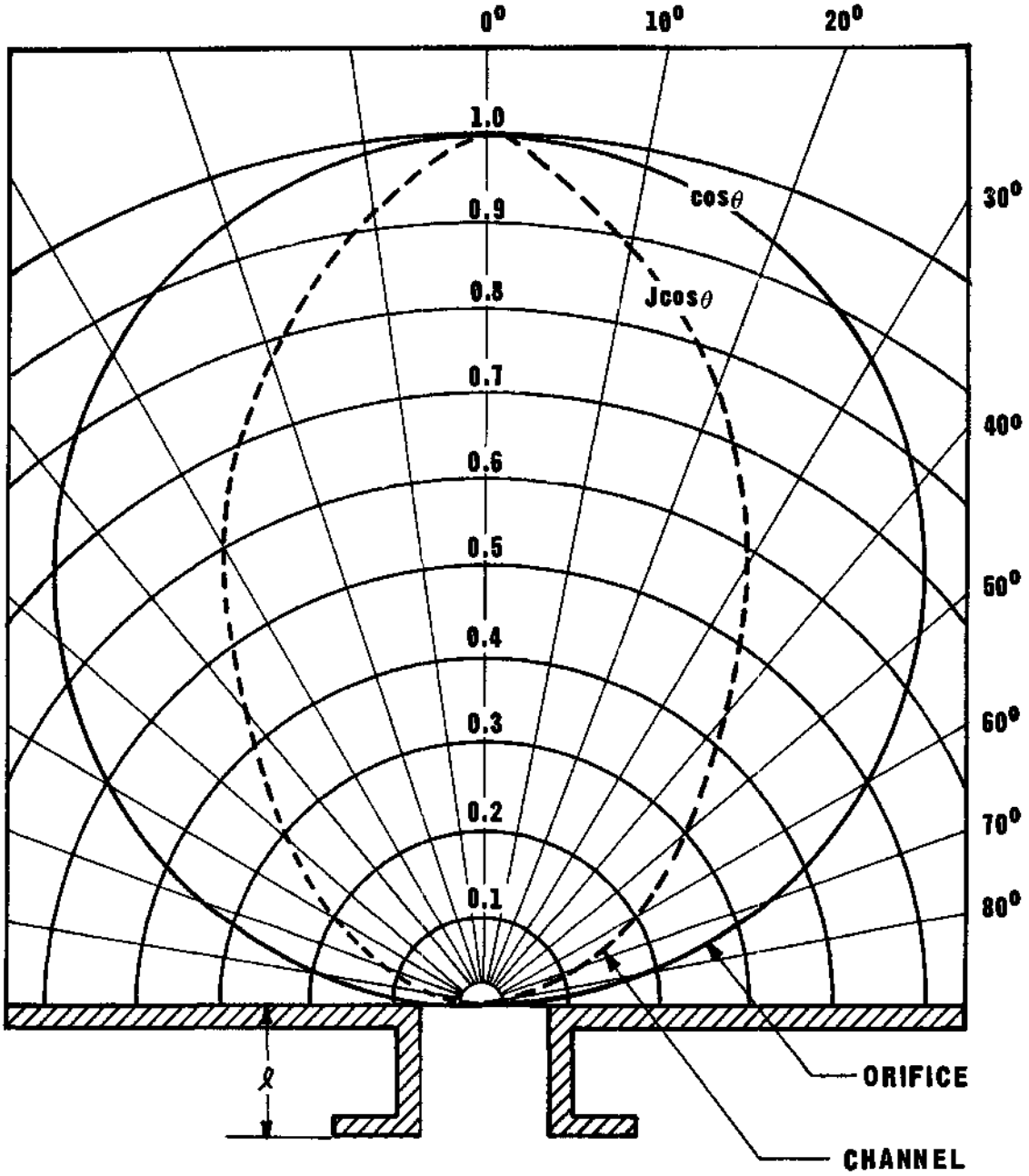

Figure 23. Polar Diagrams for the Efflux of Gas Through a Hole in a Thin Edge Orifice and Through a Channel of Length ℓ with the Same Cross-Sectional Area.

$$D(x,y,z) = \frac{N_t}{\pi\bar{v}} \cdot \frac{z}{(x^2 + y^2 + z^2)^{3/2}} \tag{8}$$

Since the probability that a given molecule will be ionized during a single pass through the electron beam is very small, it can be assumed that the number of target molecules is undiminished as a result of ionization and is therefore correctly represented by Equation (8).

Defining the sensitivity, S, as described in Chapter II,

$$S = K \int_{covol.} Ne\ \sigma_i\ dN(x,y,z) \tag{9}$$

where

$$dN(x,y,z) = D(x,y,z)\ dV(x,y,z) \tag{10}$$

and N_e and σ_i are the electron flux and ionization cross section, respectively. Fig. 24 illustrates the general rectangular effective collision covolume, covol., of the electron beam of cross section, 2a x 2b and length, $(c_2 - c_1)$, where c_1 and c_2 are the perpendicular distances from the inlet port to the nearest and far faces of the beam, respectively. Assuming that σ_i and N_e are constants and using Equations (8) and (10), Equation (9) can be written, using symmetry properties, as

$$S = (4N_tN_e\sigma_iK/\pi\bar{v}) \int_o^a \int_o^b \int_{c_1}^{c_2} [z/(x^2 + y^2 + z^2)^{3/2}]dxdydz \tag{11}$$

Integrating directly gives

$$S = (4N_tN_e\sigma_iK/\pi\bar{v}) \int_o^a \int_o^b [1/(x^2 + y^2 + c_2^2)^{1/2} - 1/(x^2 + y^2 + c_1^2)^{1/2}]dxdy \tag{12}$$

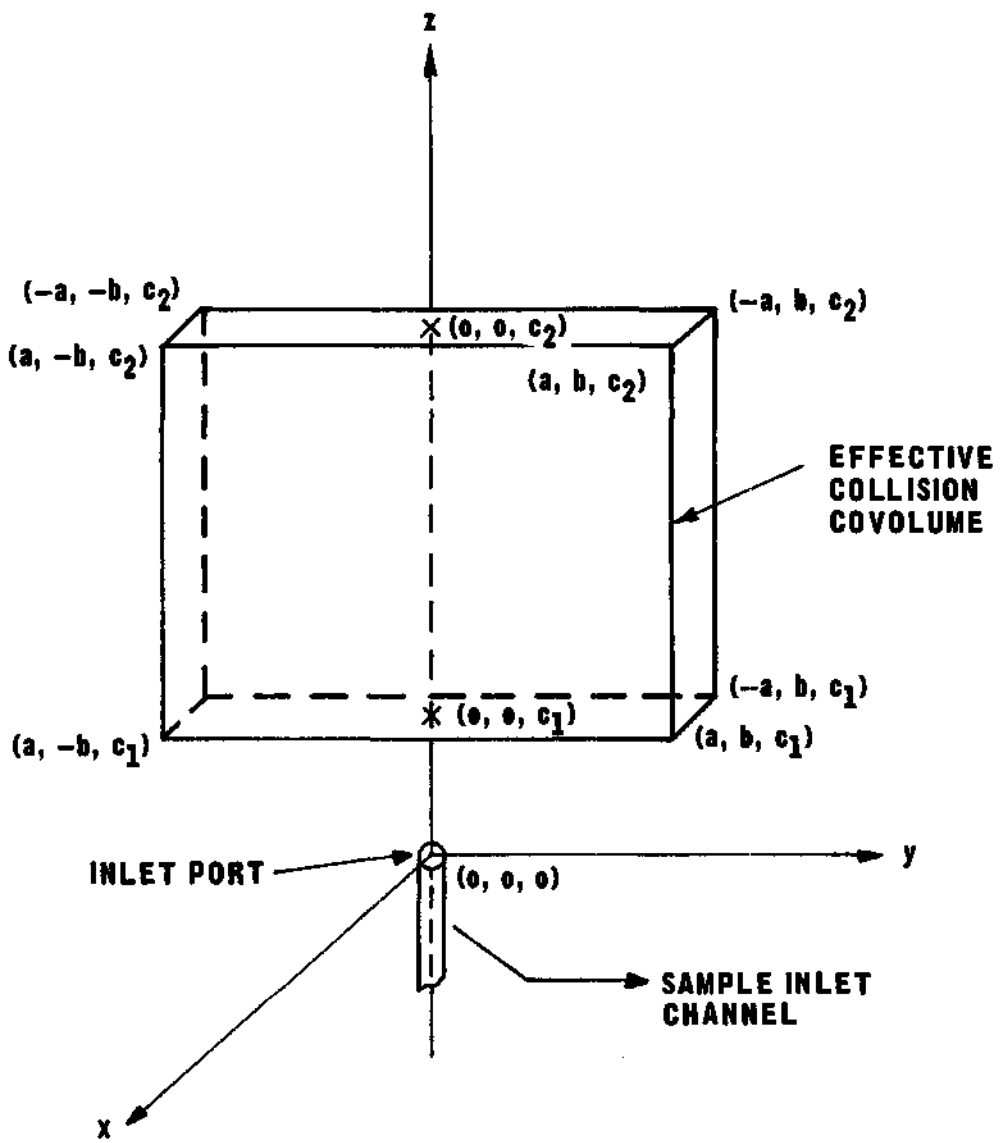

Figure 24. Rectangular Coordinate System for Integrating Over the Effective Collision Covolume to Determine the Total Sensitivity for a Given Position of the Inlet Port Relative to the Electron Beam.

$$S = (4N_t N_e \sigma_i K/\pi\bar{v}) \int_o^a \ln\{[b + (x^2+b^2+c_2^2)^{1/2}][x^2+c_1^2]^{1/2}/[b + (x^2 + b^2 + c_1^2)^{1/2}][x^2+c_2^2]^{1/2}\}\, dx \quad (13)$$

Equation (13) can be broken up into four integrals -- two of the form

$$I_1 = \int \ln [b + (x^2 + \alpha^2)^{1/2}]\, dx \quad (14)$$

and two of the form

$$I_2 = \int \ln (x^2 + c^2)^{1/2}\, dx \quad (15)$$

Evaluating the integral of Equation (14) by using parts, the trigonometric substitution $\alpha \tan\theta = x$, the algebraic substitution $z = \tan\theta/2$, and partial fractions, one obtains,

$$I_1 = x\ln[b+(x^2+\alpha^2)^{1/2}] + b\ln\{[\alpha+x+(x^2+\alpha^2)^{1/2}]/[\alpha - x + (x^2+\alpha^2)^{1/2}]\} \quad (16)$$
$$- x + 2(\alpha^2 - b^2)^{1/2} \tan^{-1}\{[(\alpha-b)/(\alpha+b)]^{1/2}\, x/[\alpha + (x^2+\alpha^2)^{1/2}]\}$$

Evaluating Equation (15) using parts yields,

$$I_2 = x \ln (x^2 + c^2)^{1/2} - x + c \tan^{-1}(x/c) \quad (17)$$

Using Equations (16) and (17) for evaluating the integral in Equation (13), one obtains,

$$S = \{4N_t N_e \sigma_i K/\pi\bar{v}\}\{a \ln[\gamma_2(b+\beta_1)/\gamma_1(b+\beta_2)] \quad (18)$$
$$+ b \ln[(\alpha_2+\beta_2-a)(\alpha_1+\beta_1+a)/(\alpha_2+\beta_2+a)(\alpha_1+\beta_1-a)]$$
$$+ c_2\tan^{-1}(a/c_2) - 2c_2\tan^{-1}[ac_2/(\alpha_2 + b)(\alpha_2+\beta_2)]$$
$$+ 2c_1\tan^{-1}[ac_1/(\alpha_1+b)(\alpha_1+\beta_1)] - c_1\tan^{-1}(a/c_1)\}$$

where, $\alpha = (b^2 + c^2)^{1/2}$; $\beta = (a^2 + \alpha^2)^{1/2}$; $\gamma = (a^2 + c^2)^{1/2}$; and where the factor, J, has been taken to be constant and equal to its maximum value of unity. Equation (18) predicts the approximate number of molecules ionized per unit time with the near face of the electron beam a distance

c_1 away from the sample inlet port for the case where (1) the flow out of the inlet channel is molecular, (2) the inlet channel is a thin edge orifice, i.e., cosine distribution of intensities out the inlet port, (3) the axis of the inlet channel is alined with the center axis of the electron beam, and (4) the inlet port is approximately a point source.

For the perpendicular arrangement of the inlet port relative to the electron beam, the geometrical parameters, a, b, and (c_2-c_1), are 0.038 cm, 0.318 cm, and 0.50 cm, respectively. For the coaxial arrangement these parameters are 0.25 cm, 0.318 cm, and 0.076 cm, respectively. Substitution of these values into Equation (18) for various values of c_1 gives the variation in sensitivity for the two arrangements as a function of the distance of the sample inlet port from the electron beam. A molecule must be considered background after a single collision with the surrounding surfaces. The factor $S\,\bar{v}/N_t N_e \sigma_i K$ (more conveniently written $F\bar{v}$) was computed from Equation (18) for both the perpendicular and and coaxial arrangements for values of c_1 between $c_1 = 0$ and $c_1 = 3.0$ cm at intervals of 0.005 cm by using the Georgia Tech B220 electronic computer. Some of the values of this factor are tabulated in Table 9. $F\bar{v}$ is equivalent to the fraction of molecules effusing from the inlet port per unit time that appear in the effective collision covolume of the electron beam multiplied by the average molecular speed (i.e., $N_b\bar{v}/N_t$) where N_b is the number of molecules in the collision covolume.

From Table 9 it was concluded that both the perpendicular and coaxial arrangements provide about the same sensitivity at equal displacements from the near face of the electron beam. The sensitivity for the coaxial case does not decrease quite as rapidly with increasing c_1 as

Table 9. Tabulated Sensitivities for Various Distances of the Inlet Port from the Electron Beam

c_1 (cms.)	$F\bar{v}$ Perpendicular Arrangement[1]	$F\bar{v}$ Coaxial Arrangement[2]	c_1 (cms.)	$F\bar{v}$ Perpendicular Arrangement	$F\bar{v}$ Coaxial Arrangement
0.000	0.156	0.134			
0.010	0.1380	0.1288	0.425	0.0171	0.0264
0.020	0.1233	0.1242	0.450	0.0159	0.0244
0.030	0.1112	0.1296	0.475	0.0148	0.0226
0.040	0.1012	0.1151	0.500	0.0138	0.0210
0.050	0.0928	0.1107	0.525	0.0130	0.0195
0.060	0.0856	0.1064	0.550	0.0122	0.0182
0.070	0.0795	0.1023	0.575	0.0114	0.0170
0.080	0.0741	0.0982	0.600	0.0108	0.0159
0.090	0.0693	0.0943	0.625	0.0102	0.0149
0.100	0.0650	0.0906	0.650	0.0096	0.0139
0.110	0.0612	0.0869	0.675	0.0091	0.0131
0.120	0.0578	0.0834	0.700	0.0086	0.0123
0.130	0.0546	0.0801	0.725	0.0082	0.0116
0.140	0.0518	0.0768	0.750	0.0078	0.0110
0.150	0.0491	0.0737	0.775	0.0074	0.0104
0.160	0.0467	0.0708	0.800	0.0070	0.0098
0.170	0.0445	0.0679	0.825	0.0067	0.0093
0.180	0.0424	0.0652	0.850	0.0064	0.0089
0.190	0.0404	0.0626	0.875	0.0061	0.0084
0.200	0.0387	0.0601	0.900	0.0059	0.0080
0.210	0.0370	0.0578	0.925	0.0056	0.0076
0.220	0.0354	0.0555	0.950	0.0054	0.0073
0.230	0.0339	0.0533	0.975	0.0052	0.0070
0.240	0.0326	0.0513	1.000	0.0050	0.0066
0.250	0.0313	0.0493	1.200	0.0038	0.0048
0.260	0.0300	0.0474	1.400	0.0028	0.0036
0.270	0.0289	0.0457	1.600	0.0023	0.0028
0.280	0.0278	0.0440	1.800	0.0018	0.0022
0.290	0.0269	0.0423	2.000	0.0015	0.0018
0.300	0.0258	0.0408	2.200	0.0013	0.0015
0.325	0.0236	0.0372	2.400	0.0011	0.0013
0.350	0.0217	0.0340	2.600	0.0009	0.0011
0.375	0.0200	0.0312	2.800	0.0008	0.0009
0.400	0.0185	0.0287	3.000	0.0007	0.0008

(1) Geometrical parameters are a = 0.038 cm., b = 0.318 cm., and c_2-c_1 = 0.500 cm.

(2) Geometrical parameters are a = 0.250 cm., b = 0.318 cm., and c_2-c_1 = 0.076 cm.

for the perpendicular case, but the difference is not significant. These predicted trends have been experimentally verified. The most striking verification of these results was obtained in the investigation of the O_2F free radical when using the perpendicular arrangement. In those experiments the sample inlet port was positioned such that a maximum O_2F^+ ion current was obtained. Moving the inlet port away from the electron beam approximately 6 mm from that optimum position resulted in a decrease in the O_2F^+ ion current of more than an order of magnitude.

Table 9 indicates that the sensitivity for the perpendicular arrangement with $c_1 = 0$ is approximately a factor of 4 greater than that for the coaxial arrangement with $c_1 = 3$ mm which is a necessary displacement for most investigations. However, this was not considered particularly significant in view of the approximations made in the calculations. The major deductions from these results were; (1) that the coaxial arangement does not offer any noticeable advantage over the perpendicular arrangement as far as sensitivity is concerned, and (2) the investigation of species that are destroyed in a single collision should be performed with the sample inlet port extremely close to the electron beam, within less than 3 mm if possible. In view of deduction (1), and the mechanical conveniences discussed earlier, it was concluded that the perpendicular arrangement was definitely preferable over the coaxial arrangement.

The calculations in this appendix have been for the case where a species is assumed destroyed after a single collision with any surrounding surface. However, it seemed that the sensitivity for a stable species would also decrease appreciably as the distance of the inlet port from the electron beam was increased, despite the fact that there would be

an appreciable background due to that stable species. Therefore, a sample of CO_2 was condensed in the cryogenic inlet system, the temperature adjusted so that an appreciable and stable CO_2^+ ion current was obtained, and the variation of this current with distance of the inlet port from the electron beam was studied. Fig. 25 illustrates the variation that was obtained. It can be seen that the intensity decreases by a factor of about 13 when the inlet port is moved from its optimum position, where the electron beam is in grazing incidence, to a distance about 2.5 cm away from the near edge of the electron beam. This is an order of magnitude less than the factor of about 150 indicated from Table 9 for an unstable species, but the decrease still represents a considerable loss of sensitivity.

The above calculations are for the case where the inlet port is a thin edge orifice which corresponds to the optimum design for a circular channel. However, a greater sensitivity could certainly be obtained by using several thin edge orifice inlet holes alined with the electron beam. The approximate sensitivity permitted with this arrangement could be readily calculated using the same approach described above and assuming that the contribution from the several inlet ports would be additive. A still better arrangement than several alined orifices would be a thin edge slit which would take advantage of the entire effective length (0.64 cm) of the electron beam. This would be particularly advantageous for the perpendicular arrangement.

It should be noted that if it is not necessary to maintain a minimum pressure, i.e., a minimum temperature, in the inlet system, then a

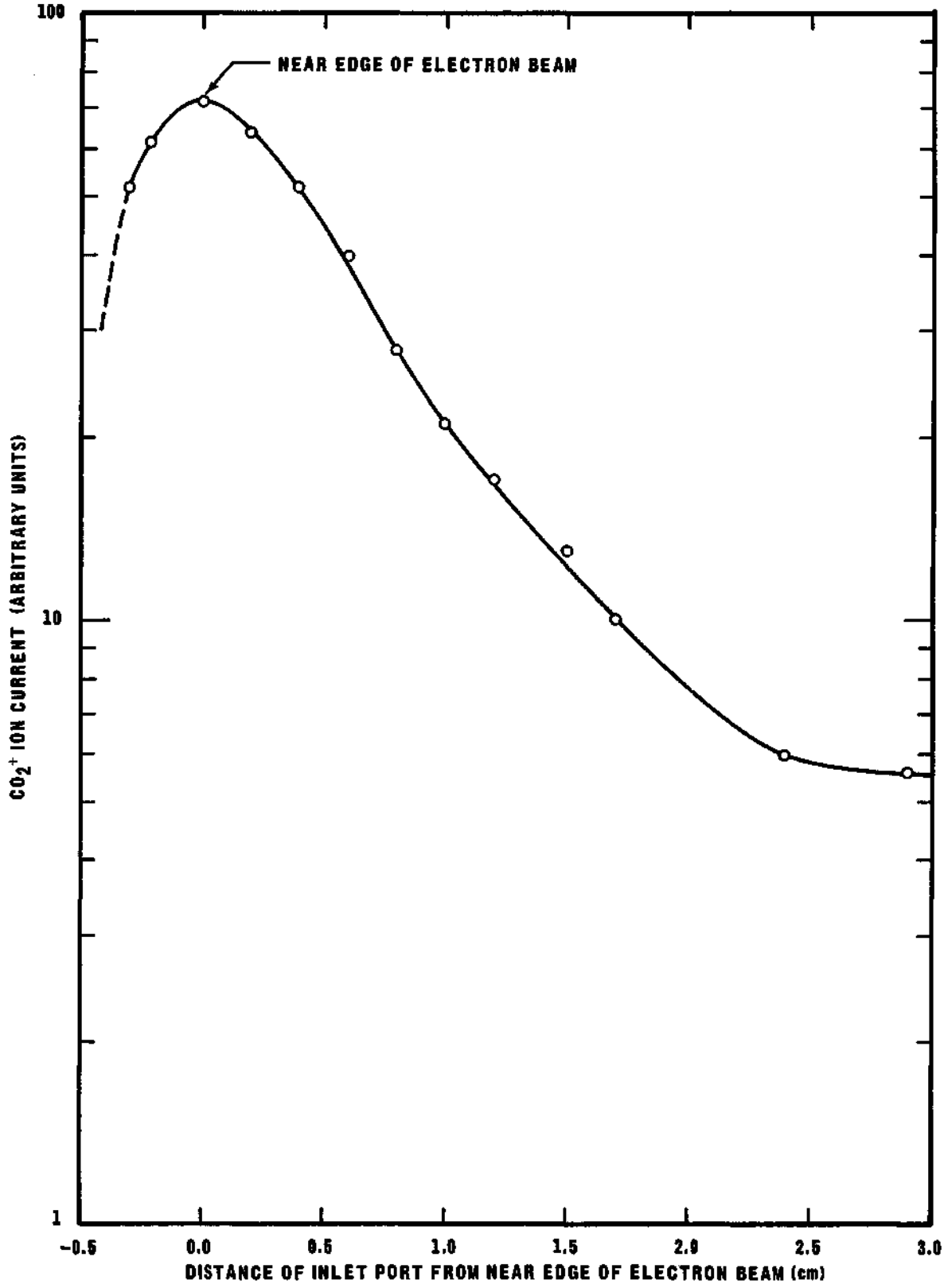

Figure 25. Variation of Sensitivity with Relative Configuration of Electron Beam and Inlet Port for the Perpendicular Arrangement Using CO_2 as a Test Gas.

greater sensitivity can be obtained by using a long inlet channel rather than a thin edge orifice. The limiting variable in this case would be the total sample influx that can be handled by the mass spectrometer pumping system. From Fig. 23, it is obvious that a more directed flow is obtained with a channel and would result in more molecules in the region of the electron beam for the same total mass flow rate through the inlet port.

Calculation of the sensitivity for this case would involve integration over the effective collision covolume where the factor J is included and is given by Equation (2) or (3). The integral involved is a very complicated function of L/r and θ and would be very difficult to compute.

A qualitative indication of the sensitivity permitted with various channels can be obtained without integrating over the collision covolume. That is, the fraction of molecules, n, entering an inlet channel of finite length which finally emerge within an angle θ with respect to the axis of the channel can be computed from the following integral

$$n = \int_0^{\theta} J \sin 2\theta \, d\theta \qquad (19)$$

where J is the deviation factor discussed above.

The value of n has recently been computed numerically and tabulated by Miller[66] for numerous values of the parameters L/r and θ. Using the results of Miller, the fraction of molecules that actually effuse from the inlet port within an angle θ with respect to the channel axis was calculated and is summarized in Table 10. The first row (i.e., for L/r = 0) is for the case of an infinitely thin edge orifice for which J = 1. It is quite obvious from Table 10 that the flow of sample becomes increasingly

Table 10. Fraction of Molecules Effusing From a Cylindrical Channel Within an Angle θ With Respect to the Axis of the Channel.

L/r	20°	30°	40°	50°	60°	70°	80°
0	0.1170	0.2500	0.4132	0.5868	0.7500	0.8830	0.9699
.1	0.1219	0.2594	0.4269	0.6034	0.7670	0.8971	0.9774
.2	0.1267	0.2686	0.4401	0.6188	0.7820	0.9084	0.9817
.5	0.1405	0.2940	0.4749	0.6573	0.8154	0.9272	0.9835
1.0	0.1610	0.3294	0.5185	0.6974	0.8383	0.9311	0.9838
1.2	0.1682	0.3411	0.5313	0.7059	0.8400	0.9315	0.9839
1.5	0.1784	0.3563	0.5461	0.7133	0.8415	0.9321	0.9840
2.0	0.1933	0.3763	0.5609	0.7179	0.8438	0.9332	0.9843
3.0	0.2167	0.3996	0.5721	0.7241	0.8471	0.9346	0.9848
4.00	0.2329	0.4100	0.5787	0.7283	0.8493	0.9352	0.9848
6.00	0.2509	0.4225	0.5871	0.7334	0.8519	0.9364	0.9850
10.0	0.2663	0.4341	0.5949	0.7385	0.8542	0.9373	0.9850

more directed in the forward direction for larger values of the length to radius ratio, L/r. For instance, the fraction of molecules emitting within an angle $\theta = 20°$ is more than twice as great for a channel with $L/r = 10$ than for an infinitely thin orifice. These results indicate that a long exit channel would be quite desirable for experiments in which it is permissible for the cold sample to be maintained at pressures of several torr.

Temperature Gradient in the Extension Piece of the Cryogenic Reactor-Inlet System

The blade-shaped extension piece (16) of the cryogenic inlet assembly shown in Fig. 2 was designed to permit its insertion between the grids of the ion source and hence directly into the ionizing electron beam. The major design parameters of the extension piece were dictated by: (1) the distance it had to extend into the ion source for the electron beam to be in grazing incidence with the sample inlet port, and (2) the space available between the ion grids. It was constructed of high thermal conductivity copper with as large a cross section as possible to minimize any thermal gradient in the axial direction, l, resulting from radiative heat transfer from the surroundings or from heat generated by decomposition of unstable species in the exit channel. The outer surface of the extension piece was nickel plated to reduce its emissivity which in turn reduced the rate of heat input by radiative transfer. The following discussion gives the basic equations and calculations for the thermal gradient in the extension piece in the axial direction assuming the worst possible case, i.e., that all the heat gained by the extension piece is transferred through its outermost end, resulting in the largest possible temperature rise.

It is assumed that the only thermal gradient in the extension piece is in the axial direction, l, and that it is rectangular shaped of width, X; height, Y; and length, L. Actually, it is slightly tapered, but not enough to significantly affect the following calculations. It has a 0.238 cm diameter sample exit channel drilled through essentially its full length.

Assuming that all heat gained by the extension piece is transferred through the end, a steady state energy balance and Fourier's law yields

$$\frac{dT}{dl} = Q_t/k_c A \tag{20}$$

Integrating Equation (20) over the length of the extension piece, with k_c taken as a constant,

$$T_L - T_o = \Delta T_L = Q_t L/k_c A \tag{21}$$

Equation (21) gives the total temperature drop in the extension piece in the axial direction. Q_t is the total heat gained per unit time, k_c is the thermal conductivity, and A = 0.753 cm^2 is the net heat transfer area for conduction in the axial direction.

The total heat Q_t added to the extension piece is the sum of the heat gained by radiation from the surroundings, Q_r, and heat gained by decomposition of unstable chemical species in the exit channel, Q_c. The negligible heat gained due to bombardment by the electron beam was calculated to be $2.09(10)^{-6}$ cal/sec for an electron energy of 70 ev and electron current of 0.125 microamp. The rate of heat transfer to the extension

piece by radiation, Q_r, is given by

$$Q_r = \sigma\, e\, A_s(T_2^4 - T_s^4) \tag{22}$$

Since T_2 is approximately 300°K and 77°K $\leq T_s \leq$ 150°K, Q_r is approximated quite accurately by

$$Q_r = \sigma\, e\, A_s T_2^4 \tag{23}$$

Using the values X = 0.4 cm, Y = 1.9 cm, L = 2.7 cm, and T_2 = 300°K, Equation (23) gives Q_r = 0.138e cal/sec where e is the emissivity of the outer surface of the extension piece.

For the case where O_3F_2 was the labile species being investigated, it could be assumed that all the sample was being decomposed into O_2 and F_2 in the exit channel. At 110°K,

$$O_3F_2 \rightarrow \frac{3}{2}\, O_2 + F_2 + 6.24 \text{ Kcal/mole} \tag{24}$$

Assuming that the exit port is a thin edge orifice (0.00515 cm^2 cross-section) and the inlet system is at 110°K (O_3F_2 has vapor pressure of about 1.0 torr at 110°K), the maximum flow rate of O_3F_2 through the exit channel can be calculated to be $3.08(10)^{-5}$ mole/sec. Hence, Q_c = 0.0192 cal/sec if all the O_3F_2 decomposes in the channel according to Equation (24).

The average value of k_c is 1.18 cal/sec-cm-°K over the temperature range of 77°-150°K. Using this value and $Q_t = Q_r + Q_c$ = 0.138 + 0.019 = 0.257 cal/sec where the emissivity, e, is taken as 1.0, Equation (21) gives ΔT_L = 0.78°K. This would correspond to the maximum temperature

rise that one would expect from the inner coolant chamber (17) to the tip of the extension piece. A more realistic value of approximately 0.1°K is obtained by assuming that e = 0.1 which would be expected for a polised nickel surface. In any case, the maximum temperature rise of less than 1°K was considered satisfactory for this work. The real temperature rise in the extension piece was actually measured while it was in analytical position as shown in Fig. 4 and was less than 2°K while the inner chamber (17) was at 77°K. Apparantly the heat transfer by conduction from the extension pieces was decreased somewhat by the solder connection to the inner chamber (17). However, this temperature rise in the extension piece of less than 2°K was still considered satisfactory.

APPENDIX C

MISCELLANEOUS MASS SPECTROMETRIC DATA

In this appendix are presented mass spectrometric results for OF_2 reported by Dibeler, et al.;[6] ionization efficiency data on OF_2 obtained in this thesis research; and positive and negative ion spectra obtained in this work for several of the most troublesome impurities observed in the oxygen fluoride experiments. Table 11 gives the relative abundance and appearance potentials of the positive and negative ions in the mass spectrum of oxygen difluoride reported by Dibeler, et al.[6] These data were obtained using a magnetic deflection mass spectrometer and the cracking pattern given is quite different from that obtained in this work using the time-of-flight machine.

Figs. 26 and 27 show the ionization efficiency data for OF^+ and OF_2^+ from OF_2 that were obtained in this work. These data permitted a rough determination of the appearance potentials of OF^+ and OF_2^+ from OF_2 from the linear intercept method. The values were determined to be $A(OF^+) = 15.7 \pm 0.3$ ev and $A(OF_2^+) = 13.6 \pm 0.3$ ev, which agree quite well with the values of Dibeler, et al., given in Table 11.

Tables 12-19 give the positive and negative ion spectra for OF_2, CF_4, C_2F_6, and SiF_4 obtained using the Bendix time-of-flight mass spectrometer. The intensities given for the negative ions were estimated from their observed intensities on the oscilloscope since the Bendix machine is not equipped to record negative ion currents. In addition, the energetics listed are estimated by observing the oscilloscope and

varying the electron energy. These energy values are hence only rough estimates in that the energy scale could not be calibrated.

Table 11. Relative Abundances and Appearance Potentials of Positive and Negative Ions in the Mass Spectrum of Oxygen Difluoride*

Ion	Relative Abundance %	Appearance Potential ev	Remarks
OF_2^+	100	13.7 ± 0.2	$I(OF_2)$ = 13.7 ± 0.2 ev
OF^+	91	15.8 ± 0.2	Negligible excess kinetic energy, KE. I(OF) = 13.0 ± 0.2 ev
O^+	4.3	--	Indeterminate threshold
F^+	0.5	--	Immeasurably small
F^-	63	1.2 ± 0.2	$KE(F^-)$ = 1.3 ev $KE(F^- + OF)$ = 2.0 ev D(FO-F) = 2.8 ev D(O-F) = 1.1 ev

*Data taken from Dibeler, et al.[6]

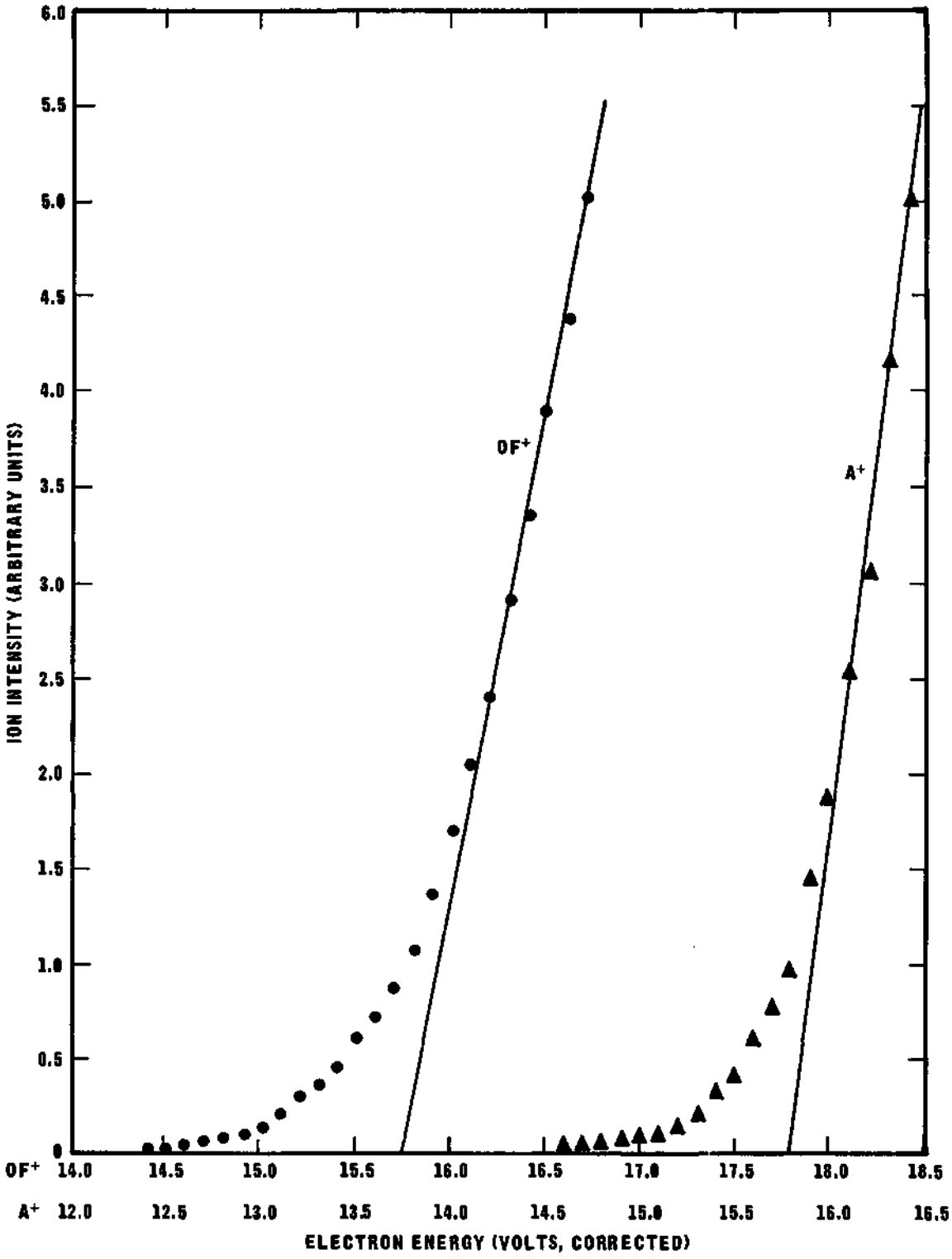

Figure 26. Ionization Efficiency Data for OF^+ from OF_2 With Argon as the Standard.

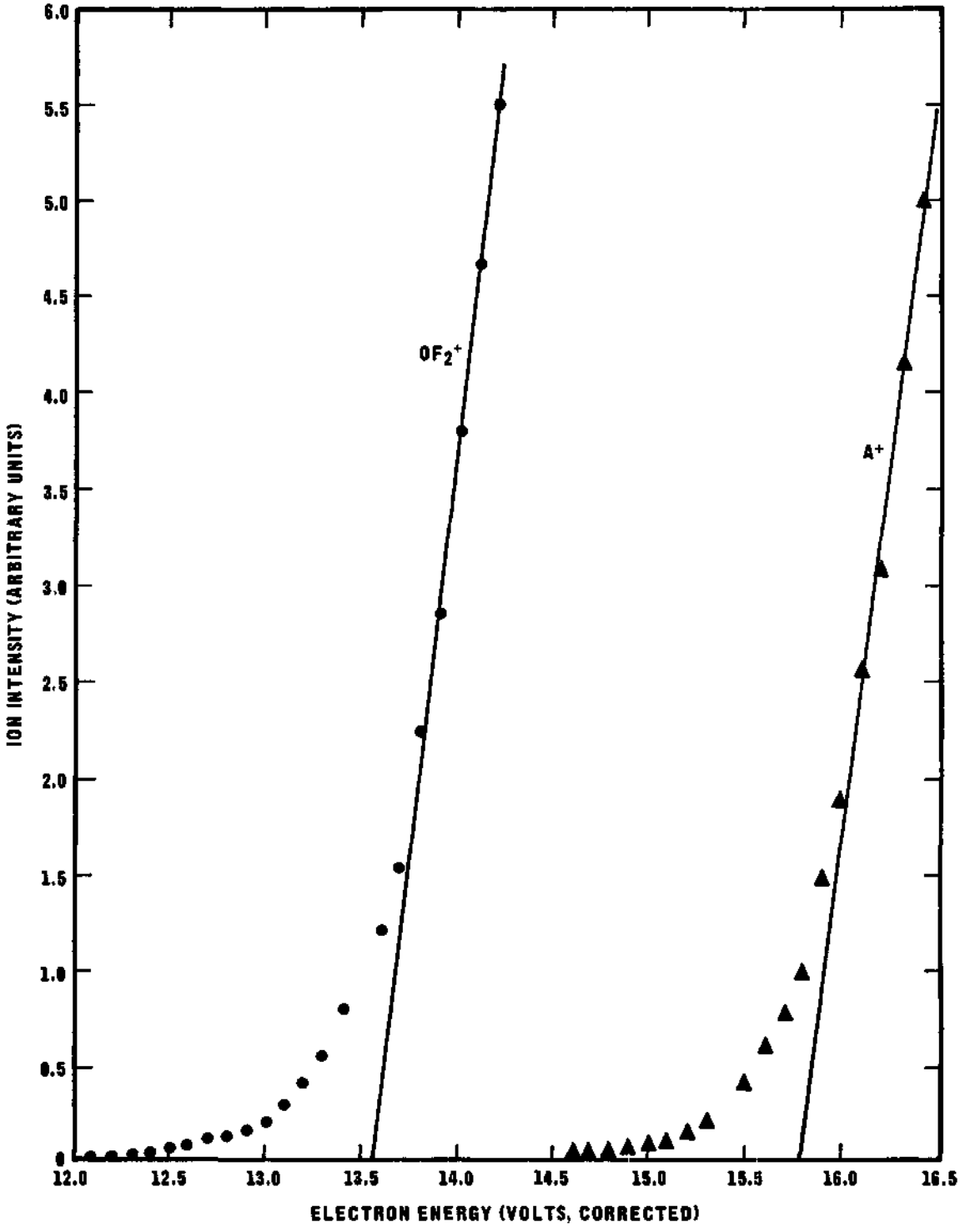

Figure 27. Ionization Efficiency Data for OF_2^+ from CF_2 With Argon as the Standard.

Table 12. Positive Ions of OF_2

Mass	Species	Relative Intensity
16	O	37.1
19	F	8.4
35	OF	100.0
54	OF_2,p	45.0

Electron Energy = 70 volts

p = parent

Table 13. Negative Ions of OF_2 (Uncalibrated Energetics)

Mass	Species	Relative Intensity[a]	Appearance Potentials, ev[b]	Electron Energy for Maximum Ion Current, ev
19	F	100	0.6	5.7
35	OF	80	1.9	17.0
38	F_2	40	2.2	17.0
54	OF_2	< 1	~ 17	c

[a]Estimated visually from oscilloscope at electron energy yielding the maximum ion current.

[b]Energy at which ion current is first observed on oscilloscope.

[c]Signal was very weak and was observed only when an extremely large sample was injected into the spectrometer.

Table 14. Positive Ions of CF_4

Mass	Species	Relative Intensity
12	C	2.7
19	F	3.5
25	CF_2,d	0.5
31	CF	6.5
34.5	CF_3, d	0.2
50	CF_2	9.1
51	CF_2, i	0.2
69	CF_3	100.0
70	CF_3, i	1.1

Electron Energy = 70 volts

d = doubly charged ion

i = isotope

Table 15. Negative Ions of CF_4 (Uncalibrated Energetics)

Mass	Species	Relative Intensity[a]	Appearance Potential, ev[b]	Electron Energy for Maximum Ion Current, ev
19	F	100	1.1	5.7 - 6.0
38	F_2	1	4.7	5.7 - 6.0
69	CF_3	65	2.1	5.7 - 6.0

[a] Estimated visually from oscilloscope at electron energy yielding the maximum ion currents.

[b] Energy at which ion current is first observed on oscilloscope.

Table 16. Positive Ions of C_2F_6

Mass	Species	Relative Intensity
12	C	1.0
19	F	0.03
31	CF	6.8
50	CF_2	5.1
51	CF_2,i	0.1
69	CF_3	100.0
70	CF_3,i	0.8
100	C_2F_4	0.3
119	C_2F_5	37.3

Electron Energy = 70 volts

i = isotope

Table 17. Negative Ions of C_2F_6 (Uncalibrated Energetics)

Mass	Species	Relative Intensity[a]	Appearance Potential, ev[b]	Electron Energy for Maximum Ion Current, ev
19	F	100	1.6	5.1 - 5.6
69	CF_3	8	2.3	6.0

[a] Estimated visually from oscilloscope at electron energy yielding the maximum ion currents.

[b] Energy at which ion current is first observed on oscilloscope.

Table 18. Positive Ions of SiF_4

Mass	Species	Relative Intensity
19	F	4.2
27	Si,i	0.2
28	Si	---
29	Si,i	0.6
47	SiF	9.0
48	SiF,i	0.6
49	SiF,i	0.4
66	SiF_2	1.6
83		0.6
85	SiF_3	100.0
86	SiF_3,i	1.5
104	SiF_4,p	2.7
105	SiF_4,i	1.1

Electron Energy = 70 volts

i = isotope

p = parent

Table 19. Negative Ions of SiF_4 (Uncalibrated Energetics)

Mass	Species	Relative Intensity[a]	Appearance Potential, ev[b]	Electron Energy for Maximum Ion Current, ev
19	F	75	7.5	9.6 - 10.0
38	F_2	2	8.3	9.6 - 10.0
85	SiF_3	100	7.5	9.6 - 10.0

[a] Estimated visually from oscilloscope at electron energy yielding maximum ion currents.

[b] Energy at which ion current is first observed on oscilloscope.

APPENDIX D

TYPICAL RAW DATA FOR THE OXYGEN FLUORIDE EXPERIMENTS

This appendix presents some typical raw data obtained in a few of the oxygen fluoride synthesis experiments. Figs. 28 and 29 show typical traces made at several temperatures during the warmup after an O_3F_2 synthesis experiment. These traces represent the mass spectrum from m/e = 16 to 90 that were obtained at the points of most interest during the warmup as indicated by Figs. 10 and 11 in Chapter III. All of them are made with an electrometer index setting of 40 except Fig. 28B for which this index was at 500. This permitted a comparison of the very large O_2^+ current with the other ion currents. The traces were made out to masses beyond m/e = 150, but only very small peaks due to impurities were observed beyond about m/e = 90. Traces were also made at electrometer settings as low as 0.1 in order to detect extremely small ion currents.

Table 20 gives the positive ions observed in the oxygen fluoride experiments, as well as the parent species of each. The relative amounts of each species varied considerably in different experiments, but most of them were observed in all of the experiments.

Tables 21, 22, and 23 give the actual ion currents (all have the same arbitrary units based on an electrometer index setting of 0.1) obtained at various temperatures in three of the O_3F_2 synthesis experiments. The intensities given are of a summary nature in that they represent an

average obtained from several traces made at that temperature. These traces were made after the ion currents had essentially stabilized at each temperature. In the cases where the mass spectrum is given twice at the same temperature, the inlet system was maintained for a relatively long time (20-45 minutes) at that temperature, and the two traces represent the change of the spectrum during that period.

In some cases very large peaks overlapped smaller adjacent peaks as indicated by the letter, b. For the case where a trace was not made at an electrometer index setting high enough to reduce the intensity of a given ion current until it was on scale, the ion current is designated by the letter, a. A dash indicates that the mass spectrum was recorded beyond that m/e, but no recordable ion current was obtained for the lowest electrometer index setting used which was usually 1.0. A blank space in the tables indicates that the mass spectrum was not recorded out to that mass.

Table 21 represents one of the initial O_3F_2 experiments illustrated by Fig. 12 in which the exit channel of the inlet system was 3.0 inches long and 0.020 in. inside diameter and the reactor space was not pumped during warmup. In this run the O_3F_2 synthesis was run for about one hour, using the <u>in situ</u> single electrode technique. The total warmup time was about 12 hours. Traces were made up to about 160°K, but no new species were detected above 140°K. From these data it can be seen that a species had to exert a vapor pressure of about 0.05-0.5 torr before it could be detected. These data may be compared with that of Table 22 which again gives the raw data obtained in a typical O_3F_2 experiment using the <u>in situ</u> synthesis technique. The total synthesis time was about 2.5 hours which

accounts partially for the relatively large ion currents obtained. The inlet system was not glass lined in this experiment, but the reactor space was pumped continuously during warmup. The total warmup time was about 10 hours. It can be seen that the species were detected in this experiment when they exerted a vapor pressure of only about 10^{-4}-10^{-5} torr which is significantly lower than in the earlier experiments. There are two reasons for this; (a) the exit port was a thin edge orifice (0.089 cm dia.), and (b) the gain of the multiplier of the mass spectrometer was increased by about an order of magnitude over that of the earlier experiments.

Table 23 gives the data obtained in an O_3F_2 experiment performed in essentially the same manner as that used for the run given by Table 22, except that the entire reactor space, transfer line, and exit channel of the inlet system was glassed lined. The synthesis ran for about 45 minutes, and the total warmup time was approximately 10 hours. The sample was pumped for about three hours at 77°K before any warming, and the change in the spectrum during that time is indicated by the two traces presented at that temperature.

In order to determine the actual sensitivity of the inlet system after the original extension piece (16), which had an exit channel with an L/r of about 300, was replaced by one that had a thin edge orifice exit port, a sample of CO_2 was condensed in the reactor space and the CO_2^+ ion current was determined as a function of temperature. CO_2 was chosen as a test species since its vapor pressure has been calculated extremely accurately by Mullins, Kirk, and Ziegler[79] down to 10^{-25} torr. Fig. 30 shows a plot of the CO_2^+ current as a function of the vapor

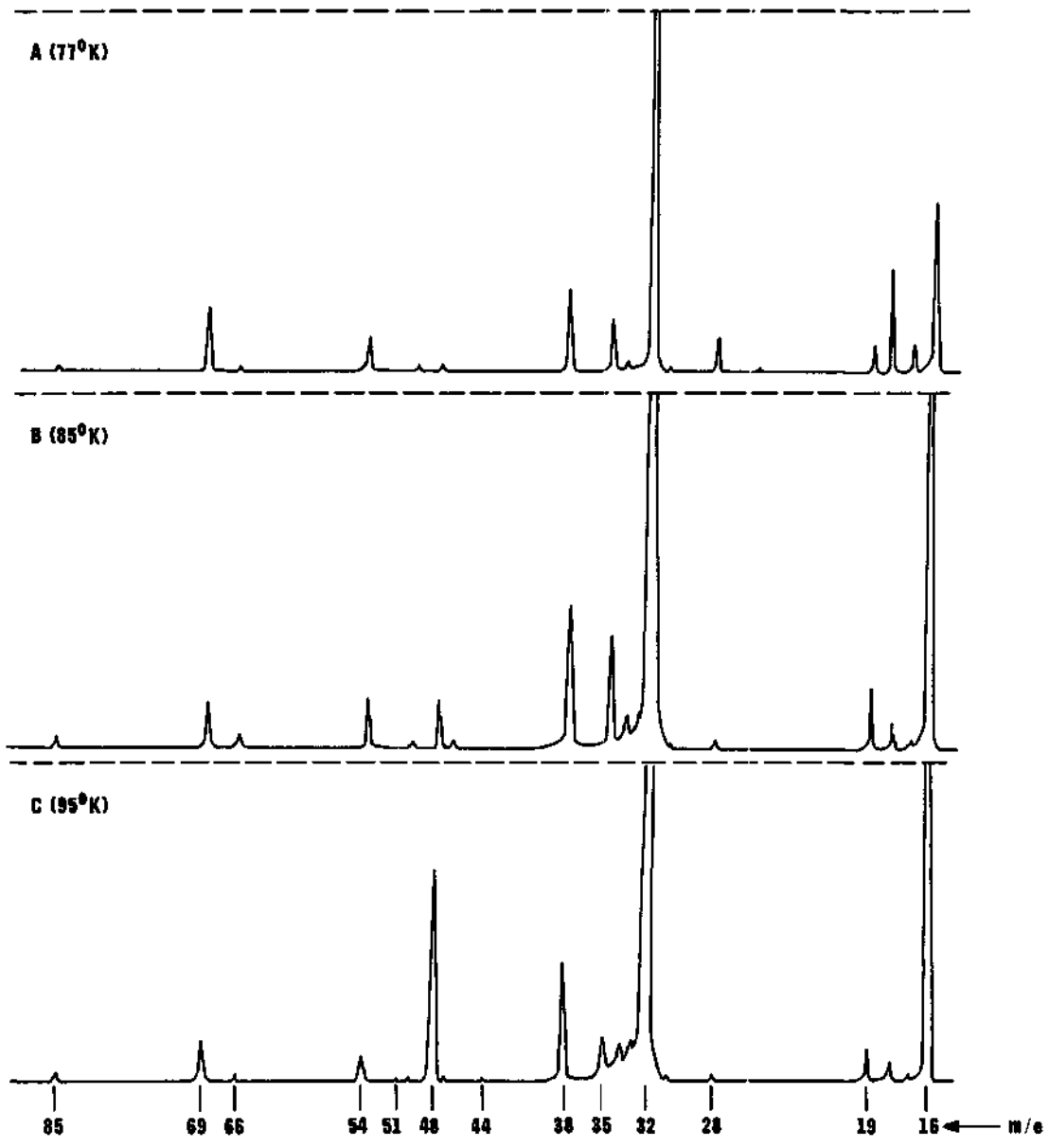

Figure 28. Positive Ion Spectrum at Three Temperatures During Warmup of Reaction Products of an O_3F_2 Synthesis.

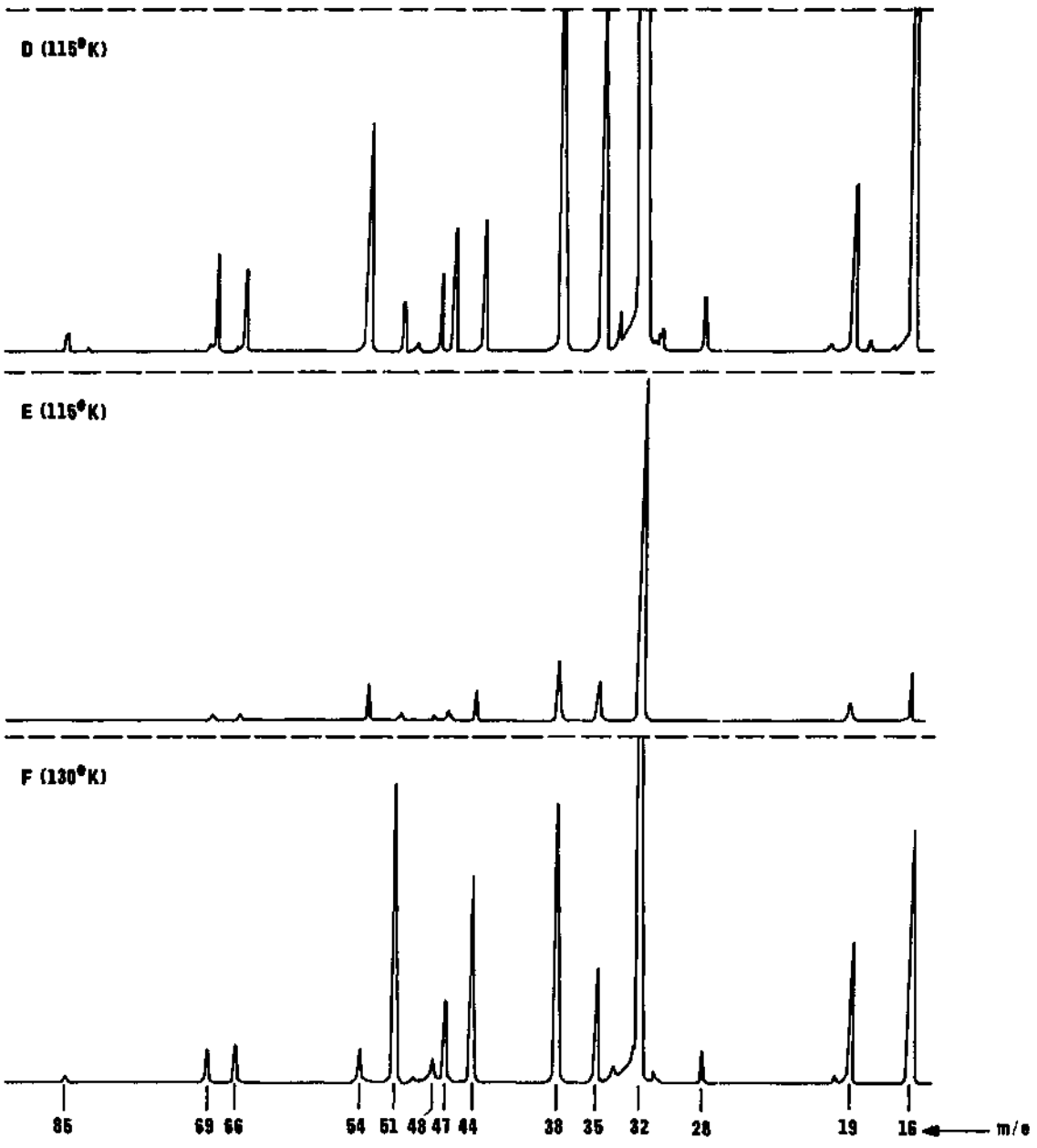

Figure 29. Positive Ion Spectrum at Two Temperatures During Warmup of Reaction Products of an O_3F_2 Synthesis.

pressure of CO_2. It shows that the CO_2 could be detected down to a vapor pressure of approximately 10^{-6} torr. However, it should be pointed out that the ion current was measured by placing the spectrometer gate on the CO_2^+ peak with a maximum gate width. This obviously results in a much larger ion current than that obtained by scanning the spectrum, since it is necessary to use a narrower gate width for scanning in order to obtain well resolved peaks. This accounts for the fact that species had to exert vapor pressures of about 10^{-4}-10^{-5} torr in the oxygen fluoride experiments before they were detected. The maximum in the CO_2^+ current where CO_2 has a vapor pressure of about $4x10^{-2}$ torr was expected since most of the species observed in the oxygen fluoride experiments gave maxima where their vapor pressures were about 0.1-1.0 torr.

Table 20. Positive Ions Observed in the Low Temperature Oxygen Fluorides Experiments (Continued)

m/e	Predominant Species		Other Species	
	Identified Ions	Parent Species	Identified Ions	Parent Species
12	C^+	CF_4, C_2F_6, COF_2		CO_2
14	N^+	N_2, N_2F_2		
16	O^+	O_2F_2, O_2, O_3, OF_2		
17	OH^+	H_2O		
18	H_2O^+	H_2O		
19	F^+	O_2F_2, F_2, CF_4, C_2F_6, SiF_4		
20	HF^+	HF		
25			CF_2^{++}	CF_4, C_2F_6
28	N_2^+	N_2	Si^+, CO^+	SiF_4, CO_2, COF_2
29			Si^+, i	SiF_4
31	CF^+	CF_4, C_2F_6		
32	O_2^+	O_2F_2, O_2, O_3	S^+	H_2S, SF_6, SO_2F_2
33	HS^+	H_2S	NF^+	NF_3, N_2F_2
34	H_2S^+	H_2S		
34.5			CF_3^{++}	CF_4, C_2F_6
35	OF^+	O_2F_2, OF_2		
38	F_2^+	F_2		
44	CO_2^+	CO_2	N_2O^+	N_2O

Table 20. Positive Ions Observed in the Low Temperature Oxygen Fluorides Experiments. (Continued)

m/e	Predominant Species: Identified Ions	Predominant Species: Parent Species	Other Species: Identified Ions	Other Species: Parent Species
47	COF^+, SiF^+	COF_2, SiF_4	N_2F^+	N_2F_2, N_2F_4
48	O_3^+	O_3	SO^+	SO_2F_2
50	CF_2^+	CF_4, C_2F_6		
51	O_2F^+	O_2F_2	CF_2^+, i	CF_4, C_2F_6
52			NF_2^+	NF_3, N_2F_4
54	OF_2^+	OF_2		
66	COF_2^+	COF_2	SiF_2^+, $N_2F_2^+$	SiF_4, N_2F_2
67			SOF^+	SO_2F_2
69	CF_3^+	CF_4, C_2F_6		
70			CF_3^+, i	CF_4, C_2F_6
71			NF_3^+	NF_3
83			SO_2F^+	SO_2F_2
85	SiF_3^+	SiF_4	$N_2F_3^+$	N_2F_4
86			SiF_3^+, i	SiF_4
100			$C_2F_4^+$	C_2F_6
102			$SO_2F_2^+$	SO_2F_2
104			SiF_4^+, $N_2F_4^+$	SiF_4, N_2F_4

Table 20. Positive Ions Observed in the Low Temperature Oxygen Fluorides Experiments (Concluded)

	Predominant Species		Other Species	
m/e	Identified Ions	Parent Species	Identified Ions	Parent Species
108			SF_4^+	SF_6
119			$C_2F_5^+$	C_2F_6
127			SF_5^+	SF_6

Table 21. Raw Data for a Typical O_3F_2 Synthesis Experiment; Reactor Space Not Pumped During Warmup

	Temperature °K									
	IC 77	77	77	77	77	80	88	88	94	94
m/e	OC 77	85	90	94	88	88	88	95	96	101
	Relative Ion Currents									
12	25	30	60	50	52	a	1100	575	75	76
14	88	100	100	85	96	110	120	180	120	124
16	160	550	2900	2500	2000	a	510	a	a	a
17	12	13	10	15	16	14	20	30	10	40
18	56	55	40	50	50	46	50	75	50	48
19	55	170	320	270	140	a	1400	920	110	92
20	-	-	-	-	-	-	-	-	-	-
25	12	25	20	32	46	90	450	320	40	36
28	1100	1120	1000	1100	1200	a	1600	1720	1100	1200
29	10	12	20	7	8	18	19	20	20	22
31	42	60	100	115	128	a	2200	1320	150	158
32	960	3300	18000	16000	11000	a	3500	a	a	a
33	10	75	b	b	68	70	75	95	b	b
34	-	30	100	180	64	66	70	85	180	220
34.5	-	10	20	40	20	58	100	170	-	-
35	112	230	400	415	430	a	100	920	105	112
38	40	490	750	650	52	60	80	160	20	20
44	6	10	5	5	3	12	40	20	10	16
47	-	-	-	-	-	-	-	-	70	84
48	-	-	-	-	-	-	-	-	25	24
50	62	115	200	220	280	a	4000	2160	250	255
51	-	-	-	4	6	12	a	a	-	-
52	6	-	12	12	16	42	60	80	20	20
54	58	150	300	410	300	a	120	520	40	64
66	-	-	-	-	-	-	-	-	170	192
67	-	-	-	-	-	-	-	-	-	-
69	1100	2000	3000	2900	a	a	a	a	a	a
70	20	30	50	52	52	b	b	b	100	96
71	6	-	-	20	16	-	-	-	20	20
85	-	-	-	-	-	-	-	-	120	112
86	-	-	-	-	-	-	-	-	-	-
108	-	-	-	-	-	-	-	-	-	-
119	-	-	-	-	-	-	-	-	-	-
127	-	-	-	-	-	-	-	-	-	-

(Continued)

Table 21. Raw Data for a Typical O_3F_2 Synthesis Experiment: Reactor Space Not Pumped During Warmup (Continued)

	Temperature °K									
	IC 96	101	106	106	106	106	110	110	116	116
m/e	OC107	107	107	110	115	115	115	118	118	122
	Relative Ion Currents									
12	122	90	60	34	60	45	50	60	30	49
14	98	60	52	44	44	40	32	35	40	38
16	a	11500	a	a	a	15800	13000	10000	5000	a
17	40	15	20	14	18	20	13	15	12	10
18	82	55	48	54	75	60	40	50	30	25
19	a	140	80	80	110	150	120	120	90	90
20	-	-	-	-	-	-	15	40	60	38
25	104	32	38	20	20	19	20	20	20	18
28	a	670	550	525	550	500	480	400	485	480
29	20	20	9	10	8	9	9	8	6	8
31	250	205	170	70	240	280	200	200	110	120
32	a	72000	a	a	a	105000	85000	63000	32000	a
33	b	b	b	b	b	b	b	b	b	b
34	b	b	b	b	780	b	b	b	215	200
34.5	b	b	b	b	390	b	b	b	32	50
35	a	160	80	a	240	220	145	140	60	85
38	78	30	-	80	60	20	32	35	20	30
44	16	20	80	82	60	45	60	90	55	60
47	a	270	190	a	380	380	300	340	150	200
48	92	95	80	a	260	410	470	800	360	550
50	a	235	200	180	170	200	190	200	140	130
51	-	-	15	15	40	80	100	100	70	80
52	92	30	10	15	20	18	12	11	10	12
54	96	50	28	32	44	40	22	40	28	40
66	a	460	330	a	770	700	500	480	180	230
67	-	-	3	14	14	18	16	15	-	-
69	a	2550	a	a	a	2500	2400	2500	1150	a
70	b	76	60	54	80	80	65	70	40	48
71	b	30	-	18	-	20	-	-	8	15
85	a	256	220	a	480	400	250	300	85	130
86	-	8	5	14	16	16	5	-	-	-
108	-	-	-	-	-	4	6	9	8	10
119	-	20	90	a	240	290	200	230	90	a
127	-	-	5	a	-	40	40	60	40	a

(Continued)

Table 21. Raw Data for a Typical O_3F_2 Synthesis Experiment; Reactor Space Not Pumped During Warmup (Concluded)

				Temperature °K						
	IC116	120	120	123	125	131	131	134	134	140
m/e	OC125	125	125	129	129	132	134	134	140	140
	Relative Ion Currents									
12	55	50	18	32	38	50	40	25	74	90
14	38	30	40	34	38	30	32	20	22	20
16	a	a	280	240	a	240	a	3600	3000	3000
17	13	12	9	12	10	9	10	6	10	11
18	30	24	18	16	20	18	16	14	16	20
19	120	132	0	480	600	1110	1280	2500	1850	1900
20	30	68	40	42	55	40	40	20	35	55
25	11	14	1	5	5	10	8	4	3	14
28	440	500	460	550	525	480	440	320	350	430
29	10	7	5	10	6	9	6	8	7	20
31	190	140	20	60	60	85	72	50	100	115
32	a	a	1800	1400	a	1400	a	26000	24000	21000
33	b	36	10	70	70	75	100	b	b	b
34	280	196	9	80	80	95	108	75	110	110
34.5	50	38	-	-	15	15	18	12	-	-
35	100	90	10	55	75	105	152	100	160	220
38	50	108	40	120	-	24	a	7200	5200	5000
44	80	144	125	450	310	370	440	200	500	800
47	280	208	150	470	370	520	320	220	600	860
48	600	112	20	60	47	50	45	25	60	80
50	132	116	14	40	55	68	60	40	75	80
51	115	124	65	430	390	740	1200	720	940	2160
52	15	16	3	10	20	20	26	20	-	40
54	45	32	3	15	18	10	-	-	-	-
66	300	176	80	170	200	285	200	140	350	400
67	8	6	2	4	6	7	5	5	-	-
69	a	a	105	380	800	880	680	400	775	770
70	40	40	4	15	15	20	14	8	-	30
71	12	10	-	4	5	-	8	-	-	-
85	150	90	11	30	50	73	45	45	75	70
86	-	-	-	-	-	-	-	-	-	-
108	10	8	-	-	-	-	-	-	-	-
119	120	88	-	15	20	20	-	-	20	-
127	85	60	-	3	7	5	-	-	-	-

Table 22. Raw Data for a Typical In Situ O_3F_2 Synthesis Experiment with Metal Walls; Reactor Space Pumped During Warmup (Continued)

		Temperature °K							
	IC	77	77	77	79	85	88	90	90
m/e	OC	77	80	77	83	92	92	92	94
	Relative Ion Currents								
16		5000	14000	4000	8000	28000	16000	21000	16000
17		800	750	450	270	600	240	340	300
18		3000	2500	1500	700	1900	850	1100	900
19		800	3900	450	1100	6400	1000	1000	950
20		110	130	30	30	40	20	30	24
25		20	50	--	--	20	--	5	5
27		--	20	--	--	--	--	5	5
28		900	480	500	200	270	340	430	340
29		20	20	10	--	20	10	15	15
31		130	130	20	--	b	110	80	100
32		35000	96000	29000	64000	184000	116000	156000	174000
33		b	b	b	b	b	b	b	b
34		200	900	140	200	2400	600	900	1000
35		1400	4000	550	1400	6000	1300	1400	1400
38		2400	6000	1500	2800	8000	3000	4300	4200
44		100	120	--	30	50	100	80	88
47		35	40	20	25	100	160	130	115
48		240	480	180	380	1300	2600	4200	5400
50		180	170	20	30	150	70	95	95
51		--	--	--	--	--	--	--	20
52		55	100	20	20	100	20	20	16
54		900	2200	280	700	3800	800	900	900
66		80	120	35	65	170	400	370	350
67		--	--	--	--	--	10	12	8
69		1800	1500	180	400	1400	1100	1000	950
70		40	60	--	--	40	20	30	30
71		40	40	--	10	35	10	15	12
83		25	--	--	--	--	--	--	--
85		50	60	20	40	140	140	180	90
86		--	--	--	--	10	--	--	--
89		--	--	--	--	--	--	--	--
100		--	--	--	--	--	--	--	--
102		--	--	--	--	--	--	--	--
104		--	--	--	--	--	--	--	--
108		--	--	--	--	--	--	--	--
119		--	--	--	--	--	50	90	90
127		--	--	--	--	--	--	20	16

Table 22. Raw Data for a Typical In Situ O_3F_2 Synthesis Experiment with Metal Walls; Reactor Space Pumped During Warmup (Continued)

m/e	IC / OC	Temperature °K							
		92 / 97	92 / 97	96 / 104	103 / 108	106 / 112	110 / 116	114 / 118	114 / 118
	Relative Ion Currents								
16		14000	22000	23000	12000	13000	18000	19000	10000
17		280	260	330	185	200	180	140	120
18		700	800	700	450	600	440	280	260
19		900	1500	1400	1800	3800	4700	5000	4800
20		25	30	80	100	95	150	160	100
25		10	12	20	35	50	40	20	15
27		10	--	15	17	10	15	10	--
28		350	370	440	480	640	1000	980	680
29		20	10	35	35	30	35	40	20
31		180	115	350	370	440	500	350	220
32		168000	220000	240000	110000	120000	135000	135000	92000
33		b	b	b	b	b	b	b	b
34		1100	1400	1000	700	800	1000	840	620
35		1300	1400	1200	2200	7400	10400	11000	9000
38		3800	5400	5200	6400	13000	18000	19000	18000
44		170	120	310	650	1700	3600	7300	5600
47		160	135	310	1200	2200	3400	1200	900
48		6400	6400	10000	3000	3000	2400	1800	1050
50		160	120	350	320	400	340	240	160
51		60	70	330	500	465	920	1600	1300
52		25	15	40	35	50	40	60	35
54		800	1100	750	1600	4600	6800	6400	5800
66		320	365	600	1400	2200	2600	1100	940
67		15	10	15	30	60	80	70	30
69		1200	1600	2800	3800	5600	3200	2600	2000
70		40	35	100	105	160	100	80	40
71		20	20	25	30	25	30	20	15
83		--	--	--	20	20	80	110	40
85		170	180	400	500	740	460	320	380
86		10	--	10	15	20	15	10	--
89		10	25	65	55	40	35	20	10
100		--	--	--	20	30	20	15	10
102		--	--	--	--	--	40	40	20
104		--	--	--	--	10	20	18	5
108		5	5	30	25	10	15	5	--
119		250	200	500	210	240	200	150	100
127		50	70	300	190	150	130	50	25

Table 22. Raw Data for a Typical In Situ O_3F_2 Synthesis Experiment with Metal Walls; Reactor Space Pumped During Warmup (Concluded)

		Temperature °K							
m/e	IC OC	119 122	121 125	121 125	106 108	122 117	130 126	130 126	135 132
	Relative Ion Currents								
16		13000	13000	12000	1200	3400	8000	6000	8000
17		120	140	110	25	30	--	--	--
18		210	180	135	95	75	70	40	40
19		6000	6600	7000	800	2300	4000	3800	4000
20		200	240	240	11	75	290	170	220
25		20	20	15	--	--	10	5	10
27		5	10	5	--	--	--	--	--
28		700	800	600	50	90	200	160	200
29		40	50	30	--	5	30	10	10
31		320	360	250	20	40	200	110	180
32		116000	120000	96000	10000	32000	72000	52000	58000
33		b	b	b	50	170	b	b	b
34		800	900	800	50	175	600	400	600
35		9000	8800	7000	800	2000	3300	2600	2500
38		20000	20000	20000	3100	8800	8800	9600	6000
44		5000	6000	4000	60	550	1200	800	1700
47		1800	2000	1200	70	160	400	350	340
48		2100	1900	1000	65	190	400	400	360
50		230	225	140	11	25	140	60	35
51		3200	5400	5800	33	1200	10000	7000	8000
52		b	b	b	5	10	b	--	--
54		6400	5200	4000	600	1200	1600	1100	840
66		1300	1400	800	160	160	350	200	160
67		50	60	40	--	5	30	30	25
69		2200	2000	1200	320	310	800	600	360
70		60	70	40	10	10	30	30	25
71		20	25	15	--	--	10	--	--
83		60	90	75	--	10	210	250	300
85		300	230	160	60	60	100	75	60
86		--	--	--	--	--	--	--	--
89		10	10	5	--	--	--	--	--
100		15	20	10	--	--	5	5	5
102		22	10	5	--	--	20	25	30
104		10	20	10	--	--	--	--	--
108		--	--	--	--	--	--	--	--
119		115	135	60	10	15	25	25	20
127		25	25	10	2	--	--	--	--

Table 23. Raw Data for a Typical In Situ O_3F_2 Synthesis Experiment with Glass Lined Walls. Reactor Space Pumped During Warmup. (Continued)

		Temperature °K							
m/e	IC OC	77 77	77 77	77 79	81 88	83 95	87 91	88 91	91 96
	Relative Ion Currents								
12		15	--	20	70	60	30	10	10
14		12	--	20	20	25	10	10	5
16		500	270	1100	4900	3800	3200	3000	5000
17		110	80	--	120	120	110	55	80
18		480	350	210	370	370	240	300	210
19		100	55	180	390	270	290	250	220
20		40	30	20	40	20	30	20	20
25		17	--	5	35	10	10	10	5
28		160	110	100	80	120	80	80	70
29		10	--	--	5	5	15	--	10
31		10	20	40	130	110	--	70	30
32		2500	1200	4900	25000	16000	15000	14000	24000
33		20	20	b	b	b	b	120	150
34		17	15	40	--	130	80	80	170
35		180	50	160	410	280	180	170	360
38		300	100	330	800	600	400	450	550
44		--	--	--	10	5	30	10	40
47		--	5	--	25	20	10	20	25
48		5	--	10	10	90	150	270	800
50		30	10	30	170	120	45	45	40
51		--	--	--	--	10	10	5	30
52		--	--	5	20	15	5	--	--
54		55	80	180	200	130	125	160	200
66		--	--	10	5	30	30	30	30
67		--	--	--	--	--	--	--	--
69		260	160	480	2100	1100	500	400	350
70		10	--	10	60	50	15	15	10
71		10	--	12	20	20	10	--	5
83		--	--	--	--	--	--	--	--
85		--	--	--	10	20	50	10	30
86		--	--	--	--	--	--	--	--
87		--	--	--	--	--	--	--	--
89		--	--	--	--	--	--	--	--
100		--	--	--	--	--	--	--	--
102		--	--	--	--	--	--	--	--
104		--	--	--	--	--	--	--	--
105		--	--	--	--	--	--	--	--
119		--	--	15	15	10	5	5	25
127		--	--	--	--	5	--	--	10

Table 23. Raw Data for a Typical In Situ O_3F_2 Synthesis Experiment with Glass Lined Walls. Reactor Space Pumped During Warmup (Continued)

		Temperature °K								
m/e	IC OC	95 98	95 101	95 101	98 104	98 104	102 112	102 112	106 110	106 110
	Relative Ion Currents									
12		10	10	10	15	35	30	30	70	15
14		5	5	10	5	20	20	10	5	10
16		5500	8000	5000	8000	12000	8000	5500	2600	2000
17		70	80	70	80	130	120	60	60	25
18		220	180	170	180	220	210	160	160	100
19		260	280	250	320	600	900	950	500	550
20		20	15	40	40	55	120	70	70	25
25		5	10	5	--	--	5	10	5	--
28		80	80	75	80	140	160	165	220	60
29		15	10	5	5	25	30	5	10	--
31		30	50	35	50	100	100	90	130	30
32		29000	44000	25000	38000	48000	40000	22000	22000	9000
33		b	b	170	260	b	b	150	b	50
34		180	250	190	250	430	360	145	150	60
35		350	460	330	340	600	500	480	480	210
38		550	455	380	520	900	950	2200	1000	1400
44		50	35	45	70	140	280	180	520	150
47		45	50	50	60	110	100	290	300	80
48		1500	2400	1300	1700	2300	1600	700	350	140
50		30	45	20	40	80	80	45	60	15
51		45	40	55	140	250	600	170	240	60
52		--	--	--	--	--	--	--	--	--
54		280	200	155	160	350	240	270	240	120
66		80	60	40	60	100	110	170	370	60
67		--	--	--	--	--	5	--	5	--
69		300	430	200	300	550	600	500	300	150
70		10	20	10	10	15	25	20	15	--
71		5	5	--	--	10	--	--	--	--
83		--	--	--	--	--	5	10	10	--
85		50	50	40	60	65	60	60	65	20
86		--	--	--	--	--	--	--	--	--
87		--	--	--	--	--	--	--	--	--
89		--	5	--	--	10	10	5	5	--
100		--	--	--	--	--	--	--	5	--
102		--	--	--	--	--	--	--	--	--
104		--	--	--	--	--	--	--	--	--
105		--	--	--	--	--	--	--	--	--
119		20	40	15	40	80	90	40	20	5
127		15	20	10	30	30	35	10	5	--

Table 23. Raw Data for a Typical In Situ O_3F_2 Synthesis Experiment with Glass Lined Walls. Reactor Space Pumped During Warmup (Concluded)

		Temperature °K								
m/e	IC OC	110 114	113 115	116 118	118 120	120 125	130 132	135 137	146 142	165 157
	Relative Ion Currents									
12		35	80	160	170	120	90	25	30	20
14		5	--	--	--	--	--	--	--	--
16		3200	4300	5000	7000	9600	9000	2600	1300	1800
17		35	30	--	--	--	--	--	--	--
18		120	65	15	40	30	--	--	--	--
19		750	800	1200	2400	3400	4400	1200	500	600
20		35	40	80	200	260	640	240	90	75
25		--	--	5	5	--	--	--	--	--
28		140	210	410	600	720	200	330	320	330
29		5	5	30	25	40	15	30	12	20
31		45	80	150	260	180	280	80	40	70
32		14000	18000	26000	32000	42000	50000	12500	7000	8600
33		b	b	b	b	b	b	b	b	b
34		100	110	150	250	300	740	140	60	150
35		390	800	1250	2000	2000	1200	450	220	230
38		1700	1700	2000	3800	4000	380	400	170	110
44		330	950	2200	1800	1350	360	250	160	190
47		180	400	700	1200	1400	400	500	375	400
48		360	430	500	600	550	140	190	150	260
50		50	45	70	120	110	100	60	25	50
51		80	250	550	1550	3600	8000	1800	4200	6000
52		--	--	--	--	--	--	--	--	--
54		250	400	750	1000	900	160	200	70	40
66		110	220	440	600	620	100	160	120	130
67		5	5	20	50	20	40	20	15	20
69		270	330	600	1000	960	520	350	170	170
70		5	10	25	35	30	20	20	5	5
71		--	--	--	--	--	--	--	--	--
83		5	10	20	40	70	280	60	25	50
85		35	40	90	4300	12000	1800	6500	5400	5200
86		--	--	5	200	1000	140	500	490	490
87		--	--	--	110	600	80	250	275	300
89		--	--	--	--	--	--	--	--	--
100		--	--	--	20	40	50	15	10	--
102		--	--	--	20	35	70	15	5	--
104		--	--	--	120	400	60	250	250	170
105		--	--	--	15	40	40	25	20	25
119		10	25	30	65	60	80	35	25	10
127		--	5	10	5	20	40	10	10	5

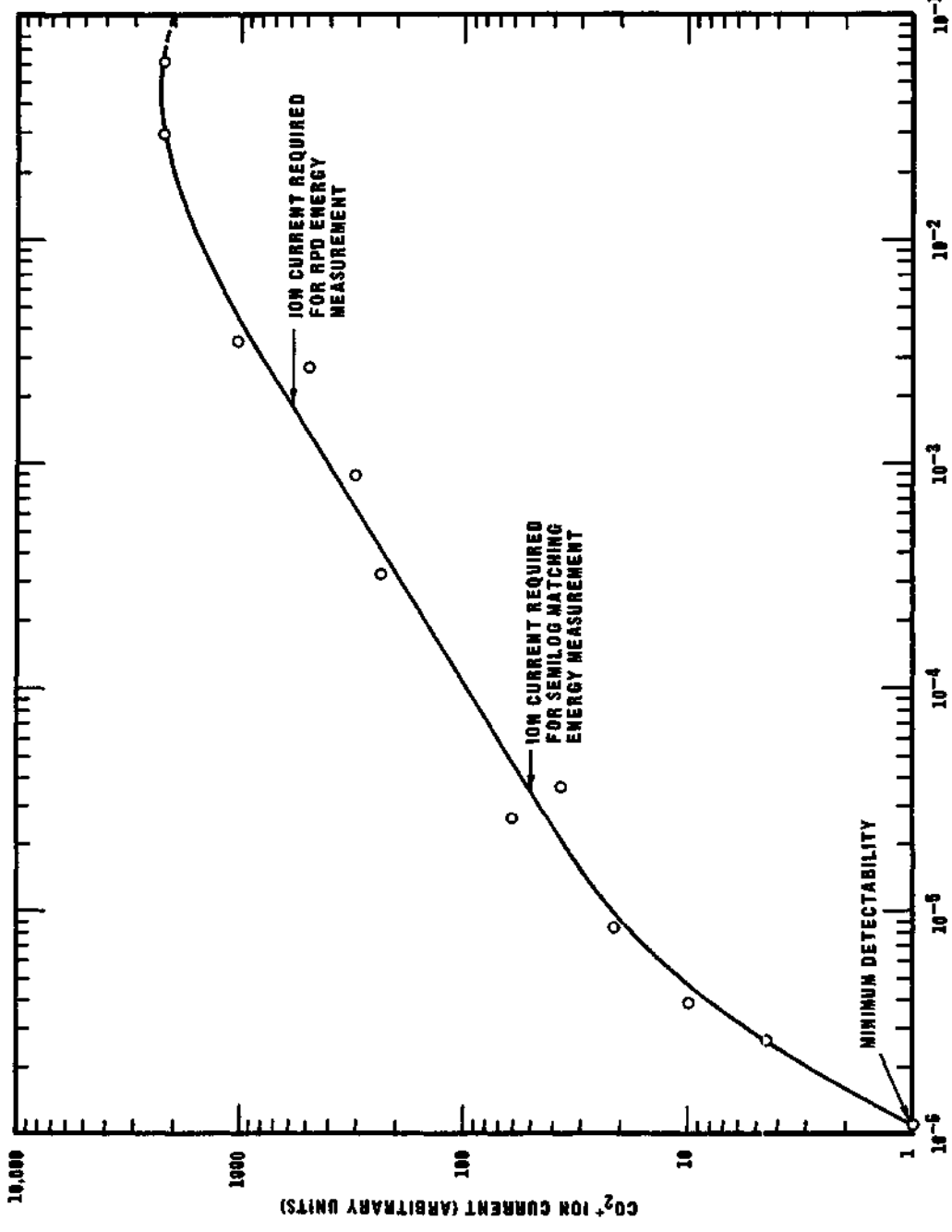

Figure 30. Variation of CO_2^+ Ion Current With the Vapor Pressure of CO_2 in the Cryogenic Reactor-Inlet System.

NOMENCLATURE

a = one-half of electron beam width, cm.

A = cross sectional area, cm^2.

A_s = surface area of extension piece of inlet system, cm^2.

$A(X)$ = appearance potential of X, ev.

b = one half of electron beam height, cm.

c_1 = distance of sample inlet port to near edge of electron beam, cm.

c_2 = distance of sample inlet port to far edge of electron beam, cm.

C = number of possible configurations.

D = molecular number density, molecules/cm^3.

$D(X-Y)$ = dissociation energy of X-Y, ev.

e = emissivity.

E_B = number of bonding electrons.

E_v = number of valence shell electrons in a given atom.

$E_a(X)_E$ = energy of atomization of X by electron impact studies, ev.

$E_a(X)_T$ = energy of atomization of X from thermochemical data, ev.

$EA(X)$ = electron affinity of X.

F = fraction of molecules effusing per sec from inlet port that is in the collision covolume.

I_1, I_2 = integrals.

$I(X)$ = ionization potential of X, ev.

J = deviation factor from cosine distribution of intensities.

k = Boltzman's constant, erg/molecule - °K.

k_c = thermal conductivity, cal/cm-sec-°K.

K = proportionality constant.

K.E. = excess kinetic energy, ev.

l = length, cm.

L = total length, cm.

m = molecular mass, gms/molecule.

m/e = mass to charge ratio.

n = fraction of molecules entering an inlet channel which finally emerge within an angle θ with respect to the axis of the channel.

N_A = number of atoms in a given molecule.

N_b = number of electrons in the effective collision covolume.

N_B = number of bonds in a given molecule.

N_e = electron flux, electrons/sec-cm^2.

N_t = total number of molecules entering a channel per unit time, molecules/sec.

$N_{t\theta}$ = number of molecules emitted from a channel per unit time per unit solid angle in the direction θ, molecules/sec.

N_θ = molecular flux in the direction θ, molecules/sec-cm^2.

p = flow parameter.

P = pressure, dyne/cm^2.

Q_c = chemical heat added per unit time, cal/sec.

Q_e = heat added per unit time by electron bombardment, cal/sec.

Q_r = radiative heat added per unit time, cal/sec.

Q_t = total heat added per unit time, cal/sec.

r = radius, cm.

R_1, R_2 = variable resistances, ohms.

S = total mass spectrometer sensitivity, molecules ionized/sec.

T = temperature, $^\circ$K.

T_2 = temperature of extension piece surface, $^\circ$K.

T_L = temperature of extension piece at connection to inner coolant chamber, °K.

T_o = temperature of extension piece at outer end, °K.

T_L = total temperature rise in the extension piece, °K.

T_s = temperature of surroundings, °K.

$\bar{v}$ = mean molecular speed, cm/sec.

X = width of extension piece, cm.

x,y,z = rectangular coordinates.

Y = height of extension piece, cm.

$\alpha,\beta,\gamma,\delta$ = constants.

ρ,θ,φ = spherical coordinates.

σ = Stefan-Boltzmann constant, cal/sec-cm^2-$°K^4$.

σ_i = ionization cross section, $Å^2$.

ω = solid angle.

BIBLIOGRAPHY*

1. H. A. McGee, Jr. and W. J. Martin, Cryogenics 2, 257 (1962).

2. R. H. Jackson, J. Chem. Soc., 4585 (1962).

3. W. J. Martin, Mass Spectrometric Studies and Cryogenic Reactivity of CF_2 and CI_2. Ph. D. Thesis, Georgia Institute of Technology (1965).

4. A. G. Streng, Chem. Rev. 63, 607 (1960).

5. P. Lebeau and A. Damiens, Compt. rend. 185, 652 (1927).

6. V. H. Dibeler, R. M. Reese, and J. L. Franklin, J. Chem. Phys. 27, 1296 (1957).

7. O. Ruff and W. Menzel, Z. anorg. allgem. Chem. 211, 204 (1933).

8. O. Ruff and W. Menzel, Z. anorg. allgem. Chem. 217, 85 (1934).

9. A. D. Kirshenbaum and A. V. Grosse, J. Am. Chem. Soc. 81, 1277 (1959).

10. A. B. Amster, J. A. Neff, and A. J. Aitken, "A Survey and Evaluation of High Energy Liquid Chemical Propulsion Systems: Preparation and Properties of Ozone Fluoride," Final Report, Stanford Research Institute, Menlo Park, California, Nov. 1, 1962.

11. A. D. Kirshenbaum, J. G. Aston, and A. V. Grosse, U. S. Dept. Com. Office Tech. Serv., P. B. Report, 149, 443 (1961).

12. A. D. Kirshenbaum, A. V. Grosse, and J. G. Aston, J. Am. Chem. Soc. 81, 6398 (1959).

13. E. Hirota, Bull. Chem. Soc. Japan 31, 130 (1958).

14. S. H. Bauer, J. Am. Chem. Soc. 69, 3104 (1947).

15. F. Seel and R. Budenz, Chem. Ber. 98, 251 (1965).

16. J. W. Linnett, J. Chem. Soc. 4663 (1963).

17. J. W. Linnett, The Electronic Structure of Molecules, John Wiley and Sons, Inc., New York (1964).

*Abbreviations in this Bibliography follow the form used by Chemical Abstracts (1965).

18. J. O. Hirshfelder, Lecture presented to Georgia Tech Chemistry Department, Atlanta, Georgia, Feb., 1965.

19. T. J. Malone, Paper presented at the 42nd annual meeting of the Georgia Academy of Sciences at Atlanta, Georgia, April, 1965.

20. S. Aoyama and S. Sakuraba, J. Chem. Soc. Japan 59, 1321 (1938).

21. S. Aoyama and S. Sakuraba, J. Chem. Soc. Japan 62, 208 (1941).

22. Irvine J. Soloman, "Research on the Chemistry of O_3F_2 and O_4F_2," NASA Accession No. N64-32 967, Sept. 1, 1964.

23. R. J. Bollbuhler and D. M. Straight, "Ignition of a Hydrogen-Oxygen Rocket Engine by Addition of Fluorine to the Oxidant," NASA Report TN-D-1308, July, 1962.

24. Irvine J. Solomon, IIT Research Institute, unpublished work.

25. A. Arkell, J. Am. Chem. Soc. 87, 4057 (1965).

26. Irvine J. Solomon, "Research on the Chemistry of O_3F_2 and O_2F_2," IIT Research Institute, Report Nos. IITRI-C227-12 and 13, 1965.

27. A. V. Grosse, A. G. Streng, and A. D. Kirshenbaum, J. Am. Chem. Soc. 83, 1004 (1961).

28. A. G. Streng and A. V. Grosse, "Addition and Substitution Compounds of Oxygen Fluorides," First Annual Progress Report for the Office of Naval Research, Contract Nonr 3085(01), Research Institute of Temple University, Philadelphia, Pa., January 3, 1961.

29. A. D. Kirshenbaum and A. G. Streng, J. Chem. Phys. 35, 1440 (1961).

30. A. G. Streng and L. V. Streng, J. Chem. Phys. 69, 1079 (1965).

31. L. Pauling, The Nature of the Chemical Bond, 3rd ed., Cornell University Press, N. Y. (1960).

32. R. P. Nielsen, Paper presented at Symposium on Advanced Propellant Chemistry, 149th National Meeting of the American Chemical Society, Detroit, Michigan, April 4-9, 1965.

33. A. G. Streng and A. V. Grosse, J. Am. Chem. Soc. 88, 169 (1966).

34. R. G. Maguire, ARL Technical Report, 60-287 (1960).

35. A. D. Kirshenbaum and A. V. Grasse, "Production, Isolation and Identification of the FO, FO_2, and FO_3 Radicals," First Annual Summary Report, Contract No. AF 04(611)-9555, Air Force Program Structure No. 3148, Research Institute of Temple University, Philadelphia, Pa., Oct. 15, 1964.

36. Paul H. Kasai, and A. D. Kirshenbaum, J. Am. Chem. Soc. 87, 3069 (1965).

37. F. Neumayr and N. Vanderkooi, Jr., Inorg. Chem. 4, 1234 (1965).

38. G. Pannetier, and A. G. Gaydon, Nature 161, 242 (1948).

39. Coleman, E. H., A. G. Gaydon, and W. W. Vaidya, Nature 162, 108 (1948).

40. G. Porter Discussions Faraday Soc. 9, 60 (1950).

41. R. A. Durie, and D. A. Ramsey, Can. J. Phys. 36, 35 (1958).

42. P. Frisch, and H. J. Schumacher, Z. anorg. allgem. Chem. 229, 423 (1936).

43. P. Frisch, and H. J. Schumacher, Z. physik. Chem. (Leipzig), B34, 322 (1936).

44. P. Frisch and H. J. Schumacher, Z. Elektrochem. 43, 807 (1937).

45. A. Glissman and H. J. Schumacher, Z. physik. Chem. (Leipzig) B24, 328 (1934).

46. R. Gatti, E. H. Staricco, J. E. Sicre, and H. J. Schumacher, Z. Physik Chem. (Frankfurt) 35, 343 (1962).

47. W. Koblitz, and H. J. Schumacher, Z. physik. Chem. (Leipzig) B25, 283 (1934).

48. H. J. Schumacher, IX Congr. intern. quim. pura. aplicada 2, 485 (1934).

49. L. Dauerman, G. Salser, and Y. A. Tajima, Paper presented at the 150th Meeting of the American Chemical Society at Atlantic City, New Jersey, Sept., 1965.

50. Viscido, Lidia del Valle, Arch. Bioquim. Quim. Farm., Tucuman 9, 89 (1961)

51. E. H. Staricco, J. E. Sicre, and H. J. Schumacher, Z. Physik. Chem. (Frankfurt) 39, 337 (1963).

52. E. H. Staricco, J. E. Sicre, and H. J. Schumacher, Z. Physik. Chem. (Frankfurt) 31, 385 (1962).

53. M. Rubenstein, J. E. Sicre and H. J. Schumacher, Z. Physik. Chem. B43, 51 (1964).

54. R. Gatti, E. H. Staricco, J. E. Sicre and H. J. Schumacher, Z. Physik. Chem. (Frankfurt) 36, 211 (1963).

55. R. Gatti, E. H. Staricco, J. E. Sicre, and H. J. Schumacher, Angew. Chem. Intern. Ed. Engl. 2, 149 (1963).

56. A. Arkell, R. R. Reinhard, and L. P. Larson, J. Am. Chem. Soc. 87, 1016 (1965).

57. G. Glocker, J. Chem. Phys. 16, 604 (1948).

58. W. C. Price, T. R. Passmore, and D. M. Roessler, Discussions Faraday Soc. 35, 201 (1963).

59. M. Green and J. W. Linnett, J. Chem. Soc., 4959 (1960).

60. J. B. Levy and B. K. Wesley Copeland, J. Phys. Chem. 69, 408 (1965).

61. H. J. Schumacher and P. Frisch, Z. physik. Chem. 37, 1 (1937).

62. L. P. Blanchard and P. LeGoff, Can. J. Chem., 37, 515 (1959).

63. "Collected Works of Sir James Dewar," edited by Lady Dewar, Cambridge University Press, Vol. I and II, 1927.

64. D. C. Damoth, "Advances in Analytical Chemistry and Instrumentation," Vol. 4, edited by C. N. Reilley, Wiley, New York, 1965.

65. P. Clausing, Z. Physik. 66, 471 (1930).

66. A. N. Miller, J. Chem. Phys. 42, 3734 (1965).

67. K. Biemann, "Mass Spectrometry, Organic Chemical Applications," McGraw-Hill, New York, 1962.

68. C. E. Melton and W. H. Hamill, J. Chem. Phys. 41, 546 (1964).

69. S. N. Foner and R. L. Hudson, J. Chem. Phys. 25, 602 (1956).

70. S. N. Foner and R. L. Hudson, J. Chem. Phys. 36, 2681 (1962).

71. J. T. Herron and H. I. Schiff, J. Chem. Phys. 24, 1266 (1956).

72. B. Siegel and L. Schieler, "Energetics of Propellant Chemistry ," Wiley and Sons, Inc., New York (1964).

73. F. B. Dudley, G. H. Cady, O. F. Eggers, Jr., J. Am. Chem. Soc. 78 1553 (1956).

74. T. J. Malone and H. A. McGee, Jr., J. Phys. Chem. 69, 4338 (1965).

75. A. J. B. Robertson, Trans. Faraday Soc. 48, 229 (1952).

76. A. F. Wells, "Structural Inorganic Chemistry," Oxford, at the Claredon Press (1962).

77. R. L. Kuczkowski, J. Am. Chem. Soc. 86, 3617 (1964).

78. P. J. Durant and B. Durant, "Introduction to Advanced Inorganic Chemistry, Wiley and Sons, Inc., New York (1962).

79. J. C. Mullins, B. S. Kirk, and W. T. Ziegler, "Calculation of the Vapor Pressure and Heats of Vaporization and Sublimation of Liquids and Solids, Especially Below One Atmosphere. V. Carbon Monoxide and Carbon Dioxide." Georgia Tech Report No. 2, Project No. A-663, Aug. 15, 1963.

VITA

Thomas Joseph Malone was born in Jackson, Mississippi on March 27, 1939. He attended public schools in Hattiesburg Mississippi and graduated from Hattiesburg High School in 1957. Upon graduation he served six months active duty with the U. S. Army and received training in Army Finance Disbursement. He entered Pearl River Junior College in Poplarville, Mississippi in September 1958 on an athletic scholarship and was a member of the varsity football and basketball teams. He received an Associate of Science Degree from Pearl River Junior College in May 1960 and was named valedictorian of his graduating class. In June 1960 he entered Georgia Institute of Technology under the cooperative plan and was awarded the degree of Bachelor of Chemical Engineering with honors in June 1963. He was employed by Hercules Powder Company, Hattiesburg, Mississippi, under the cooperative plan. He received scholarships from Union Bag-Camp, Inc. during the academic years 1961-62 and 1962-63.

In June 1963 he enrolled in the Graduate Division of the Georgia Institute of Technology as a predoctoral student. He was employed by the Engineering Experiment Station and received graduate fellowships from the National Science Foundation, Proctor and Gamble Company, and Ethyl Corporation.

He is a member of Phi Kappa Phi, Tau Beta Pi, Phi Theta Kappa, and the Society of Sigma Xi. He is a member of Phi Sigma Kappa social fraternity, of which he is a past president.

In 1962 he was married to the former Patricia Ellen Stewart of

Poplarville, Mississippi and they have one daughter, Deborah Ellen. They now live in Spartanburg, South Carolina, where he is employed by the Deering-Milliken Research Corporation.